

MAJOR REPORT • OPEN ACCESS

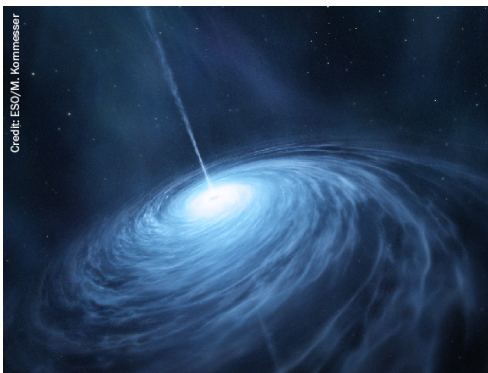
Physics beyond colliders at CERN: beyond the Standard Model working group report

To cite this article: J Beacham *et al* 2020 *J. Phys. G: Nucl. Part. Phys.* **47** 010501

View the [article online](#) for updates and enhancements.

Recent citations

- [The quest for new physics with the Physics Beyond Colliders programme](#)
Joerg Jaeckel *et al*
- [New long-lived particle searches in heavy-ion collisions at the LHC](#)
Marco Drewes *et al*
- [Probing the freeze-in mechanism in dark matter models with U\(1\) gauge extensions](#)
Saniya Heeba and Felix Kahlhoefer



AMERICAN
ASTRONOMICAL
SOCIETY




IOP | ebooks™

Your first choice for astronomy, astrophysics,
solar physics, and planetary science ebooks.

Start exploring the collection—download the
first chapter of every title for free.

Major Report

Physics beyond colliders at CERN: beyond the Standard Model working group report

J Beacham¹ , C Burrage^{2,30}, D Curtin³ , A De Roeck⁴,
J Evans⁵, J L Feng⁶, C Gatto^{7,8}, S Gninenko⁹, A Hartin¹⁰,
I Irastorza¹¹, J Jaeckel¹², K Jungmann^{13,30}, K Kirch^{14,30},
F Kling⁶, S Knapen¹⁵, M Lamont⁴, G Lanfranchi^{4,16,30,31} ,
C Lazzeroni¹⁷, A Lindner¹⁸, F Martinez-Vidal¹⁹,
M Moulson¹⁶, N Neri²⁰, M Papucci^{4,21}, I Pedraza²²,
K Petridis²³, M Pospelov^{24,30}, A Rozanov^{25,30}, G Ruoso^{26,30},
P Schuster²⁷, Y Semertzidis²⁸, T Spadaro¹⁶, C Vallée²⁵ and
G Wilkinson²⁹

¹ Duke University, Durham, NC 27708, United States of America

² University of Nottingham, Nottingham, United Kingdom

³ Department of Physics, University of Toronto, Toronto, Ontario M5S 1A7, Canada

⁴ European Organization for Nuclear Research (CERN), Geneva, Switzerland

⁵ Department of Physics, University of Cincinnati, Cincinnati, OH 45221, United States of America

⁶ Department of Physics and Astronomy, University of California, Irvine, CA 92697-4575, United States of America

⁷ Sezione di Napoli, INFN, Napoli, Italy

⁸ Northern Illinois University, United States of America

⁹ Institute for Nuclear Research of the Russian Academy of Sciences, 117312 Moscow, Russia

¹⁰ University College London, Gower Street, London WC1E 6BT, United Kingdom

¹¹ Grupo de Física Nuclear y Altas Energías, Universidad de Zaragoza, Zaragoza, Spain

¹² Institute for Theoretical Physics, Heidelberg University, Heidelberg, Germany

¹³ VSI (Van Swinderen Institute), University of Groningen, Groningen, The Netherlands

¹⁴ ETH Zurich and Paul Scherrer Institute, Villigen, Switzerland

¹⁵ Institute for Advanced Study, Princeton, NJ, United States of America

¹⁶ Laboratori Nazionali di Frascati, INFN, Frascati (Rome), Italy

¹⁷ University of Birmingham, Birmingham, United Kingdom

¹⁸ DESY, Hamburg, Germany

¹⁹ IFIC/University of Valencia-CSIC, Valencia, Spain

²⁰ INFN Sezione di Milano and Università di Milano, Milano, Italy

²¹ Lawrence Berkeley National Laboratory and UC Berkeley, Berkeley, CA, United States of America

²² Benemerita Universidad Autonoma de Puebla, Mexico

²³ University of Bristol, Bristol, United Kingdom

²⁴ Perimeter Institute, Waterloo and University of Victoria, Victoria, Canada

²⁵ CPPM, CNRS-IN2P3 and Aix-Marseille University, Marseille, France

²⁶ Laboratori Nazionali di Legnaro, INFN, Legnaro, Italy

²⁷ SLAC National Accelerator Laboratory, Menlo Park, CA 94025, United States of America

²⁸ KAIST/IBS, Daejeon, Republic of Korea

²⁹ University of Oxford, Oxford, United Kingdom

E-mail: Gaia.Lanfranchi@Inf.infn.it

Received 5 September 2019

Accepted for publication 10 October 2019

Published 11 December 2019



CrossMark

Abstract

The Physics Beyond Colliders initiative is an exploratory study aimed at exploiting the full scientific potential of the CERN's accelerator complex and scientific infrastructures through projects complementary to the LHC and other possible future colliders. These projects will target fundamental physics questions in modern particle physics. This document presents the status of the proposals presented in the framework of the Beyond Standard Model physics working group, and explore their physics reach and the impact that CERN could have in the next 10–20 years on the international landscape.

Keywords: beyond standard Model, dark matter, dark sector, axions, particle physics, accelerators

Executive summary

The main goal of this document follows very closely the mandate of the Physics Beyond Colliders (PBC) study group and is *'an exploratory study aimed at exploiting the full scientific potential of CERN's accelerator complex and its scientific infrastructure through projects complementary to the LHC, HL-LHC and other possible future colliders. These projects would target fundamental physics questions that are similar in spirit to those*

³⁰ PBC–BSM Coordinators and Editors of this Report.

³¹ Author to whom any correspondence should be addressed.



Original content from this work may be used under the terms of the [Creative Commons Attribution 3.0 licence](https://creativecommons.org/licenses/by/3.0/). Any further distribution of this work must maintain attribution to the author(s) and the title of the work, journal citation and DOI.

*addressed by high-energy colliders, but that require different types of beams and experiments*³².

Fundamental questions in modern particle physics such as the origin of the neutrino masses and oscillations, the nature of dark matter and the explanation of the mechanism that drives the baryogenesis are still open today and do require an answer.

So far an unambiguous signal of New Physics (NP) from direct searches at the Large Hadron Collider (LHC), indirect searches in flavor physics and direct detection dark matter experiments is absent. Moreover, theory provides no clear guidance on the NP scale. This imposes today, more than ever, a broadening of the experimental effort in the quest for NP. We need to explore different ranges of interaction strengths and masses with respect to what is already covered by existing or planned initiatives.

Low-mass and very-weakly coupled particles represent an attractive possibility, theoretically and phenomenologically well motivated, but currently poorly explored: a systematic investigation should be pursued in the next decades both at accelerator-based experiments and with proposals aiming at detecting axions and axion-like particles (ALPs) with terrestrial experiments.

Very high energy scales (~ 100 TeV) will not be reachable with colliders that exist now or in the foreseeable future and can be explored only using extremely rare or forbidden decays as probe to the NP in the multi-TeV range. Electric dipole moments (EDMs) are simultaneously probes of NP in the extremely low ($< 10^{-15}$ eV) and in the very large (> 100 TeV) mass scale range.

The CERN laboratory could offer an unprecedented variety of high-intensity, high-energy beams and scientific infrastructures that could be exploited to this endeavor. This effort would nicely complement and further broaden the already rich physics program ongoing at the LHC and HL-LHC.

This document presents the status of the proposals presented in the framework of the PBC beyond the standard model (BSM) physics working group, and explore their physics reach and the impact that CERN could have in the next 10–20 years on the international landscape.

1. Introduction

The PBC BSM study group has considered about 18 different proposals aiming at exploiting the CERN accelerator complex and scientific infrastructure. These proposals will be sensitive to New Physics in a range of masses and couplings inaccessible to other existing or planned initiatives in the world, as the experiments at the LHC or at a future circular collider (FCC), dark matter (DM) direct detection experiments and flavor physics initiatives.

This document focusses on searches for Physics BSM also known as NP. It introduces the physics motivations and the complementarity of the proposals presented within the PBC–BSM activity with respect to the LHC and other initiatives in the world in the quest for NP. NP is required to answer open questions in modern particle physics, as the origin of neutrinos masses and oscillations, baryogenesis and the nature of DM. A viable possibility is so called *hidden sector physics*, that comprises new particles with masses below the electro-weak (EW) scale that couple very weakly to the Standard Model (SM) world via *portals*. Another viable possibility is that NP is well above the EW scale (and therefore well beyond the direct reach of the LHC and any other future high-energy collider), and can be only probed via indirect effects in extremely rare or forbidden processes in the SM or by testing the presence of electric dipole moments (EDMs) either in proton and deuteron or in more complex systems.

³² See <https://pbc.web.cern.ch>.

Three main categories of experiments have been identified, following the NP mass range they are sensitive to:

- (1) *Experiments sensitive to NP with mass in the sub-eV range and very weakly coupled to SM particles:* these are mostly experiments searching for axions and ALPs using a large variety of experimental techniques;
- (2) *Experiments sensitive to NP with mass in the MeV–GeV range and very weakly coupled to SM particles:* these are accelerator-based experiments that could exploit the large variety of high-intensity high-energy beams currently available or proposed at CERN;
- (3) *Experiments sensitive to NP with mass in the multi-TeV range and strongly coupled to SM particles:* these are experiments searching for extremely rare or forbidden processes, that could be produced via high-intensity beams.

The document is organized as follows. Section 2 presents a brief summary of the main physics motivations. In particular section 2.1 discusses in detail portals to a hidden sector along with a set of benchmark cases that have been identified as theoretically and phenomenologically motivated target areas to explore the physics reach of the PBC proposals and put them in the world-wide landscape. The proposals presented in the framework of the PBC–BSM study group are briefly described in section 3 and classified in terms of their sensitivity to a given mass range and to a set of benchmark cases. A more detailed description is then given in sections 4–6 ordered along the identified main mass ranges. The physics reach of the PBC–BSM proposals is shown in sections 7–10 along with the current status of these searches at ongoing and/or planned initiatives in the world that are or will be important players on the same timescale of the PBC proposals. Brief conclusions are drawn in section 11.

2. Physics motivations

With the discovery at the LHC of the Higgs boson [1, 2], the last missing piece for the experimental validation of the SM is now in place. An additional LHC result of great importance is that a large new territory has been explored and no unambiguous signal of NP has been found so far. These results, together with several constraints from flavor phenomenology and the absence of any charged lepton flavor violation process, indicate that there might be no NP with a direct and sizeable coupling to SM particles up to energies $\sim 10^5$ TeV unless specific flavor structures/symmetries are postulated.

The possibility that the SM holds well beyond the electroweak (EW) scale must now be seriously considered. The SM is renormalizable and predictive and the measured masses of the Higgs boson and the top quark fall into a narrow region of parameters where consistency of the SM does not require new particles up to a very high energy scale, possibly all the way up to the Planck scale [3–5]. However, some yet unknown particles or interactions are required to explain a number of observed phenomena in particle physics, astrophysics, and cosmology such as neutrino masses and oscillations, baryon asymmetry of the Universe, DM and cosmological inflation.

(1) *Neutrino oscillations*

Propagating neutrinos have been seen to oscillate between different flavors. This implies the existence of a neutrino mass matrix which differentiates the flavor eigenstates from the mass eigenstates. This is absent in the SM. It is, additionally, challenging to explain why the observed neutrino masses are so much smaller than the masses of other leptons. One common mechanism to generate such a mass matrix is the, so called, *seesaw* mechanism, which introduces one or more heavy sterile neutrinos. This heavy mass scale, combined with the SM scales, allows for the generation of very light mass

eigenstates for the EW neutrinos. Estimates for the mass of these additional neutrinos range from $(10^{-9}-10^{15})$ GeV.

(2) *Abundance of matter, absence of anti-matter*

All of the structure that we see in the Universe is made of matter, and there is no indication of the presence of significant amounts of anti-matter.

The dominance of matter over anti-matter can be explained by out of equilibrium processes in the early universe violating B -number conservation, as well as the C and CP symmetries, and occurring out of equilibrium. These Sakharov conditions [6] are necessary to generate the baryon asymmetry when assuming symmetric initial conditions and CPT conservation. Neither the CP -violation nor the out-of-equilibrium condition can be accommodated without extending the SM in some way. In particular our new understanding of the Higgs mechanism means that we now know that the EW phase transition is not a strong first order transition, and so cannot be the explanation for the asymmetry between matter and antimatter that we see in the present universe³³.

(3) *Dark Matter*

Evidence that the particles of the SM are not abundant enough to account for all of the matter in the Universe comes from a multitude of galactic and cosmological observations. Two key observations are galactic dynamics and the cosmic microwave background (CMB). The stability of spiral galaxies, and their observed rotation curves require an additional (cold) matter component to be clustered on galactic scale. This additional component contains a significant fraction of the total mass of the Galaxy and has a greater spatial extent than the visible galactic matter. Observations of the CMB tell us about the average properties of the Universe that these microwave photons have passed through since the epoch of decoupling. Again this tells us that, on average, SM matter can only account for approximately 5% of the Universe that we see, and that there is an additional 25% of our current universe which appears to be cold and dark non-relativistic matter.

There are many proposed models of DM which would be compatible with these observations, ranging from ultra-light scalars with masses 10^{-31} GeV to a distribution of black holes with masses up to $10 M_{\text{sun}}$, being M_{sun} the mass of the Sun.

(4) *Cosmological inflation and dark energy*

Additionally, observations of the CMB indicate that our universe began with a period of exponential inflation, and is currently undergoing a second period of accelerated expansion. No explanation for either of these periods of the Universe's evolution exists within the SM. A widely accepted hypothesis to explain these observations is that the space is permeated by an unknown form of energy (or *dark energy*) which tends to accelerate the expansion of the Universe and accounts for the remaining 70% of the existing Universe.

In addition to the evidence described above there are a number of other hints that physics beyond the SM is required. These are typically unusually large fine tunings of parameters which are challenging to explain within the SM framework. These should not be taken to have the same status, regarding motivating NP, as the observational evidence described above, but rather as possible sign posts to parts of the model which are not yet fully understood.

³³ An alternative model assumes CPT and B -number violation. It could create a matter anti-matter asymmetry in thermal equilibrium [7, 8]. An active field with a multitude of experimental searches for CPT violating processes exists worldwide, among which leading activities are located at the CERN AD facility [9]. They have yielded many tight bounds already on Lorentz and CPT violation.

(1) *Higgs mass fine tuning*

The Higgs boson is the only scalar field present in the SM. In contrast to the other particles we observe, it is not understood how to protect the mass of the scalar Higgs field from quantum corrections driving it to a much higher scale without a high degree of fine tuning. Possible solutions to this problem include low-scale supersymmetry, the existence of extra spatial dimensions, and dynamical relaxation mechanisms.

(2) *Strong CP problem*

There is no reason to expect that the strong sector of the SM would respect CP symmetry. Without a large degree of fine tuning, this level of CP violation would produce an EDM for the neutron at an observable level. Unlike the other fine tuning problems we discuss here, it is not even possible to make an anthropic argument for why the degree of CP violation in the strong sector should be unobservably small.

The most common solution for this issue is the introduction of a pseudo scalar field, the axion, which dynamically relaxes the degree of CP violation to small values. With an appropriately chosen mass the axion may also make up all or part of the DM in our universe.

(3) *Cosmological constant and dark energy*

As mentioned above, the CMB combined with other cosmological observations, in particular of Type 1a supernovae, indicates that approximately 70% of the energy density in our current universe is due to a cosmological constant, or something that behaves very similarly. A cosmological constant term in the Einstein equations is naturally generated by quantum fluctuations of the vacuum, but unfortunately this is many orders of magnitude too large to be compatible with cosmological observations. Explaining why such a large cosmological constant is not seen typically requires a significant amount of fine tuning.

There is a vast landscape of theoretical models to address some, or all, of the above-mentioned motivations for NP. This often involves introducing new particles which can be bosons or fermions, heavy or light, depending on the theory and the problems it addresses. There are theories that aim to make the most minimal modification possible to the SM, whilst still addressing all of the motivations for new physics that we have described here, as well as model independent approaches, which try to parametrize all of the possible ways certain types of new physics could extend the SM. Here we will outline the most popular classes of current theoretical ideas for BSM physics.

(1) *New physics at the TeV scale and beyond*

If there is an intermediate scale between the EW and the Planck scale, it is necessary to introduce a mechanism to protect the Higgs mass from receiving large quantum corrections. The most commonly studied possibility, by far, is the introduction of supersymmetry. No compelling hints for supersymmetry have yet been seen at the LHC, which suggests that, if this symmetry is realized in nature, it may only be restored at an energy scale much higher than can currently be reached with collider experiments. We will see that precision measurements, such as Kaon physics, B physics, and EDM measurements, can indirectly search for NP at a much higher scale than can be directly probed with the LHC or any future high-energy collider.

(2) *Right-handed neutrinos*

The introduction of right-handed neutrinos is motivated by explanations of neutrino masses, in particular their smallness via the see-saw mechanism. However, it can also be a useful ingredient for generating baryon asymmetry via leptogenesis. The introduction of such right-handed neutrinos can generate CP violation, but as yet the scale at which this happens is not constrained, if it lies near the EW scale it could lead to observable EDMs. The masses

of the right-handed neutrinos can lie anywhere from the GUT scale down to ~ 100 MeV. A viable example including right-handed neutrinos is the *Neutrino Minimal Standard Model* (ν MSM) [10, 11] which accounts for neutrino masses and oscillations, for the evidence of DM and for the baryon asymmetry of the Universe. This model adds to the SM only three right-handed singlet sterile neutrinos or heavy neutral leptons (HNLs), one with a mass in the keV range that acts as DM candidate and the other two with a mass in the GeV range and Yukawa couplings in the range 10^{-11} – 10^{-6} .

(3) *WIMP dark matter models*

The idea that the DM is a thermal relic from the hot early universe motivates non-gravitational interactions between dark and ordinary matter. The canonical example involves a heavy particle with mass between 100 and 1000 GeV interacting through the weak force (WIMPs), but so far no WIMP has been observed. However a thermal origin is equally compelling even if DM is not a WIMP: DM with any mass from a MeV to tens of TeV can achieve the correct relic abundance by annihilating directly into SM matter. Thermal DM in the MeV–GeV range with SM interactions is overproduced in the early Universe so viable scenarios require additional SM neutral mediators to deplete the overabundance [12–20]. The sub-GeV range for the DM mediators can additionally provide a solution to some outstanding cosmological puzzles including an explanation of why the mass distribution at the center of a galaxy is smoother than expected.

(4) *Axion DM models*

Axions are another well motivated DM candidate, that may simultaneously solve the *CP* problems of QCD. Axion DM particles are sufficiently light that they must be produced non-thermally through a gravitational or misalignment production mechanism.

The minimal axion model relates the mass and coupling constant of the axion. If this condition is relaxed the theory can be generalized to one of axion-like-particles (ALPs) and such a generalization may also be motivated from string theory. The search for axions and ALPs in the sub-eV mass range comprises a plethora of different experimental techniques and experiments as *haloscopes*, *solar helioscopes* and *pure laboratory experiments* among which, for example, regeneration or *light-shining-through a wall* (LSW) experiments. ALPs with masses in the MeV–GeV range can be produced, and possibly detected, at accelerator-based experiments.

So far most of the experimental efforts have been concentrated on the discovery of new particles with masses at or above the EW scale with sizeable couplings with SM particles. Another viable possibility, largely unexplored, is that particles responsible for the still unexplained phenomena beyond the SM are below the EW scale and have not been detected because they interact very feebly with the SM particles. Such particles are thought to be linked to a so called *hidden sector*. Given the exceptionally low-couplings, a high intensity source is necessary to produce them at a detectable rate: this can be astrophysical sources, or powerful lasers, or high-intensity accelerator beams. The search for NP in the low-mass and very low coupling regime at accelerator beams is what is currently called the *intensity frontier*.

Hidden Sector particles and *mediators* to the SM can be light and long-lived. They interact very weakly with SM fields that do not carry electromagnetic charge, like the Higgs and the Z^0 bosons, the photon and the neutrinos. They are singlet states under the SM gauge interactions and the couplings between the SM and hidden-sector particles arise via mixing of the hidden-sector field with a SM ‘portal’ operator. In the following section we will present the generic framework for *hidden sector portals* along with a set of specific benchmark cases that will be used in this document to compare the physics reach of a large fraction of proposals presented within this study.

2.1. Hidden sector portals

The main framework for the BSM models, the so-called *portal* framework, is given by the following generic setup (see e.g. [21–23]). Let O_{SM} be an operator composed from the SM fields, and O_{DS} is a corresponding counterpart composed from the dark sector fields. Then the portal framework combines them into an interaction Lagrangian

$$\mathcal{L}_{\text{portal}} = \sum O_{\text{SM}} \times O_{\text{DS}}. \quad (2.1)$$

The sum goes over a variety of possible operators of different composition and dimension. The lowest dimensional renormalisable portals in the SM can be classified into the following types:

Portal	Coupling
Dark photon, A_μ	$-\frac{\epsilon}{2 \cos \theta_W} F'_{\mu\nu} B^{\mu\nu}$
Dark Higgs, S	$(\mu S + \lambda S^2) H^\dagger H$
Axion, a	$\frac{a}{f_a} F_{\mu\nu} \tilde{F}^{\mu\nu}, \frac{a}{f_a} G_{i,\mu\nu} \tilde{G}_i^{\mu\nu}, \frac{\partial_\mu a}{f_a} \bar{\psi} \gamma^\mu \gamma^5 \psi$
Sterile neutrino, N	$y_N LHN$

Here, $F'_{\mu\nu}$ is the field strength for the dark photon, which couples to the hypercharge field, $B^{\mu\nu}$; S is a new scalar singlet that couples to the Higgs doublet, H , with dimensionless and dimensional couplings, λ and μ ; a is a pseudoscalar axion that couples to a dimension-4 diphoton, di-fermion or di-gluon operators; and N is a new neutral fermion that couples to one of the left-handed doublets of the SM and the Higgs field with a Yukawa coupling y_N .

According to the general logic of quantum field theory, the lowest canonical dimension operators are the most important. All of the portal operators respect all of the SM gauge symmetries. Even the global symmetries are kept intact with the only exception being the (accidental) lepton number conservation if the HNL is Majorana. The kinetic mixing and $S^2 H^\dagger H$ operators are generically generated at loop level unless targeted symmetries are introduced to forbid them³⁴.

The PBC–BSM working group has identified a set of *benchmark physics cases*, presented the corresponding Lagrangians, and defined the parameter space to be examined in connection with experimental sensitivities. In the subsequent section, we formulate the benchmark models in some detail.

2.1.1. Vector portal models. A large class of BSM models includes interactions with light new vector particles. Such particles could result from extra gauge symmetries of BSM physics. New vector states can mediate interactions both with the SM fields, and extra fields in the dark sector that e.g. may represent the DM states.

The most minimal vector portal interaction can be written as

$$\mathcal{L}_{\text{vector}} = \mathcal{L}_{\text{SM}} + \mathcal{L}_{\text{DS}} - \frac{\epsilon}{2 \cos \theta_W} F'_{\mu\nu} B_{\mu\nu}, \quad (2.2)$$

where \mathcal{L}_{SM} is the SM Lagrangian, $B_{\mu\nu}$ and $F'_{\mu\nu}$ are the field strengths of hypercharge and new $U(1)'$ gauge groups, ϵ is the so-called kinetic mixing parameter [24], and \mathcal{L}_{DS} stands for the dark sector Lagrangian that may include new matter fields χ charged under $U'(1)$

³⁴ E.g. a Z_2 symmetry for the hidden photon field.

$$\mathcal{L}_{\text{DS}} = -\frac{1}{4}(F'_{\mu\nu})^2 + \frac{1}{2}m_{A'}^2(A'_\mu)^2 + |(\partial_\mu + ig_D A'_\mu)\chi|^2 + \dots \quad (2.3)$$

If χ is stable or long-lived it may constitute a fraction of entirety of DM. At low energy this theory contains a new massive vector particle, a dark photon state, coupled to the electromagnetic current with ϵ -proportional strength, $A'_\mu \times \epsilon J_{EM}^\mu$.

We define the following important benchmark cases (BC1–BC3) for the vector portal models.

- *BC1, Minimal dark photon model:* in this case the SM is augmented by a single new state A' . DM is assumed to be either heavy or contained in a different sector. In that case, once produced, the dark photon decays back to the SM states. The parameter space of this model is $\{m_{A'}, \epsilon\}$.
- *BC2, Light DM coupled to a dark photon:* here a minimally coupled WIMP DM model can be constructed [14, 15]. The preferred values of dark coupling $\alpha_D = g_D^2/(4\pi)$ are such that the decay of A' occurs predominantly into $\chi\chi^*$ states. These states can further rescatter on electrons and nuclei due to ϵ -proportional interaction between SM and DS states mediated by the mixed AA' propagator [22, 25]. The parameter space for this model is $\{m_{A'}, \epsilon, m_\chi, \alpha_D\}$ with further model-dependence associated to the properties of χ (boson or fermion). The suggested choices for the PBC evaluation are 1. ϵ versus $m_{A'}$ with $\alpha_D \gg \epsilon^2\alpha$ and $2m_\chi < m_{A'}$, 2. y versus m_χ plot where the *yield* variable y , $y = \alpha_D \epsilon^2 (m_\chi/m_{A'})^4$, is argued [26] to contain a combination of parameters relevant for the freeze-out and DM–SM particles scattering cross section. One possible choice is $\alpha_D = 0.1$ and $m_{A'}/m_\chi = 3$.
- *BC3, Millicharged particles:* this is the limit $m_{A'} \rightarrow 0$, in which case χ has an effective electric charge of $|Q_\chi| = |\epsilon g_D e|$ [24, 27]. The suggested choice of parameter space is $\{m_\chi, Q_\chi/e\}$, and χ can be taken to be a fermion.

The kinetic mixing coupling of A' to matter is the simplest and most generic, but not the only possible vector portal. Other cases considered in the literature include gauged $B - L$ and $L_\mu - L_\tau$ models, and somewhat less motivated leptophylic and leptophobic cases, when A' is assumed to be coupled to either total lepton current, or total baryon current with a small coupling g' .

Such other exotic vector mesons however, generically mix with the SM photon at one loop, which is often enhanced by the number of flavors and/or colors of the quarks/leptons running in the loop. This means that the kinetically mixed dark photon benchmarks outlined above also cover these scenarios, to some extent (see, e.g. [28]).

2.1.2. Scalar portal models. The 2012 discovery of the BEH mechanism, and the Higgs boson h , prompts to investigate the so called scalar or Higgs portal, that couples the dark sector to the Higgs boson via the bilinear $H^\dagger H$ operator of the SM. The minimal scalar portal model operates with one extra singlet field S and two types of couplings, μ and λ [29],

$$\mathcal{L}_{\text{scalar}} = \mathcal{L}_{\text{SM}} + \mathcal{L}_{\text{DS}} - (\mu S + \lambda S^2)H^\dagger H. \quad (2.4)$$

The dark sector Lagrangian may include the interaction with DM χ , $\mathcal{L}_{\text{DS}} = S\bar{\chi}\chi + \dots$. Most viable DM models in the sub-EW scale range imply $2 \cdot m_\chi > m_S$ [30].

At low energy, the Higgs field can be substituted for $H = (v + h)/\sqrt{2}$, where $v = 246$ GeV is the EW vacuum expectation value, and h is the field corresponding to the physical 125 GeV Higgs boson. The non-zero μ leads to the mixing of h and S states. In the limit of small mixing it can be written as

$$\theta = \frac{\mu\nu}{m_h^2 - m_S^2}. \quad (2.5)$$

Therefore the linear coupling of S to SM particles can be written as $\theta_S \times \sum_{\text{SM}} O_h$, where O_h is a SM operator to which Higgs boson is coupled and the sum goes over all type of SM operators coupled to the Higgs field.

The coupling constant λ leads to the coupling of h to a pair of S particles, λS^2 . It can lead to pair-production of S but cannot induce its decay. An important property of the scalar portal is that at loop level it can induce flavor-changing transitions, and in particular lead to decays $K \rightarrow \pi S$, $B \rightarrow K^{(*)}S$ etc [29, 31, 32] and similarly for the hS^2 coupling [33]. We define the following benchmark cases for the scalar portal models:

- *BC4, Higgs-mixed scalar*: in this model we assume $\lambda = 0$, and all production and decay are controlled by the same parameter θ . Therefore, the parameter space for this model is $\{\theta, m_S\}$.
- *BC5, Higgs-mixed scalar with large pair-production channel*: in this model the parameter space is $\{\lambda, \theta, m_S\}$, and λ is assumed to dominate the production via e.g. $h \rightarrow SS$, $B \rightarrow K^{(*)}SS$, $B^0 \rightarrow SS$ etc. In the sensitivity plots shown in section 9.2 a value of the branching fraction $BR(h \rightarrow SS)$ close to 10^{-2} is assumed in order to be complementary to the LHC searches for the Higgs to invisible channels.

We also note that while the 125 GeV Higgs-like resonance has properties of the SM Higgs boson within errors, the structure of the Higgs sector can be more complicated and include e.g. several scalar doublets. In the two-Higgs doublet model the number of possible couplings grows by a factor of three, as S can couple to 3 combinations of Higgs field bilinears, $H_1^\dagger H_1$, $H_2^\dagger H_2$ and $H_1 H_2$. Therefore, the experiments could investigate their sensitivity to a more complicated set of the Higgs portal couplings that are, however, beyond the present document.

2.1.3. Neutrino portal models. The neutrino portal extension of the SM is very motivated by the fact that it can be tightly related with the neutrino mass generation mechanism. The neutrino portal operates with one or several dark fermions N , that can be also called *heavy neutral leptons* or HNLs. The general form of the neutrino portal can be written as

$$\mathcal{L}_{\text{vector}} = \mathcal{L}_{\text{SM}} + \mathcal{L}_{\text{DS}} + \sum F_{\alpha I} (\bar{L}_\alpha H) N_I, \quad (2.6)$$

where the summation goes over the flavor of lepton doublets L_α , and the number of available HNLs, N_I . The $F_{\alpha I}$ are the corresponding Yukawa couplings. The dark sector Lagrangian should include the mass terms for HNLs, that can be both Majorana or Dirac type. For a more extended review, see [23, 34]. Setting the Higgs field to its v.e.v., and diagonalizing mass terms for neutral fermions, one arrives at $\nu_i - N_j$ mixing, that is usually parametrized by a matrix called U . Therefore, in order to obtain interactions of HNLs, inside the SM interaction terms, one can replace $\nu_\alpha \rightarrow \sum_I U_{\alpha I} N_I$. In the minimal HNL models, both the production and decay of an HNL are controlled by the elements of matrix U .

PBC has defined the following benchmark cases:

- *BC6, Single HNL, electron dominance*: assuming one Majorana HNL state N , and predominantly mixing with electron neutrinos, all production and decay can be determined as function of parameter space $(m_N, |U_e|^2)$.
- *BC7, Single HNL, muon dominance*: assuming one Majorana HNL state N , and predominantly mixing with muon neutrinos, all production and decay can be determined as function of parameter space $(m_N, |U_\mu|^2)$.
- *BC8, Single HNL, tau dominance*: one Majorana HNL state with predominantly mixing to tau neutrinos. Parameter space is $(m_N, |U_\tau|^2)$.

These are representative cases which do not exhaust all possibilities. Multiple HNL states, and presence of comparable couplings to different flavors can be even better motivated than the above choices. The current choice of benchmark cases is motivated by simplicity.

2.1.4. Axion portal models. QCD axions are an important idea in particle physics [35–37] that allows for a natural solution to the strong CP problem, or apparent lack of CP violation in strong interactions. Current QCD axion models are restricted to the sub-eV range of axions. However, a generalization of the minimal model to ALPs can be made [27]. Taking a single pseudoscalar field a one can write a set of its couplings to photons, quarks, leptons and other fields of the SM. In principle, the set of possible couplings is very large and in this study we consider only the flavor-diagonal subset

$$\begin{aligned} \mathcal{L}_{\text{axion}} = & \mathcal{L}_{\text{SM}} + \mathcal{L}_{\text{DS}} + \frac{a}{4f_\gamma} F_{\mu\nu} \tilde{F}_{\mu\nu} + \frac{a}{4f_G} \text{Tr} G_{\mu\nu} \tilde{G}_{\mu\nu} \\ & + \frac{\partial_\mu a}{f_l} \sum_\alpha \bar{l}_\alpha \gamma_\mu \gamma_5 l_\alpha + \frac{\partial_\mu a}{f_q} \sum_\beta \bar{q}_\beta \gamma_\mu \gamma_5 q_\beta. \end{aligned} \quad (2.7)$$

The DS Lagrangian may contain new states that provide a UV completion to this model (for the case of the QCD axion they are called the Peccei–Quinn sector). All of these interactions do not lead to large additive renormalization of m_a , making this model technically natural. Note, however, that the coupling to gluons does lead to a non-perturbative contribution to m_a .

The PBC proposals have considered the following benchmark cases:

- *BC9, photon dominance:* assuming a single ALP state a , and predominant coupling to photons, all phenomenology (production, decay, oscillation in the magnetic field) can be determined as functions on $\{m_a, g_{a\gamma\gamma}\}$ parameter space, where $g_{a\gamma\gamma} = f_\gamma^{-1}$ notation is used.
- *BC10, fermion dominance:* assuming a single ALP state a , and predominant coupling to fermions, all phenomenology (production and decay) can be determined as functions on $\{m_a, f_l^{-1}, f_q^{-1}\}$. Furthermore, for the sake of simplicity, we take $f_q = f_l$.
- *BC11, gluon dominance:* this case assumes an ALP coupled to gluons. The parameter space is $\{m_a, f_G^{-1}\}$. Notice that in this case the limit of $m_a < m_{a,\text{QCD}}|_{f_a=f_G}$ is unnatural as it requires fine tuning and therefore is less motivated.

The ALP portals, *BC9 – BC11*, are *effective* interactions, and would typically require UV completion at or below the f_i scales. This is fundamentally different from vector, scalar and neutrino portals that do not require external UV completion. Moreover, the renormalization group (RG) evolution is capable of inducing new couplings. All the sensitivity plots shown in section 7 assume a cut-off scale of $\Lambda = 1$ TeV. Details about approximations and assumptions assumed in computing sensitivities for the BC10 and BC11 cases are reported in appendices A and B.

3. Experiments proposed in the PBC context

The PBC–BSM working group has considered about 18 different initiatives which aim at exploiting the CERN accelerator complex and scientific infrastructure with a new, broad and compelling physics program that complement the quest of NP at the TeV scale performed at the LHC or other initiatives in the world. The proposals have been classified in terms of their sensitivity to NP in a given mass range, as reported below.

1. Sub-eV mass range

Axions and ALPs with gluon- and photon-coupling can have masses ranging from 10^{-22} eV³⁵ to 10^9 eV.

Axions and ALPs that are DM and feature a gluon coupling, with masses in the sub-eV mass range can generate a non-zero oscillating electric dipole moment (oEDM) in protons. The PBC proposal related to the study of oEDMs in protons is *CPEDM*.

The search for axions and ALPs with photon-coupling and mass in the sub-eV range comprises a plethora of different experimental techniques and experiments as *haloscopes*, *solar helioscopes* and *pure laboratory experiments* among which, for example, regeneration or *light-shining-through a wall* (LSW) experiments. Two experiments have been proposed in the framework of the PBC–BSM study: the *International AXion Observatory (IAXO)* aims at searching axions/ALPs coming from the Sun by using the axion-photon coupling, and the *JURA* experiment, considered as an upgrade of the ALPS II experiment, currently under construction at DESY, and exploiting the LSW technique.

2. MeV–GeV mass range

HNLs, ALPs, light dark matter (LDM) and corresponding light mediators (dark photons, dark scalars, etc) could have masses in the MeV–GeV range and can be searched for using the interactions of proton, electron and muon beams available (or proposed) at the PS and SPS accelerator complex and at the LHC interaction points. Ten proposals discussed in the PBC–BSM working group are aiming to search for hidden sector physics in the MeV–GeV range and are classified in terms of the accelerator complex they want to exploit:

- *PS extracted beam lines: REDTOP.*
- *SPS extracted beam lines: NA62⁺⁺ or NA62 in dump mode* at the K12 line currently used by the NA62 experiment; *NA64⁺⁺(e)* and *NA64⁺⁺(μ)* proposed at the existing H4 and M2 lines of the CERN SPS; *light dark matter eXperiment* at a proposed slow-extracted primary electrons line at the SPS; *SHiP* at the proposed *beam dump facility (BDF)* at the SPS, and *AWAKE* at the IP4 site of the SPS.
- *LHC interaction points: MATHUSLA, FASER, MilliQan, and CODEX-b* at the ATLAS/CMS, ATLAS, CMS and LHCb interaction points of the LHC, respectively. These experiments probe New Physics from below the MeV to the TeV scale, but their physics case is beyond the scope of this document. We focus on comparing their reach to NP in the MeV–GeV range to the other proposals at the PS and SPS lines.

3. TeV mass range

The search for new particles at a very high mass scale is traditionally performed by studying clean and very rare flavor processes, as for example $K^+ \rightarrow \pi^+ \nu \bar{\nu}$ and $K_L \rightarrow \pi^0 \nu \bar{\nu}$ rare decays or lepton-flavor-violating (LFV) processes as $\tau \rightarrow 3\mu$. The *KLEVER* project aims at measuring the branching fraction of the very rare and clean decay $K_L \rightarrow \pi^0 \nu \bar{\nu}$ using an upgraded P42/K12 line at the SPS; *TauFV* is a fixed-target experiment proposed at the BDF to search for the LFV decay $\tau \rightarrow 3\mu$ and other LFV τ decays produced in the interactions of a primary high-energy proton beam with an active target. Proposals searching for permanent EDMs in protons, deuterons or charmed hadrons, can also probe NP at the $\mathcal{O}(100)$ TeV scale, if there are new sources of CP violation. PBC proposals aiming at studying permanent EDM in proton and deuteron, and EDMs/MDMs in charmed and strange hadrons are *CPEDM* and *LHC-FT*, respectively.

Table 1 summarizes the projects presented in the PBC–BSM study group framework divided on the basis of their sensitivity to NP at a given mass scale, along with

³⁵ This case applies only if the axion is DM.

Table 1. Projects considered in the PBC–BSM working group categorized in terms of their sensitivity to a set of benchmark models in a given mass range. The characteristics of the required beam lines, whenever applicable, are also displayed.

Proposal	Main physics cases	Beam line	Beam type	Beam yield
Sub-eV mass range:				
IAXO	Axions/ALPs (photon coupling)	—	Axions from sun	—
JURA	Axions/ALPs (photon coupling)	Laboratory	eV photons	—
CPEDM	p, d oEDMs	EDM ring	p, d	—
	axions/ALPs (gluon coupling)		p, d	—
LHC-FT	Charmed hadrons oEDMs	LHCb IP	7 TeV p	—
MeV–GeV mass range:				
SHiP	ALPs, dark photons, dark scalars	BDF, SPS	400 GeV p	$2 \times 10^{20}/5$ years
NA62 ⁺⁺	LDM, HNLs, lepto-phobic DM, ALPs, dark photons, dark scalars, HNLs	K12, SPS	400 GeV p	up to $3 \times 10^{18}/\text{year}$
NA64 ⁺⁺	ALPs, dark photons, dark scalars, LDM $+ L_\mu - L_\tau$	H4, SPS	100 GeV e^-	5×10^{12} eot/year
	$+ CP, CPT, \text{leptophobic DM}$	M2, SPS	160 GeV μ	$10^{12} - 10^{13}$ mot/year
LDMX	Dark photon, LDM, ALPs	H2-H8, T9	~ 40 GeV π, K, p	$5 \times 10^{12}/\text{year}$
AWAKE/NA64	Dark photon	eSPS	8 (SLAC) -16 (eSPS) GeV e^-	$10^{16} - 10^{18}$ eot/year
REDTOP	Dark photon, dark scalar, ALPs	AWAKE beam	30-50 GeV e^-	10^{16} eot/year
MATHUSLA200	Weak-scale LLPs, dark scalar, Dark photon, ALPs, HNLs	CERN PS	1.8 or 3.5 GeV	10^{17} pot
FASER	Dark photon, dark scalar, ALPs, HNLs, $B - L$ gauge bosons	ATLAS or CMS IP	14 TeV p	3000 fb^{-1}
MilliQan	Dark photon, dark scalar, ALPs, HNLs, $B - L$ gauge bosons	ATLAS IP	14 TeV p	3000 fb^{-1}
MilliQan	Milli charge	CMS IP	14 TeV p	$300-3000 \text{ fb}^{-1}$
CODEX-b	Dark scalar, HNLs, ALPs, LDM, Higgs decays	LHCb IP	14 TeV p	300 fb^{-1}
>> TeV mass range:				
KLEVER	$K_L \rightarrow \pi^0 \nu \bar{\nu}$	P42/K12	400 GeV p	5×10^{19} pot /5 years

Table 1. (Continued.)

Proposal	Main physics cases	Beam line	Beam type	Beam yield
TauFV	LFV τ decays	BDF	400 GeV p	$\mathcal{O}(2\%)$ of the BDF proton yield
CPEDM	p, d EDMs axions/ALPs (gluon coupling)	EDM ring	p, d p, d	— —
LHC-FT	Charmed hadrons MDMs, EDMs	LHCb IP	7 TeV p	—

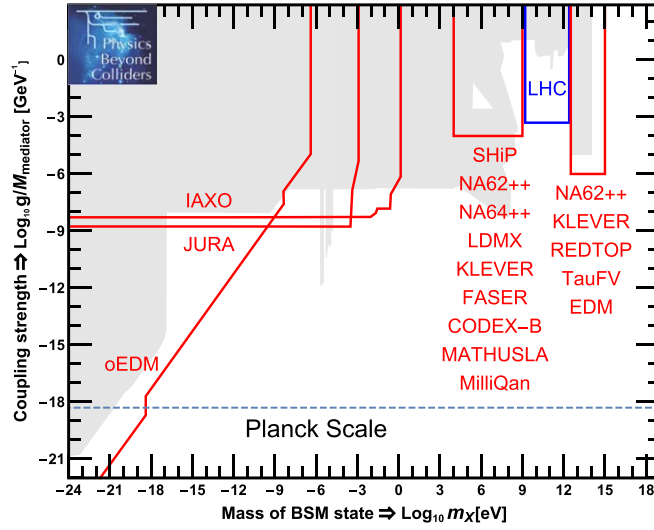


Figure 1. Schematic overview of the BSM landscape, based on a selection of specific models, with a rough outline of the areas targeted by the PBC experiments. The x -axis corresponds to the mass m_X of the lightest BSM state, and the y -axis to the scale of the effective new interaction $f = M_{\text{Mediator}}/g$, where M_{Mediator} is the mass of a heavy mediator and g its (dimensionless) coupling constant to the Standard Model. The gray shaded area outlines the currently excluded regions for a class of models corresponding to the benchmarks BC9 and BC11 (see [27, 38, 39]).

their main physics cases and the characteristics of the required beam, whenever is applicable.

The physics reach of the PBC BSM projects is schematically shown in figure 1 in a generic plane of coupling versus mass, along with the parameter space currently explored at the LHC: the PBC–BSM projects will be able to explore a large variety of ranges of NP couplings and masses using very different experimental techniques and are fully complementary to the exploration currently performed at the high energy frontier and at DM direct detection experiments.

4. Proposals sensitive to new physics in the sub-eV mass range

Axions and ALPs have been searched for in dedicated experiments since their proposal, however to date no detection has been reported and only a fraction of the available parameter space has been probed. Indeed, nowadays there are experiments or proposals that study masses starting from the lightest possible value of 10^{-22} eV up to several GeV. The apparatuses employed in such a search are highly complementary in the mass reach and use detection techniques that are not common in HEP, taking advantage for example of solid state physics, optical and microwave spectroscopy, resonant microwave cavities, precision force measuring system, highly sensitive optical polarimetry.

A relevant point which characterizes the detector is the choice of the axion source: in fact, due to the extremely weak coupling with ordinary matter, axion production in a laboratory will be suffering from extremely small fluxes compared with possible natural sources like the Sun or the Big Bang.

Table 2. Comparison between the main techniques employed in the search for axion like particles in the sub eV range.

Category	Haloscopes	Helioscopes	Lab experiments
Physics reach	ALPs and QCD axion	ALPs and QCD axion	ALPs
Model dependence	Strong	Weak	Absent
Ranges	Resonance detector	Wide band	Wide band
Flux	Very high	High	Low
Typical photon	Microwave	X-rays	Optical

Different experiments can probe different couplings, but the majority of the running or proposed experiment are actually exploiting the coupling of the axion to two photons through the Primakoff effect.

The following categories can then be identified:

(1) *Dark matter haloscopes*

Taking advantage of the large occupation number for the axion in the local DM halo, an axion haloscope searches for the reconversion of DM axions into visible photons inside a magnetic field region. A typical detector is a resonant microwave cavity placed inside a strong magnetic field [40]. The signal would be a power excess in the cavity output when the cavity resonant frequency matches the axion mass. Current searches are limited in range to a few μeV masses, but several new proposals are on the way.

(2) *Solar helioscopes*

Axions and ALPs can be efficiently produced in the solar interior via different reactions: Primakoff conversion of plasma photons in the electrostatic field of a charged particle, thus exploiting the axion to photon coupling; axio-recombination, Bremsstrahlung and Compton are other possible channels based on the axion electron coupling. Solar axions escape from the Sun and can be detected in an earth laboratory by their conversion into photons (x-rays) in a strong electromagnetic field.

(3) *Pure laboratory experiment*

Laboratory searches for axions can be essentially divided into three categories: polarization experiments [41], regeneration experiments (light-shining-through wall—LSW) [42] and long range forces experiments [43]. The key advantage for these apparatuses is the model independence of the detection scheme. However, at present fluxes are so low that only ALPs can be probed. Typically apparatuses feature an axion source, for example a powerful laser traversing a dipolar magnetic field, and an axion reconverter placed after a barrier, again based on a static electromagnetic field. Reconverted photons can be detected with ultra low background detectors.

Table 2 compares the physics reach, the model dependency, the mass range of a possible axion or ALP particle, the intensity of the expected flux and the wavelength of the detected photons for three categories of experiments sensitive to axions/ALPs with photon-coupling.

4.1. Solar axions helioscopes: IAXO

Brief presentation, unique features. The IAXO is a new generation axion helioscope [44], aiming at the detection of solar axions with sensitivities to the axion-photon coupling $g_{a\gamma}$ down to a few 10^{-12}GeV^{-1} , a factor of 20 better than the current best limit from CAST (a factor of more than 10^4 improvement in signal-to-noise ratio). Its physics reach is highly

complementary to all other initiatives in the field, with unparalleled sensitivity to highly motivated parts of the axion parameter space that no other experimental technique can probe. The proposed baseline configuration of IAXO includes a large-scale superconducting multi-bore magnet, specifically built for axion physics, together with the extensive use of x-ray focusing based on cost-effective slumped glass optics and ultra-low background x-ray detectors. The unique physics potential of IAXO can be summarized by the following statements:

- (1) IAXO follows the only proposed technique able to probe a large fraction of QCD axion models in the meV to eV mass band. This region is the only one where astrophysical, cosmological (DM) and theoretical (strong CP problem) motivations overlap.
- (2) IAXO will fully probe the ALP region invoked to solve the transparency anomaly, and will largely probe the axion region invoked to solve observed stellar cooling anomalies.
- (3) IAXO will partially explore viable QCD axion DM models, and largely explore a subset of predictive ALP models (dubbed *ALP miracle*) recently studied to simultaneously solve both DM and inflation.
- (4) The above sensitivity goals do not depend on the hypothesis of axion being the DM, i.e. in case of non-detection, IAXO will robustly exclude the corresponding range of parameters for the axion/ALP.
- (5) IAXO relies on detection concepts that have been tested in the CAST experiment at CERN. Risks associated with the scaling up of the different subsystems will be mitigated by the realization of small scale prototype BabyIAXO.
- (6) IAXO will also constitute a generic infrastructure for axion/ALP physics with potential for additional search strategies (e.g. the option of implementing RF cavities to search for DM axions).

Key requirements. The main element of IAXO is a new dedicated large-scale magnet, designed to maximize the helioscope figure of merit. The IAXO magnet will be a superconducting magnet following a large multi-bore toroidal configuration, to efficiently produce an intense magnetic field over a large volume. The design is inspired by the ATLAS barrel and end-cap toroids, the largest superconducting toroids ever built and presently in operation at CERN. Indeed the experience of CERN in the design, construction and operation of large superconducting magnets is crucial for the project. IAXO will also make extensive use of novel detection concepts pioneered at a small scale in CAST. This includes x-ray focussing and low background detectors. The former relies on the fact that, at grazing incident angles, it is possible to realize x-ray mirrors with high reflectivity. IAXO envisions newly-built optics similar to those used onboard NASA's NuSTAR satellite mission, but optimized for the energies of the solar axion spectrum. Each of the eight ~ 60 cm diameter magnet bores will be equipped with such optics. For BabyIAXO, using existing optics from the ESA's XMM mission is being considered. At the focal plane of each of the optics, IAXO will have low-background x-ray detectors. Several technologies are under consideration, but the most developed one are small gaseous chambers read by pixelised microbulk Micromegas planes. They involve low-background techniques typically developed in underground laboratories, like the use of radiopure detector components, appropriate shielding, and the use of offline discrimination algorithms. Alternative or additional x-ray detection technologies are also considered for IAXO, like GridPix detectors, magnetic metallic calorimeters, transition edge sensors, or silicon drift detectors. All of them show promising prospects to outperform the baseline Micromegas detectors in aspects like energy threshold or resolution, which are of interest, for example, to search for solar axions via the axion-electron coupling, a process featuring both lower energies than the standard Primakoff ones, and monochromatic peaks in the spectrum.

Open questions, feasibility studies. As a first step the Collaboration pursues the construction of BabyIAXO, an intermediate scale experimental infrastructure. BabyIAXO will test magnet, optics and detectors at a technically representative scale for the full IAXO, and, at the same time, it will be operated and will take data as a fully-fledged helioscope experiment, with sensitivity beyond CAST and potential for discovery.

Status, plans and collaboration. After a few years of preparatory phase, project socialization and interaction with funding bodies, the IAXO Collaboration was eventually formalized in July 2017. A Collaboration agreement document (bylaws) was signed by 17 institutions from Croatia, France, Germany, Italy, Russia, Spain, South Africa, USA, as well as CERN. They include about 75 physicists at the moment. It is likely that this list will increase with new members in the near future. A Collaboration management is already defined and actively implementing steps towards the BabyIAXO design and construction. The experiment will likely be sited at DESY, and it is expected to be built in 2–3 years, entering into data taking in 3–4 years.

The Collaboration already nicely encompasses all the know-how to cover BabyIAXO needs, and therefore a distribution of responsibilities in the construction of the experiment exists already. The magnet of (Baby)IAXO is of a size and field strength comparable to that of large detector magnets typically built in high energy physics. For this IAXO relies on the unique expertise of CERN in large superconducting magnets. The CERN magnet detector group has led all magnet design work so far in the IAXO CDR. The technical design of the BabyIAXO magnet, for which CERN has allocated one Applied Fellow, has started in January 2018. Further CERN participation is expected in terms of, at the least, allocation of expert personnel to oversee the construction of the magnet, as well as the use of existing CERN infrastructure. Other groups with magnet expertise in the Collaboration are CEA-Irfu and INR. The groups of LLNL, MIT and INAF are experts in the development and construction of x-ray optics, in particular in the technology chosen for the IAXO optics. Detector expertise exists in many of the Collaboration groups, encompassing the technologies mentioned above. Experience in general engineering, large infrastructure operation and management is present in several groups and in particular in centers like CERN or DESY. Many of the groups have experience in axion phenomenology and the connection with experiment, and more specifically experience with running the CAST experiment. Following these guidelines the Collaboration board is in the process of defining a Collaboration agreement (MoU) to organize the distribution of efforts and commitments among the collaborating institutes.

IAXO has also submitted a separate document³⁶ to be considered in the update of the European Strategy for Particle Physics (ESPP).

4.2. Laboratory experiments: JURA

Brief presentation, unique features. The pioneer LSW experiment was conducted in Brookhaven by the BFRT Collaboration [45], and the two most recent results are those of the experiments ALPS [46] and OSQAR [47]. ALPS is DESY based and used a decommissioned HERA magnet. ALPS is currently performing a major improvement to phase II, where a set of 10 + 10 HERA magnets will be coupled to two 100 m long Fabry–Perot cavities. ALPS II [48] will in fact take advantage of a resonant regeneration apparatus [49, 50], thus expecting a major improvement of the current limit on LSW experiment given by OSQAR. ALPS II will

³⁶ *The IAXO: case, status and plans. Input to the ESPP*, <https://indico.cern.ch/event/765096/contributions>.

represent the current state of the art LSW experiment, and for this reason its activities are monitored with interest by the PBC since they will give key elements to judge the proposal Joint Undertaking on the Research for ALPs (JURA).

ALPS II aims to improve the sensitivity on ALP-photon couplings by three orders of magnitude compared to existing exclusion limits from laboratory experiments in the sub-meV mass region. ALPS II will inject a 30 W laser field into the 100 m long production cavity (PC) which is immersed in a 5.3 T magnetic field. The circulating power inside the PC is expected to reach 150 kW. The 100 m long regeneration cavity (RC) on the other side of the wall will have a finesse of 120 000. The RC is also placed inside a similar 5.3 T magnetic field. The employed two different photon detection concepts are expected to be able to measure fields with a photon rate as low as $\sim 10^{-4}$ photons per second. A next generation experiment for a LSW techniques will mainly rely on improved magnetic field structure, since from the optical part only limited improvements seems to be feasible. The project *JURA* basically combines the optics and detector development at ALPS II with dipole magnets for future accelerators under development at CERN.

The sensitivity of ALPS II in the search for ALPs is mainly limited by the magnetic field strength and the aperture (which limits the length of the cavities) of the HERA dipole magnets. *JURA* assumes the usage of magnets under development for an energy upgrade of LHC or a future FCC.

Key requirements. Several variants of these future magnets are of interest to the *JURA* initiative. In one of them the inner high temperature superconductor part would be omitted, so that magnets with a field of about 13 T and 100 mm aperture would be available (the modified HERA dipoles provide 5.3 T and 50 mm). In table 3 experimental parameters of ALPS II and this option of *JURA* are compared. They follow from assuming the installation of optical cavities inside the magnet bore in a (nearly) confocal configuration.

Open questions, feasibility studies. The project *JURA* is a long term development, for which the experiment ALPS II can be considered as a feasibility study, especially for the resonant regeneration scheme. There are in fact some open questions: for example, the possibility of running mutually resonant cavities of very high finesses for distances of the order of several hundreds meters is still open. The linewidth of such cavities is in fact of the order of a few Hz, about one order of magnitude smaller than current state of the art. Another issue is the detector noise, however recent developments using coherent detection schemes seem to be very promising. Of course, the development of new magnets at CERN is not related to *JURA*, and thus this project will just rely on other projects' results.

JURA in the abovementioned configuration would surpass IAXO by about a factor of 2 in the photon-ALP coupling. It would allow to determine the photon-coupling of a lightweight ALP discovered by IAXO unambiguously and in a model-independent fashion or probe a large fraction of the IAXO parameter space model independently in case IAXO does not see anything new.

Status, plans and collaboration. ALPS II is currently being constructed at DESY in the HERA tunnels. The tunnels and hall are currently being cleared and magnet installation will begin in 2019. The optics installation will begin at the end of 2019 and first data run is scheduled for 2020. About two years of operation is then expected. The time schedule for *JURA* is foreseen to be for a 2024–2026 starting time by using a LHC dipole magnet in a first phase. At the moment there is no real Collaboration and *JURA* might be considered an idea for a possible experiment which should grow within the years to come.

Table 3. Comparison of experimental parameters of ALPS II at DESY and the JURA proposal.

Parameter	Sensitivity	ALPS II	JURA	Rel. sensitivity JURA/ALPS II
Magnet aperture		50 mm	100 mm	
Magnetic field amplitude B	$g_{a\gamma} \propto B^{-1}$	5.3 T	13 T	2.5
Magnetic field length L	$g_{a\gamma} \propto L^{-1}$	189 m	960 m	5.1
Effective laser power P	$g_{a\gamma} \propto P^{-1/4}$	0.15 MW	2.5 MW	2.0
Regeneration build up (finesse F)	$g_{a\gamma} \propto F^{-1/4}$	40 k	100 k	1.3
Detector noise rate R	$g_{a\gamma} \propto R^{1/8}$	10^{-4} Hz	10^{-6} Hz	1.8
Total gain				56

5. Proposals sensitive to new physics in the MeV–GeV mass range

Accelerator experiments are a powerful tool to probe feebly-interacting particles with masses in the MeV–GeV region. They can be produced directly, but also in the decay of beauty, charm and strange hadrons produced in the interactions of a proton, electron or muon beam with a dump or an active target. Usually, their couplings to SM particles are very suppressed leading to exceptionally low expected production rates. Therefore high-intensity beams are required to improve over the current results.

Importantly such accelerator experiments are a unique tool to test models with light dark matter (LDM) in the MeV–GeV range, under the hypothesis that DM annihilates directly to SM particles via new forces/new dark sector mediators. The advantage of accelerator experiments is that the DM is produced in a relativistic regime, and therefore its abundance depends very weakly on the assumptions about its specific nature, while the rates can be predicted from thermal freeze-out.

In addition, accelerator based experiments can probe the existence of HNLs with masses between 100 MeV and $\mathcal{O}(100)$ GeV in a range of couplings phenomenologically motivated and challenge the see-saw mechanism in the freeze-in regime.

More general hidden sector physics in the MeV–GeV mass range can also be studied at fixed-target, dump and colliders experiments. The focus of this document is on initiatives that want to exploit the CERN accelerator complex beyond the LHC, as e.g. extracted beam lines at the PS and SPS injectors, however proposals designed to be operated at or near the LHC interaction points have been included in the study to provide a complete landscape scenario of the physics reach at CERN achievable in the next 10–20 years. Several experimental approaches can be pursued to search for HNLs, ALPs, LDM and corresponding light mediators, depending on the characteristics of the available beam line and the proposed experiment. These can be classified as follows:

(1) *Detection of visible decays:*

HNLs, ALPs and LDM mediators are very weakly coupled to the SM particles and can therefore decay to visible final states with a probability that depends on the model and scenario. The detection of visible final state is a technique mostly used in beam-dump experiments and in collider experiments (Belle, ATLAS, CMS and LHCb), where typical

signatures are expected to show up as narrow resonances over an irreducible background. This approach is of particular importance when the light mediator has a mass which is less than $2m_\chi$, being m_χ the mass of the LDM, in which case the mediator can decay only to visible final states.

(2) *Direct detection of LDM scattering in the detector material:*

LDM produced in reactions of electrons and/or protons with a dump can travel across the dump and be detected via the scattering with electrons and/or protons of a heavy material. This technique has the advantage of probing directly the DM production processes but requires a large proton/electron yield to compensate the small scattering probability. Moreover the signature is very similar to that produced by neutrino interactions. This is a limiting factor unless it is possible to use a bunched beam and time-of-flight techniques.

(3) *Missing momentum/energy techniques:*

Invisible particles (as LDM or HNLs, ALPs, and light mediators with very long lifetimes) can be detected in fixed-target reactions as, for example, $e^- + Z \rightarrow e^- + Z + A'$, with Z the atomic number of the nucleus and $A' \rightarrow \chi\bar{\chi}$, by measuring the missing momentum or missing energy carried away from the escaping invisible particle(s). Main challenge of this approach is the very high background rejection that must be achieved, that relies heavily on the detector hermeticity and, in some cases, on the exact knowledge of the initial and final state kinematics. This technique guarantees an intrinsic better sensitivity for the same luminosity than the technique based on the detection of HNLs, ALPs and light mediator going to visible decays or based on the direct detection of LDM scattering in the detector, as it is independent of the probability of decays or scattering. However it is much more model-dependent and more challenging as far as the background is concerned. Moreover, if the mediator decays promptly or with a short lifetime to detected SM particles, these techniques have no sensitivity.

(4) *Missing mass technique:*

This technique is mostly used to detect invisible particles (as DM candidates) in reactions with a well-known initial state, as for example $e^+ + e^- \rightarrow \gamma + A'$ with $A' \rightarrow \chi\bar{\chi}$. This technique requires detectors with very good hermeticity that allow to detect all the other particles in the final state. Characteristic signature of this reaction is the presence of a narrow resonance emerging over a smooth background in the distribution of the missing mass. Main limitation of this technique is the knowledge of the background arising from processes in which particles in the final state escape the apparatus without being detected.

The timescale of the PBC–BSM projects that will explore the MeV–GeV mass range is shown in figure 2 and compared with other similar initiatives in the world. A concise description of each proposal along with beam request, key requirements for the detectors, open questions and feasibility studies, is shown in the following section, which we order along the required CERN beam lines.

5.1. Proposals at the PS beam lines

5.1.1. REDTOP

Brief presentation, unique features. REDTOP is a fixed target experiment searching for physics BSM primarily in ultra-rare decays of the η and η' mesons produced in the interactions of the high-intensity, low-energy (few GeV) proton beam with a target. REDTOP

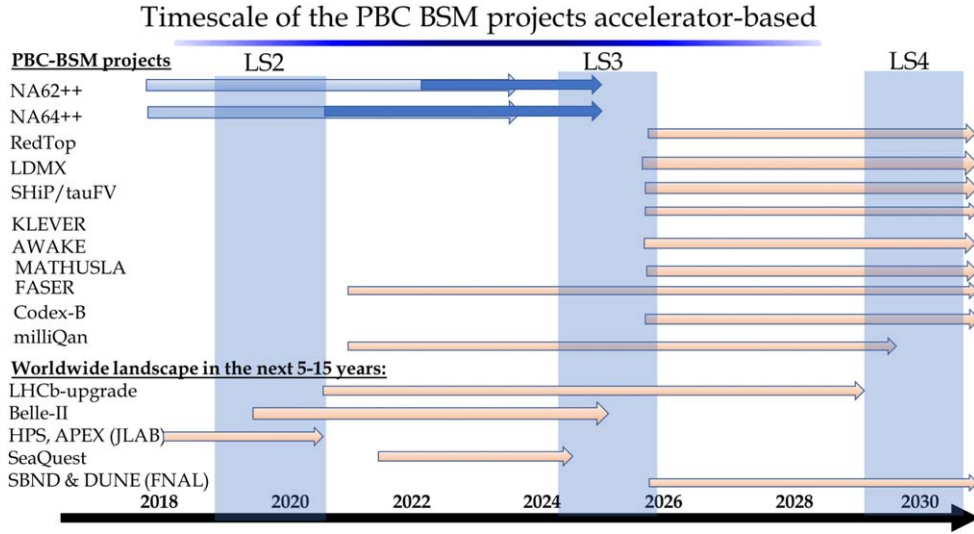


Figure 2. Tentative timescale for PBC projects exploring the MeV–GeV mass range compared to other similar initiatives in the world that could compete on the same physics cases.

was originally proposed at FNAL³⁷ but recently expressed interest to be hosted at CERN. The experiment requires to collect approximately 10^{13} η and 10^{11} η' mesons produced in the interactions of 10^{17} protons with energy in the range 1.7–1.9 GeV (for η production) and about the same number of protons with an energy of about 3.5 GeV (for η' production). A fast detector, blind to most hadrons and baryons produced from the inelastic scattering of the beam, surrounds the target systems and covers about 98% of the solid angle.

The η and η' mesons are quite unique in nature. The additive quantum numbers for these particles are all zero, the same as for the vacuum and the Higgs, with the exception of their negative parity, leading to the suppression of SM decays. An attractive feature of the η and η' mesons is that they are flavor-neutral, so its SM C - and CP -violating interactions are known to be very small.

Thus, rare η/η' decays are a promising place to look for BSM effects. They complement analogous searches performed with K and B mesons with the unique feature that their decays are flavor-conserving. Such decays, therefore, can provide distinct insights into the limits of conservation laws, and open unique doors to new BSM models at branching fraction sensitivity levels typically below 10^{-9} . In contrast, current experimental upper limits for η decays are many orders of magnitude larger, so η decays have not been competitive with rare decays of flavored mesons so far.

Rare η/η' decays can be also exploited to search for dark photons as, e.g. in the process $\eta \rightarrow \gamma A'$, $A' \rightarrow \mu^+ \mu^-$. ALPs and Dark Photons could be radiated from the beam through multiple processes [51] (Primakoff effect, Drell–Yan, proton bremsstrahlung, etc).

Beam, beam time. In order to generate 10^{13} η mesons on the 10 foils target systems of the experiment, approximately 10^{17} protons with energy in the range 1.7–1.9 GeV are required. The same number of protons with an energy of about 3.5 GeV would generate approximately

³⁷ http://redtop.fnal.gov/wp-content/uploads/2016/02/REDTOP_EOI_v10.pdf.

10^{11} η' mesons. These yields give enough sensitivity for exploring physics BSM as they correspond to a sample of mesons a factor about 10^4 larger than the existing world sample. A near-Continuous Wave (cw) beam is necessary in order to limit the pile-up of events and to suppress the combinatorial background. Only about 0.5% of the beam interacts inelastically with the target systems. Consequently, the power dissipated in the latter corresponds to only 15 mW total (1.5 mW/target foil) for a 1.8 GeV proton beam and 24 mW total (2.4 mW/target foil) for a 3.5 GeV proton beam. The remaining (99.5%) of the beam is unaffected and it could be deviated toward other experimental apparatuses downstream of REDTOP.

The Collaboration aims to integrate about 10^{17} pot at 1.8 GeV (η' -factory) and 10^{17} pot at 3.5 GeV (η' - factory). These yields could be provided in one or multiple years, depending on the availability of such beam at CERN.

Key requirements for detector. The REDTOP detector is being designed to sustain a maximum inelastic interaction rate of about 5×10^8 evt s^{-1} . These capabilities exceed the event rate expected at CERN by about one order of magnitude and could portend to running the detector at future, high-intensity proton facility (for example, PIP-II at Fermilab). In order to sustain such an event rate, the detector must be: (a) very fast; (b) blind to baryons. The latter are produced within the target with a multiplicity of about 5/event and could easily pile-up if detected. On the other hand, since BSM physics is being searched for mostly in channels with charged leptons in the final state, the detector must have good efficiency to electrons and muons and excellent PID capabilities. The above requirements are fulfilled by adopting an Optical-TPC [52] for the tracking systems and a high-granularity, dual-readout ADRIANO calorimeter [53].

A fiber tracker, with identical features as that under construction for the LHCb experiment [54], has been recently included in the detector layout.

The schematic layout of the detector is shown in figure 3.

Open questions, feasibility studies. A few open questions exist, at this stage, for REDTOP. The largest unknown is related to the available accelerator complex and the experimental hall where the experiment could be operated. Both LEAR and Booster were considered as options for REDTOP but have been rejected. A possibility could be to use the 24 GeV, T8 proton beam line that currently serves CHARM and IRRAD facilities with a maximum intensity of 6.5×10^{11} protons-per-pulse (ppp) over 0.4 s. REDTOP would require a lower kinetic energy (2–3 GeV) and a much longer flat-top. No showstoppers have been identified but machine studies would be required and, in any case, the impact on the rest of the CERN physics program would be significant.

The second unknown is related to the Detector R&D still necessary to complete the design of the apparatus. In fact, while a multi-year R&D effort has been in place for ADRIANO and for the fiber tracker, very little has been done for the moment towards the development of an optical-TPC (O-TPC) prototype. The latter is conditional to the availability of R&D funding which, at present, is still not in place. The Collaboration is meanwhile considering, to launch a simulation campaign to understand if alternative, more conventional solutions could be found that can sustain the event rate expected at REDTOP.

Timeline. The Collaboration has estimated that about two years of detector R&D are necessary (dominated by the R&D on the O-TPC) and about 1 year for the construction and installation of the detector. The solenoid and the lead-glass required for the Cerenkov component of ADRIANO are readily available from INFN while the fibers for the Tracker and for the Scintillating component of ADRIANO are commercially available with short lead

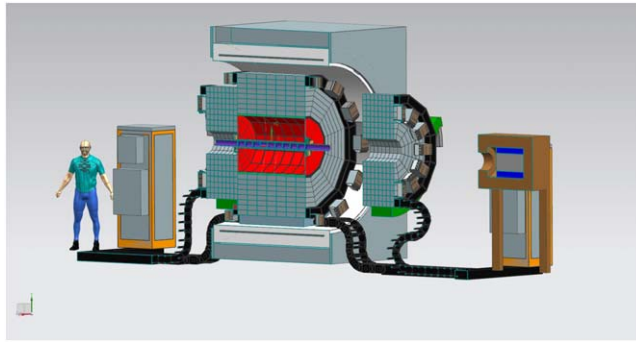


Figure 3. Schematic layout of REDTOP detector.

times. The low cost, large area photo-detectors required for the O-TPC are becoming commercially available at Incom³⁸ and the production of about 100 units for REDTOP seems not to represent a problem for the company.

Under the assumption that the funding for the Optical-TPC is available starting in 2020, REDTOP would be ready to install in 2022 and run in 2023, one year before LS3. The proposed schedule is very aggressive but considered feasible by the Collaboration. However, the PBC coordinators decided to have a conservative approach and consider REDTOP a proposal for Run 4. A full proposal will be presented to the SPSC immediately after the conclusion of the ESPP process (mid-2020). A coincide document³⁹ has been submitted for the next update of the ESPP.

Status of the Collaboration. REDTOP Collaboration counts, presently, 23 institutions and 67 collaborators, as reported here: <http://redtop.fnal.gov/collaboration/>.

5.2. Proposals at the SPS beam lines

5.2.1. NA64⁺⁺

Brief presentation, unique features. The NA64 is a hermetic general purpose detector to search for dark sector particles in missing energy events from high-energy (~ 100 GeV) electrons, muons, and hadrons scattering off nuclei in an active dump. A high energy electron beam, for example, can be used to produce a vector mediator, e.g. dark photon A' , via the reaction $e^- + Z \rightarrow e^- + Z + A'$ $A' \rightarrow \chi\bar{\chi}$ where Z is the atomic number of the nuclei and A' is produced via kinetic mixing with bremsstrahlung photons and then decay promptly and invisibly into light (sub-GeV) DM particles [55, 56] in a hermetic detector [57, 58]. The signature of possible A' would appear as a single isolated electromagnetic shower in the active dump with detectable energy accompanied by missing energy in the rest of the detector.

The advantage of this technique compared to traditional beam dump experiments is that the sensitivity to A' scales as ϵ^2 instead of ϵ^4 , ϵ being the kinetic mixing strength, as the A' is required to be produced but not detected in the far apparatus. Another advantage of the NA64

³⁸ Incom Inc., Charlton, MA (US).

³⁹ REDTOP: Rare Eta Decays with a TPC for Optical Photons, <https://indico.cern.ch/event/765096/contributions>.

approach is the high energy of the incident beam, that boosts the center-of-mass system relative to the laboratory system: this results in an enhanced hermeticity of the detector which provides a nearly full solid angle coverage.

The missing energy technique can be used also with high energy muon and hadron beams. The reaction of muon scattering off nuclei $\mu + Z \rightarrow \mu + Z + Z'_\mu$ is sensitive to dark sector particles predominantly coupled to muons [59, 60], and, as such, is fully complementary to the dark photon searches. This search is quite appealing and very timely in particular in connection to the $g_\mu - 2$ anomaly [61], and will be competing with another proposal at Fermilab [62] and elsewhere (see, e.g. [63] for a review). A Z_μ model gauging the $L_\mu - L_\tau$ lepton number could also explain the hints of LFU violations in R_K and R_{K^*} ratios observed by LHCb [64, 65]. The sensitivity to a Z_μ particle compatible with the observed B -anomalies and other constraints is currently under study by the Collaboration.

High energy hadron beams can be used to search for dark sector particles in the decays $K_L, K_S, \pi^0, \eta, \eta' \rightarrow$ invisible, where the neutral mesons M^0 are produced via the charge-exchange reactions $\pi(K) + p \rightarrow M^0 + n + E_{\text{miss}}$ [66–68]. This type of search with neutral kaons is also quite complementary, see e.g. [68, 69] to the current CERN and the proposed PBC program in the kaon sector.

Key requirements for detector, beam, beam time, timeline. NA64 is currently taking data at the H4 beam line of the SPS [70–72]. The beam line is a 100 GeV electron beam with a maximum intensity of $\sim 10^7 e^-$ per SPS spill. Beam intensity and transverse size have been optimized to guarantee an efficient detection of the synchrotron radiation during NA64 operation. The detection of synchrotron radiation is necessary to reach the required beam purity.

NA64 has collected about 3×10^{11} eot before LS2, and aims at reaching 5×10^{12} eot during Run 3.

The NA64 detector is a spectrometer with a low material budget tracker, micro-MEGAS, GEM and straw-tubes based, followed by an active target, which is a hodoscopic electromagnetic calorimeter (ECAL), shashlik-type, for the measurement of the energy of the recoil electrons. A high-efficient veto counter and a massive hermetic hadronic calorimeter are positioned just after the ECAL to efficiently detect muons or hadronic secondaries produced in the e^- -nucleus interactions in the active target.

The key feature of the NA64 apparatus is the detection of the synchrotron radiation from 100 GeV electrons in the magnetic field to significantly enhance electron identification and suppress background from the hadron contamination in the beam. The addition of a compact tungsten calorimeter after the synchrotron radiation detector as an active target for the production of energetic A' or X -boson explaining the *Be anomaly [73, 74], enables the search of $A' \rightarrow e^+e^-$ visible decays. The first results obtained in 2016–2017 for the both $A' \rightarrow \chi\bar{\chi}$ and $A' \rightarrow e^+e^-$ decay modes [70–72] confirm the validity and sensitivity of the NA64 technique for searching for dark sector physics.

The NA64⁺⁺ experiment proposed in the PBC context aims at using high-energy electron, muon and hadron beams extracted at the SPS and currently available at the CERN North Area, starting in Run 3.

(1) NA64⁺⁺(e):

NA64 plans to continue the data taking after LS2 with the main goal to integrate up to 5×10^{12} eot at the H4 line in about (6–8) months. The preparation of an area able to host a quasi-permanent installation of NA64 began in 2018.

An upgrade of the detector is also needed in order to cope with a high intensity beam: this

includes the replacement of the electromagnetic calorimeter electronics, the addition of a zero-degree hadron calorimeter, and the upgrade of the data acquisition system.

(2) $NA64^{++}(\mu)$:

A new detector served by the M2 beam line and located in the EHN2 experimental hall in the CERN North Area is proposed to be built after LS2 to investigate dark sector predominantly coupled to the second and third generation and LFV $\mu\text{-}\tau$ conversion with a high energy muon beam. The M2 line, currently serving the COMPASS experiment, is able to provide muons with momentum of $\simeq(100\text{--}160)$ GeV/c, and intensity up to $\sim 10^8$ μ /spill.

The detector setup follows closely the one currently operating with e^- beam: an active (muon) target followed by a large hadron calorimeter located in a magnetic field, which is used both to measure the outgoing muon momentum and to veto events with associated hadrons. The signal consists of a muon with outgoing momentum significantly lower than the incoming one and no energy deposition in the rest of the detector.

A key issue is the purity of the incoming muon beam: a background study performed in 2017 shows that the level of the hadron contamination in the muon beam can be reduced down to the negligible level $\leq 10^{-6}$ by using nine *Be* absorbers. Another key issue is the precise measurement of the momentum of the outgoing muon and its identification with high purity.

Some modification of the M2 upstream part are also foreseen, as described in the PBC Conventional Beams WG Report [75]. Assuming a muon beam intensity of $\sim 3 \times 10^7$ μ /spill, with $\sim 4 \times 10^3$ spills per day, about 1.5 years are necessary to accumulate $\sim 5 \times 10^{13}$ mot. NA64 has submitted in October the addendum for the SPSC⁴⁰ for the Phase 1 of $NA64^{++}(\mu)$, which requires 10^6 muons s^{-1} at 100 GeV.

(3) $NA64^{++}(h)$:

The NA64 studies with hadron beams are less advanced and will continue during the coming years. Integrated luminosities of 10^{13} pions-on-target, 10^{12} kaons-on-target, and 10^{12} protons-on-target could investigate dark sector models complementary to the dark photon one. These searches would require (20–50) GeV hadron beams that could be provided by the H4 line without modification. The Collaboration aims to start data taking with hadron beams after LS3.

Open questions, planned feasibility studies. The main open question for $NA64^{++}(e)$ is the detector ability to cope with the higher beam intensity, which is already available, and hence increased pile-up: this has already been positively answered based on the preliminary analysis of the data sample collected during the 2018 run where an intensity close to $\sim 10^7 e$ /spill has been reached. With such an intensity and 4000/spills/day, about four months will be required to collect 4×10^{12} eot. Upgrades of the detector and data acquisition system are planned during LS2. As for $NA64^{++}(e)$, key issues for $NA64^{++}(\mu)$ are the beam purity and beam momentum measurement, and detector hermeticity. In both cases, the time sharing in the two (highly demanded) beam lines (H4 and M2) with other potential users (eg. COMPASS, MUonE, etc) is an issue and will require a careful planning and prioritization of the operations.

Status of the Collaboration. The Collaboration currently consists of $\simeq 50$ participants representing 14 institutions from Chile, Germany, Greece, Russia, Switzerland, and USA. An

⁴⁰ CERN-SPSC-2018-024/SPSC-P-348-ADD-3.

updated list of authors and institutions can be found at: <https://na64.web.cern.ch>. The NA64 Collaboration has also submitted a separate document⁴¹ for the next update of the ESPP.

5.2.2. NA62⁺⁺.

Brief presentation, unique features. NA62 [76] is a fixed target experiment at the CERN SPS with the main goal of measuring the BR of the ultra-rare decay $K^+ \rightarrow \pi^+ \nu \bar{\nu}$ with 10% precision. It is currently taking data at the K12 beam line at the CERN SPS. The NA62 long decay volume, hermetic coverage, low material budget, full PID capability and excellent tracking performance, make NA62 a suitable detector for the search for hidden particles (SHiP). The possibility of dedicating part of Run 3 to this physics case is timely, since the projected sensitivity surpasses that of competitive experiments in the same time range. NA62 proposes to integrate $\sim 10^{18}$ pot operating the detector in dump mode for few months during Run 3 [77].

Location, beam requirements, beam time, timeline. NA62 is currently operating at the K12 beam line in the North Area. At full intensity, a beam of 3×10^{12} protons-per-pulse (ppp), 400 GeV momentum, in 3.5 s long effective spills from the SPS hit a beryllium target to produce a 75 GeV momentum-selected 750 MHz intense secondary beam of positive particles, 6% of which are charged kaons. The beryllium target used by NA62 is followed by two 1.6 m long, water-cooled, beam-defining copper collimators (TAX) which can act also as a dump of ~ 10.7 nuclear interaction lengths each. In the standard NA62 operation, roughly 50% of the beam protons punch through the beryllium target and are absorbed by the TAX collimators.

At the NA62 nominal beam intensity, 10^{18} pot can be acquired in $\mathcal{O}(3)$ months of data taking. The dump-mode operation can be obtained by lifting the NA62 Beryllium target away from the beam line and by closing the first TAX collimator, placed ~ 22 m downstream of the target. The muon halo emerging from the dump is partially swept away by the existing muon clearing system. The switching from the standard beam mode to the beam-dump mode takes a few minutes and it is already done regularly. About 3×10^{16} pot in dump mode have already been collected and are being analyzed for background studies.

The NA62 Collaboration is preparing a thorough plan for running after the end of LS2 with a fraction of the beam time in dump mode during Run 3 (2021–2023). A possible sharing could be two years in beam mode to complete the measurement of the branching fraction (BR) of the $K^+ \rightarrow \pi^+ \nu \bar{\nu}$ mode and $\mathcal{O}(1)$ year in beam dump mode. The proposal will take into account the results obtained on the measurement of the $BR(K^+ \rightarrow \pi^+ \nu \bar{\nu})$ based on the analysis of data taken in recent (2016–2018) run.

Detector description, key requirements for detector. A schematic layout of the NA62 detector is shown in figure 4.

The secondary positively charged hadron beam of 75 GeV/c momentum reaches the 120 m long, 2 m diameter, in-vacuum decay volume, placed 100 m downstream of the target. A Cherenkov counter (KTAG) filled with N_2 along the beam line identifies and timestamps kaons, which are about 6% of the hadron beam. Three silicon pixel stations (Gigatracker, GTK) measure the momentum and the time of all the particles in the beam at a rate of 750 MHz. A guard ring detector (CHANTI) tags hadronic interactions in the last GTK station

⁴¹ *Prospects for exploring the Dark Sector physics and rare processes with NA64 at the CERN SPS*, <https://indico.cern.ch/event/765096/contributions/>.

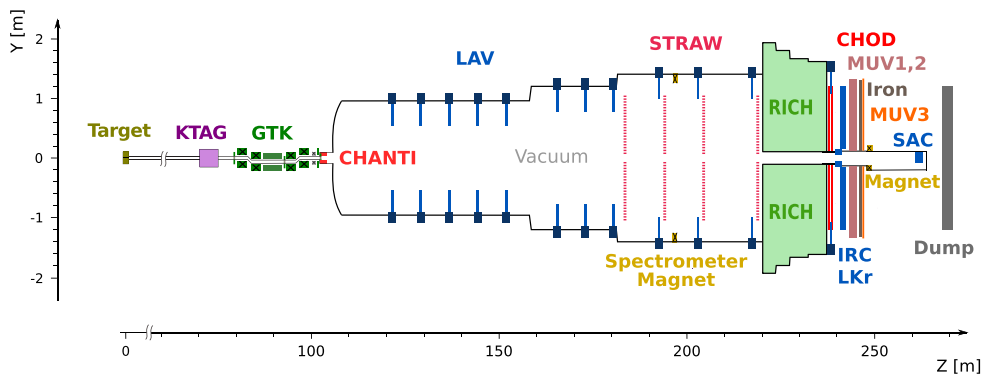


Figure 4. Layout of the NA62 experiment.

at the entrance of the decay volume. Large angle electromagnetic calorimeters (LAV) made of lead glass blocks surround the decay vessel can be used to veto particles up to 50 mrad. A magnetic spectrometer made of straw tubes in vacuum measures the momentum of the charged particles.

A 17 m long RICH counter filled with Neon separates π , μ and e up to 40 GeV/c. The time of charged particles is measured both by the RICH and by scintillator hodoscopes (CHOD and NA48-CHOD) placed downstream to the RICH. The electromagnetic calorimeter filled with liquid krypton (LKr) covers the forward region and complements the RICH for the particle identification. A shashlik small-angle calorimeter (IRC) in front of LKr detects γ directed on the inner edges of the LKr hole around the beam axis. The hadronic calorimeter made of two modules of iron-scintillator sandwiches (MUV1 and MUV2) provides further π - μ separation based on hadronic energy. A fast scintillator array (MUV3) identifies muons with sub-nanosecond time resolution. A shashlik calorimeter (SAC) placed on the beam axis downstream of a dipole magnet bending off-axis the beam at the end of the NA62 detector, detects γ down to zero angle. A multi-level trigger architecture is used when operated in beam mode. The hardware-based level-0 trigger uses timing information from CHOD, RICH and MUV3, and calorimetric variables from electromagnetic and hadronic calorimeters. Higher-level software-based trigger requirements are based on variables from KTAG, LAV and magnetic spectrometer.

Such a setup is perfectly suited to perform a comprehensive SHiP in a large variety of visible final states.

Open questions, feasibility studies. The operation of NA62 in dump mode does not pose particular problems and no show-stoppers have been identified. The analysis of $\mathcal{O}(10^{16})$ pot collected in dump mode shows that the background can be kept under control for hidden particles decaying to final states that are then fully reconstructed. The addition of an Upstream Veto at the front of the fiducial volume is currently being studied: this detector should be able to further reduce the combinatorial di-muon background coming from random combinations of halo muons and to open the possibility of detecting also partially reconstructed final states. In normal operation mode half of the protons do not interact with the Be target and impinge upon the TAXes: these data are used for some specific background studies, namely for the di-muon background.

Minor modifications to the beam line are possible, too, aimed at reducing the upstream-produced background (again mainly halo muons). A full GEANT4-based simulation of the

beam line has been implemented and is being used to study optimized settings of the existing magnetic elements of the line and possibly an optimized new layout for the beam-dump operation. Preliminary studies show that the component of the muon flux above 20 GeV can be reduced by two orders of magnitude with an appropriate setting of the magnetic elements of the beam line. The maximum intensity achievable is under study, as well, with some prospects of increase beyond the present nominal one. These aspects are under study within the PBC Conventional Beams working group.

Status of the Collaboration. The NA62 Collaboration is made of 213 authors from 31 institutions. An updated list of authors and institutions can be found at: <https://na62.web.cern.ch>.

5.2.3. LDMX @ eSPS

Brief presentation, unique features. The LDMX aims to probe dark matter (DM) parameter space far below expectations from the thermal freeze-out mechanism by exploiting the missing-momentum technique in a fixed-target experiment with a primary electron beam of modest GeV-range energy, low current and high duty-cycle. LDMX is the only experiment exploiting this technique among those presented in the PBC framework, and it has a unique physics reach. Apart from its unparalleled sensitivity to sub-GeV DM scenarios over a wide mass range, it will have sensitivity to a variety of other BSM phenomena [78].

A high-intensity primary electron beam can be provided via an X-band 70 m long linac based on CLIC technologies that could accelerate electrons to 3.5 GeV and fill the SPS in 1–2 s. The beam could be further accelerated up to 16 GeV by the SPS and then slowly extracted to a Meyrin site. The eSPS Collaboration has recently submitted an expression of interest to the SPSC [79].

The design of the experiment is driven by two main goals: to *measure* the distinguishing properties of DM production and to efficiently reject potential backgrounds, in particular photo-nuclear reactions of bremsstrahlung photons. The signal signature has two main features: (i) a reconstructed recoiling electron with energy substantially less than the beam energy but detectable, with measurable transverse momentum, and (ii) the absence of any other activity in the final state. A constraint on the DM particle production rate can be transferred into robust bounds on the interaction strength which in turn can be compared to direct freeze-out rates that would yield the observed cosmic DM abundance.

The missing-momentum approach has distinct advantages compared to other techniques such as missing mass (requires the reconstruction of all final state particles and allows only much lower luminosity), missing-energy only (suffers from higher backgrounds due to fewer kinematic handles and lack of discrimination between electrons and photons), or beam-dump experiments (have to pay the penalty of needing an additional interaction of the DM in the detector).

Key requirements for detector, beam, beam time, timeline. Reaching the full potential of the missing-momentum technique places demanding constraints on the experiment and the beamline supporting it. A high repetition rate of electrons is required (as much as $\sim 10^9$ electrons-on-target (eot) per second) in order to reach the envisaged integrated luminosities of 10^{14} – 10^{16} eot, while keeping an extremely low electron density per bunch ($1 - 5 e^-/\text{bunch}$).

This requires a fast detector that can individually resolve the energies and angles of incident electrons, while simultaneously rejecting a variety of potential background processes that vary in rate over many orders of magnitude. The LDMX design makes use of a low-mass,

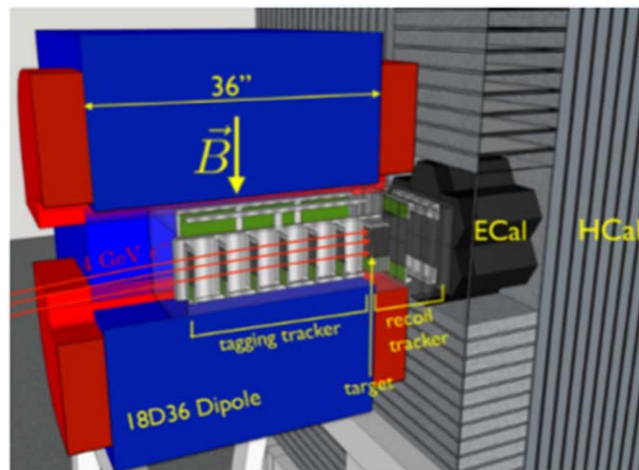


Figure 5. The LDMX experiment layout.

silicon-based tracking system in a 1.5 T dipole magnet to measure the momentum of the incoming electrons, and to cleanly reconstruct electron recoils, thereby providing a measure of missing momentum. A high-speed, high-granularity SiW calorimeter with MIP sensitivity is used to reject potential high rate bremsstrahlung background at trigger level, and to work in tandem with a scintillator-based hadron calorimeter to veto rare photo-nuclear reactions. The design leverages new and existing calorimeter technology under development for the HL-LHC, as well as existing tracking technology and experience from the HPS experiment [80]. The experiment is fairly small-scale for HEP standards. Thus it could be built, commissioned and run over the course of a few years. A rendering of the proposed experimental design is shown in figure 5.

The scenario for a CERN SPS beam outlined below envisages a beam energy between 3.5 and 16 GeV [79]. Further requirements for the beam are a low current and large beam-spot to ease the identification of individual electrons, paired with a high duty factor for large integrated luminosity.

All of this can be provided at CERN in three basic steps: a new LINAC providing electrons with 3.5 GeV, injecting into the SPS where the electrons are accelerated to up to 16 GeV, followed by a slow extraction of electrons to be delivered to the experiment. The bunch spacing can be any multiple of 5 ns up to 40 ns, the average number of electrons per bunch can range from <1 up to anything that can be tolerated by the experiment, and there is a high flexibility in the beam size, such that for example a beam spot of $2\text{ cm} \times 30\text{ cm}$ is perfectly feasible. To achieve 10^{16} eot in one year would require approximately one third of the time currently used by the SPS to accelerate protons.

The Collaboration anticipates the beamline could be available conservatively in 2025 (or even a few years earlier depending on CERN priorities) and that this would accommodate comfortably the time needed for the final design and construction of the detector. Hence, data taking could start in 2025 (or earlier), and be completed within a few years, as little as 1–2 years for the most optimistic luminosity scenarios. In addition to the LDMX experiment itself, the main construction needs are the electron linac as injector to the SPS, a 50 m tunnel for last path of the extracted beam, and a small experimental hall. The potential of such a primary electron beam facility goes beyond LDMX: (i) It also opens for a beam-dump search

for visibly decaying dark photons, (ii) gives a Jefferson laboratory type facility with extended energy range for Nuclear Physics, and (iii) would be a significant Accelerator Physics R&D-asset at CERN.

Open questions, planned feasibility studies. The design studies up to now [78] have been based on the assumption of a 4 GeV beam with on average one electron at a rate of 46 MHz. They have demonstrated the experiment's ability to reach close to 0 background for 4×10^{14} eot. Within this scenario, in-depth studies of the simulation of photo-nuclear backgrounds are progressing, in order to refine the hadron calorimeter design. This will be followed by detector prototyping in 2019/20.

The sensitivities for the other BSM phenomena outlined in [78] will be studied in the near future. Other plans for the near future include further studies of multi-electron events (starting now with $2e/\text{bunch}$) as well as 16 GeV beam energy; how many electrons/bunch can be tolerated in terms of triggering, reconstruction and identification, how high a granularity is needed and feasible, and how short a bunch spacing can be handled. This will feed into the determination of the exact run conditions in terms of the beam parameters described above, in order to achieve a luminosity of 10^{16} EOT, which will allow to probe all thermal targets below a few hundred MeV. A further handle on the effective luminosity especially for the study of high-mass signals (where degradation in momentum resolution is tolerable) is the target material and thickness, that can be modified from the default 10% X_0 W. The exploration of these parameters has only just begun.

Status of the Collaboration. LDMX@eSPS is currently being proposed by 78 physicists from 23 institutions as listed in the Letter of Intent submitted to the SPSC⁴² in September 2018. A condensed version of the LOI has been submitted for the next update of ESPP⁴³.

5.2.4. AWAKE

Brief presentation, unique features. The AWAKE experiment is placed underground at point 4 of the SPS, at the former site of the CNGS target complex. The AWAKE phase-I consisted of a 10 m long plasma cell impinged by 400 GeV proton bunches extracted from the SPS. A laser pulse, co-propagating with a proton bunch, creates a plasma in a column of rubidium vapor and seeds the modulation of the bunch into microbunches. Recently electrons have been accelerated in the wakefield of the proton microbunches. Based on the success of AWAKE phase-I, the Collaboration is currently investigating the possibility of accelerating an electron beam to 5–10 GeV in a 10–20 m plasma cell. A possible implementation of this phase is an electron beam dump experiment where electrons are accelerated to $\mathcal{O}(50)$ GeV using SPS bunches with 3.5×10^{11} ppp every 5 s.

Electron bunches of 5×10^9 electrons/bunch can be impinged upon a tungsten target where a Dark Photon could be produced and detected by an NA64-like experiment downstream. The experiment aims to detect visible dark photon decays to e^+e^- initially, with the possibility of extending to $\mu^+\mu^-$ and $\pi^+\pi^-$ final states.

Key requirements for detector, beam, beam time, timeline. The dark photons decay in a decay volume of order 10 m long, and the decay products are detected in three micromegas trackers

⁴² CERN-SPSC-2018-023/SPSC-EOI-018.

⁴³ Dark Sector Physics with a Primary Electron Beam Facility at CERN, <https://indico.cern.ch/event/765096/contributions/>.

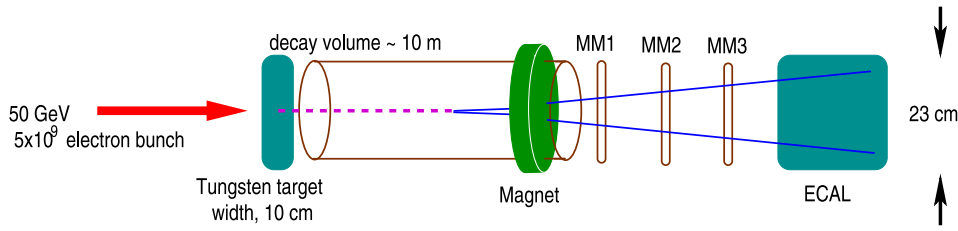


Figure 6. The AWAKE/NA64 conceptual layout.

MM1, MM2, MM3 as well as a tungsten plastic shashlik calorimeter, ECAL and the further possible addition of a HCAL. A downstream magnet separates decay products and allows the momentum reconstruction. A schematic layout of the experiment is shown in figure 6.

The advantage of this experimental setup is the luminosity gain provided by deploying bunches of electrons. This enables a larger $e\sigma$ in a shorter time frame and results in an extended coverage of the sensitivity parameter space. Taking into account the LIU-SPS with upgraded extraction kickers and a 12 week experimental run with a 70% SPS duty cycle, AWAKE/NA64 expects to integrate 10^{16} $e\sigma$ in one year of operation. This is more than three orders of magnitude larger than the expected integrated $e\sigma$ by NA64 in Run 3.

The proposed experiment requires a location accessible to SPS protons that drive the AWAKE accelerator and tunnel length long enough to accommodate a 50–100 m long plasma cell as well as 20 m of dump, drift volume and detectors.

A possible location is in the former CNGS target hall and decay tunnel. This project relies on the successful implementation of the AWAKE acceleration concept and could be installed at earliest during LS3.

Open questions, planned feasibility studies. Ongoing feasibility studies will include full reconstruction of the dark photon mass, as well as GEANT4 studies which incorporate realistic AWAKE electron bunches at different average beam energies.

The simulation of a NA64-like experiment on a possible AWAKE-based beam line is still in a very early stage: the evaluation of the background rates and experimental efficiencies needs still to be done and therefore are not contained in the sensitivity curves shown in section 10.

Status of the Collaboration. The AWAKE/NA64 team consists of the people belonging to the following institutes: CERN, University College London (London, UK), Institute for Nuclear Research (Moscow, Russia), Max Planck Institute for Physics (Munich, Germany), ETH (Zurich, Switzerland), Budker Institute of Nuclear Physics (Novosibirsk, Russia).

The AWAKE/NA64 Collaboration has submitted a separate document for the next update of the ESPP⁴⁴.

5.2.5. KLEVER. The main goal of the KLEVER experiment is to look for New Physics in the multi-TeV mass range via a measurement of the rare decay $K_L \rightarrow \pi^0 \nu \bar{\nu}$ and is discussed in section 6. However, the experiment may also be sensitive to specific signatures of hidden sector physics at the MeV–GeV scale, as discussed in section 9.

⁴⁴ Particle physics applications of the AWAKE acceleration scheme, <https://indico.cern.ch/event/765096/contributions/3295624/>.

5.2.6. SHiP @ BDF

Brief presentation, unique features. The SHiP experiment has been proposed to study a wide variety of models containing light long-lived particles (LLPs) with masses below $\mathcal{O}(10)$ GeV with unprecedented sensitivity.

This will be achieved through main features. Firstly, it benefits from the copious amounts of charm, beauty, τ leptons and photons produced in an interaction of the intense beam designed to be operated at the BDF [81] at the SPS which, in turn, can produce hidden sector particles such as a HNLs, dark scalars, Dark Photons, Axion Like Particles, light dark matter, R-parity violating neutralinos etc. The BDF will be able to provide 4×10^{13} 400 GeV protons in 1 s long spills, corresponding to an integrated yield of 2×10^{20} pot in 5 years of operation. Secondly, by reducing the background to zero over the experiment lifetime through the combination of a magnetic *muon shield* to sweep away muons from reaching the detector acceptance, decay volume under vacuum, veto systems surrounding the detector, timing coincidence through a dedicated fast timing detector, and a magnetic spectrometer within the decay volume.

Detector description, key requirements for detector. The main experimental challenge concerns the requirement of highly efficient reduction of beam-induced backgrounds to below 0.1 events in the projected sample of 2×10^{20} protons on target. To this end, the experimental configuration includes a long target made of heavy material to stop pions and kaons before their decay, a decay volume in vacuum, a muon shield based on magnetic deflection able to reduce the flux of muons emerging from the target by six orders of magnitude in the detector acceptance, and a hermetic veto system surrounding the whole decay volume.

The SHiP experiment incorporates two complementary apparatuses. The first detector immediately downstream of the muon shield consists of an emulsion based spectrometer optimized for recoil signatures of hidden sector particles and τ neutrino physics. The second detector system aims at measuring the decays of Hidden Sector particles to fully reconstructible final states as well as partially reconstructible final states that involve neutrinos. The spectrometer is designed to accurately reconstruct the decay vertex, the mass, and the impact parameter of the hidden particle trajectory at the proton target. A set of calorimeters and muon stations provide particle identification. A dedicated timing detector with ~ 100 ps resolution provides a measure of coincidence in order to reject combinatorial backgrounds. The decay volume is surrounded by background taggers to tag neutrino and muon interactions in the vacuum vessel walls and in the surrounding infrastructure.

A schematic diagram of the detector layout is shown in figure 7.

Beam requirements, beam time, timeline The BDF facility is described in a separate report⁴⁵. It consists of a 400 GeV momentum primary proton beam line slowly extracted from the SPS in 1 s long spills per 7.2 s long cycle. It is able to provide up to 4.0×10^{13} protons per cycle. The SHiP operational scenario is based on a similar fraction of beam time as the past CERN Neutrinos to Gran Sasso (CNGS) program. In the baseline scenario, the beam sharing delivers an annual yield of 4×10^{19} protons to the SHiP experimental facility and a total of 10^{19} to the other physics programs at the CERN North Area, while respecting the beam delivery required by the LHC and HL-LHC. The physics sensitivities are based on acquiring a total of 2×10^{20} protons on target, which may thus be achieved in five years of nominal operation.

⁴⁵ *Beam Dump Facility Report*, in preparation for the ESPP.

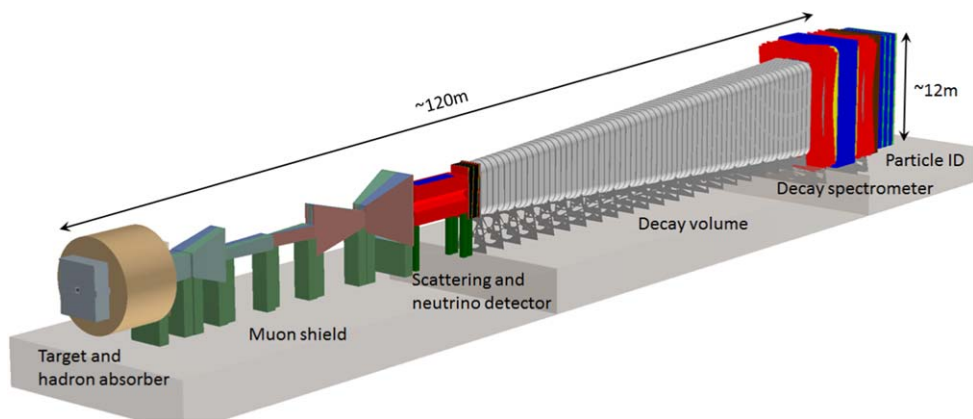


Figure 7. Layout of the SHiP detector.

CERN’s North Area has a large space next to the SPS beam transfer lines which is largely free of structures and underground galleries, and is entirely located on the current CERN territory. The proposed implementation is based on minimal modification to the SPS complex and maximum use of the existing beam lines. The design foresees space for future extensions. SHiP profits from the unique feature in the SPS of slow extraction of a debunched beam over a timescale of around a second. It allows tight control of combinatorial background, and allows diluting the large beam power deposited on the proton target both spatially and temporally. Should an observation require consolidation, a second mode of operation with slow extraction of bunched beam is also foreseen in order to further increase the discrimination between the signature of a light dark matter object, by measuring their different times of flight, and background induced by neutrino interactions.

The schedule for the SHiP experiment and the experimental facility is largely driven by the CERN long-term accelerator schedule. Accordingly, the schedule aims at profiting as much as possible from data taking during Run 4 (currently 2027–2029). Most of the experimental facility can be constructed in parallel to operating the North Area beam facilities. The connection to the SPS has been linked to Long Shutdown 3 (i.e. for LHC 2024–2026) but requires that the stop of the North Area is extended by one year (2025–2026). The schedule requires preparation of final prototypes and the TDRs for both the detector and the facility by beginning 2022, and construction and installation between 2023 and beginning 2027.

Background and feasibility studies. An extensive simulation campaign was performed to optimize the design of the muon shield, detector setup as well as to develop a selection that reduces all possible sources of background to <0.1 events over the experiment lifetime. The backgrounds considered were: neutrinos produced through the initial collision that undergo deep inelastic scattering anywhere in the SHiP facility producing V^0 s; muons deflected by the shield that undergo deep inelastic scattering in the experimental hall or anywhere within the decay volume producing V^0 s; muons in coincidence from the same spill (combinatorial muons) escaping the shield; cosmic muons interacting anywhere in the decay volume or with experimental hall.

The rate and momentum spectrum of the muon halo obtained with the full simulation is being calibrated using data from a dedicated 1 month long run performed in July 2018 where

a smaller replica of the SHiP target was exposed to $\mathcal{O}(5 \times 10^{11})$ 400 GeV protons. Results are expected by the Comprehensive Design Report, due by the end of 2019.

All samples rely on GEANT4 to simulate the entire SHiP target, muon shield, detector, and experimental hall (walls, ceiling, floor). In addition, neutrino interactions were simulated through GENIE.

A highly efficient selection is devised to reject all types of backgrounds and is detailed in the SHiP Technical Proposal. This selection requires two good quality tracks reconstructed in the SHiP spectrometer. Additional criteria are placed on the vertex quality, distance of closest approach, and impact parameter of the two-track system. In addition, candidates are rejected if the veto systems either at the front or around the decay vessel are compatible with an interaction within them. Tracks are also required to be in coincidence within a 300 ps timing window ($\sim 3\sigma$).

A neutrino sample equivalent to ten years of SHiP operation resulted in exactly zero events surviving a basic selection. In order to ensure this background source is negligible, a sample corresponding to 50 years of operation is being simulated. The combinatorial, deep inelastic and cosmic muon backgrounds are expected to produce $\leq 10^{-3}$ events over the experiment lifetime. Further studies will be conducted with even larger samples to further optimize the selection. In addition, backgrounds to light dark matter signatures are currently under evaluation.

In addition to simulation studies, a thorough R&D campaign on all sub-detectors has been carried out in the last three years with the aim to have realistic estimate of detector performance obtained with suitable technological choices.

Open questions: The main challenges concern the beam losses and activation during the slow extraction process, the design of the large muon shield, and the exact knowledge of the spectrum of the muon halo.

- (1) Significant progress has been made in the studies of techniques to reduce the beam losses and activation. Studies in 2017 confirmed the intensity reach to within a factor of two. Deployment of crystal channeling in conjunction with modified optics to reduce the beam density at the end of 2018, both in MD and in operation, now shows that the baseline proton yield is realistically within reach.
- (2) The design and performance of the muon shield poses certain technological challenges. These include how to best assemble sheets of grain oriented (GO) steel without disrupting the magnetic circuit, how to cut the GO sheets into desired configurations, and how to best connect the GO sheets to achieve the desired stacking factor. In order to address these questions a prototyping campaign is underway.
- (3) The design of the muon shield and the residual rate of muons depends on the momentum distribution of the muons produced in the initial proton collision. The latest shield optimization and rate estimates were performed using PYTHIA simulations. In order to validate these simulations a test beam campaign was performed in July 2018 to measure the muon flux using a replica of SHiP's target. The data are currently being analyzed. Depending on the outcome of this test beam campaign, a further optimization of the shield configuration will be performed.

Status of the collaboration. The SHiP Expression of Interest was submitted to SPSC in October 2013. This was followed by the Technical Proposal submitted to the SPSC in April 2015. The SHiP Technical Proposal was successfully reviewed by the SPSC and the CERN RB up to March 2016, with a recommendation to prepare a comprehensive design study (CDS) report by 2019.

SHiP is currently a Collaboration of 295 members from 54 institutes (out of which 4 are associate Institutes) representing 18 countries, CERN and JINR. The status of the

Collaboration is kept up-to-date in the CERN greybook⁴⁶. In addition to the experimental groups, about 40 people from the CERN Accelerator Division are currently working on the design and R&D of the BDF.

The formal organization of SHiP consists of a country representative board (CRB), Interim Spokesperson, Technical Coordinator and Physics Coordinator, and the group of project conveners as elected and ratified by the CRB. The organization has been adopted for the Comprehensive Design Study phase. A recent report⁴⁷ which summarizes the simulation studies and R&D activities has been submitted to the SPSC in January 2019.

A contribution related to the SHiP experiment has been submitted to the ESPP update⁴⁸.

5.3. Proposals at the LHC interaction points

5.3.1. FASER

Brief presentation, unique features. FASER (ForwArd SEarch experiment at the LHC) is a proposed small and inexpensive experiment designed to search for light, weakly-interacting particles at the LHC. Such particles are dominantly produced along the beam collision axis and are typically LPs, traveling hundreds of meters before decaying. To exploit both of these properties, FASER is to be located along the beam collision axis, 480 m downstream from the ATLAS interaction point (IP). At this location, FASER and a larger successor, FASER2, will enhance the LHC's discovery potential by providing sensitivity to dark photons, dark Higgs bosons, HNLs, ALPs, and many other proposed new particles.

The FASER signal is LLPs that are produced at or close to the IP, travel along the beam collision axis, and decay visibly in FASER:

$$p + p \rightarrow \text{LLP} + X, \quad \text{LLP travels } \sim 480 \text{ m}, \quad \text{LLP} \rightarrow \text{charged tracks} + X \text{ (or } \gamma\gamma + X\text{).} \quad (5.1)$$

These signals are striking: two oppositely charged tracks (or two photons) with very high energy (\sim TeV) that emanate from a common vertex inside the detector and which have a combined momentum that points back through 100 m of rock and concrete to the IP.

The sensitivity reach of FASER has been investigated for a large number of new physics scenarios [28, 82–92]. FASER will have the potential to discover a broad array of new particles, including dark photons, other light gauge bosons, HNLs with dominantly τ couplings, and ALPs. FASER2 will extend FASER's physics reach in these models to larger masses and also probe currently uncharted territory for dark Higgs bosons, other types of HNLs, and many other possibilities.

Location, beam requirements, beam time, timeline. FASER will be located 480 m downstream from the ATLAS IP in service tunnel TI12 as shown in figure 8. TI12 was formerly used to connect the SPS to the LEP tunnel, but is currently empty and unused.

The planned timeline for FASER is to be installed in TI12 during Long Shutdown 2 (LS2), in time to collect data during Run 3 of the 14 TeV LHC from 2021 to 2023. FASER's cylindrical active decay volume has a radius $R = 10$ cm and length $L = 1.5$ m, and the detector's total length is under 5 m. To allow FASER to maximally intersect the beam

⁴⁶ See <https://greybook.cern.ch/greybook/experiment/detail?id=SHiP>.

⁴⁷ SHiP Collaboration, *SHiP experiment—Progress Report*, CERN-SPSC-2019-010; SPSC-SR-248.

⁴⁸ SHiP Collaboration, *The Search for Hidden Particles experiment at the CERN SPS accelerator*, <https://indico.cern.ch/event/765096/contributions/3295624/>.

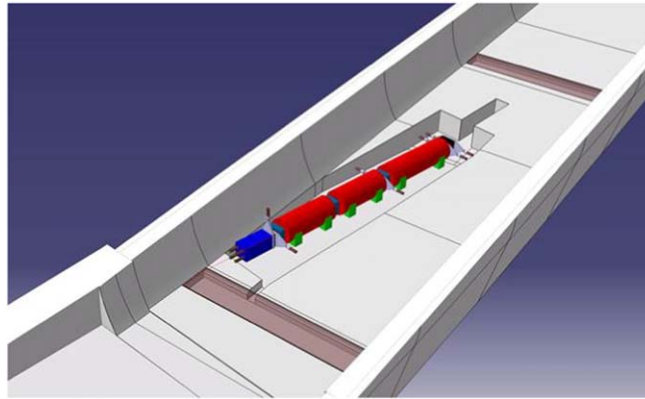


Figure 8. View of FASER in tunnel TI12. The trench lowers the floor by 45 cm at the front of FASER to allow FASER to be centered on the beam collision axis. Credit: CERN Site Management and Buildings Department.

collision axis, the floor of TI12 should be lowered by 45 cm. This will not disrupt essential services, and no other excavation is required. FASER will run concurrently with the LHC and requires no beam modifications. Its interactions with existing experiments are limited only to requiring bunch crossing timing and luminosity information from ATLAS.

If FASER is successful, a larger version, FASER2, with an active decay volume with $R = 1$ m and $L = 5$ m, could be installed during LS3 and take data in the 14 TeV HL-LHC era. FASER2 would require extending TI12 or widening the staging area UJ12 adjacent to TI12.

Detector description, key requirements for detector. The layout of the FASER detector is illustrated in figure 9. At the entrance to the detector on the left is a double layer of scintillators (gray) to veto charged particles coming through the cavern wall from the IP, primarily high-energy muons. The veto layer is followed by a 1.5 m long, 0.6 T permanent dipole magnet (red) with a 20 cm aperture. This serves as the decay volume for LLPs decaying into a pair of charged particles, with the magnet separating these to a detectable distance. Next is a spectrometer consisting of two 1 m long, 0.6 T dipole magnets with three tracking stations (blue), each composed of layers of precision silicon strip detectors located at either end and in between the magnets. Scintillator planes (gray) for triggering and precision time measurements are located at the entrance and exit of the spectrometer. The final component is an electromagnetic calorimeter (purple) to identify high energy electrons and photons and measure the total electromagnetic energy.

Open questions, feasibility studies. The FASER signals are two extremely energetic (\sim TeV) coincident tracks or photons that start at a common vertex and point back to the ATLAS IP. Muons and neutrinos are the only known particles that can transport such energies through 100 m of rock and concrete between the IP and FASER. Preliminary estimates show that muon-associated radiative processes and neutrino-induced backgrounds may be reduced to negligible levels.

Recently a FLUKA study [93–95] from the CERN Sources, Targets and Interactions group has been carried out to assess possible backgrounds and the radiation level in the FASER location. The study shows that no high energy (>100 GeV) particles are expected to

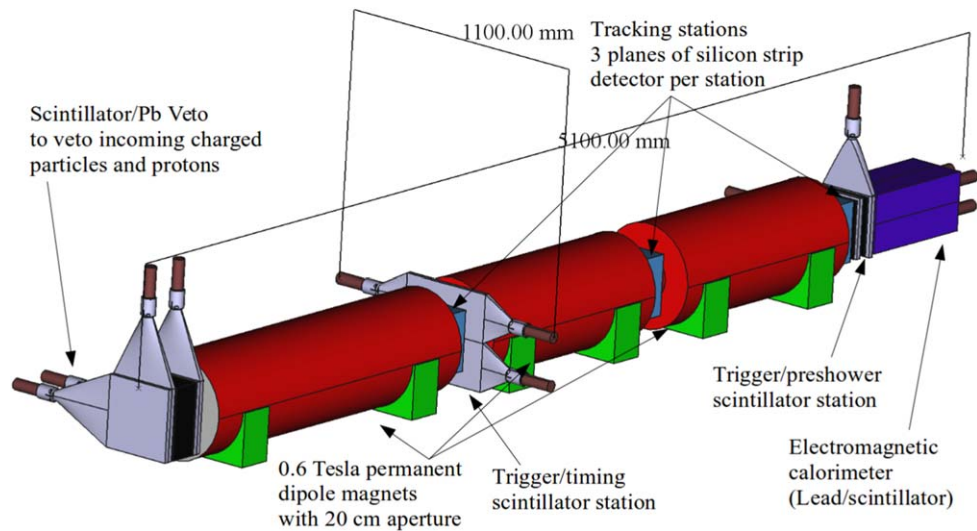


Figure 9. Layout of the FASER detector. See text for description of the detector components.

enter FASER from proton showers in the dispersion suppressor or from beam-gas interactions. In addition, the radiation level expected at the FASER location is very low due to the dispersion function in the LHC cell closest to FASER.

Emulsion detectors and battery-operated radiation monitors were installed in TI12 and TI18 during Technical Stops in 2018. The results from these *in situ* measurements have validated the FLUKA estimates, confirming that the high-energy particle background is highly suppressed and radiation levels are also very low and not expected to be problematic for detector electronics. Additional work is ongoing to refine background estimates, evaluate signal efficiencies, and optimize the detector.

Status of the collaboration. FASER submitted a Letter of Intent [96] to the LHCC in July 2018. At its September meeting, the LHCC reviewed the LoI favorably and encouraged the FASER Collaboration to submit a Technical Proposal. This was submitted to the LHCC in November 2018, and based on a positive review, the LHCC has approved FASER in March 2019. A working group has also been created within the PBC activities to study the interplay between the detector, the civil engineering, the backgrounds and radiation levels at the FASER installation point. Two private foundations contribute to support FASER's construction and operation costs.

The FASER group currently (December 2018) consists of 27 collaborators (22 experimentalists and 5 theorists) from 16 institutions in China, Germany, Israel, Japan, Poland, Switzerland, the United Kingdom, and the United States. The list of institutes is the following: Tsinghua University (China), University of Mainz (Germany), Technion (Israel), Weizmann Institute (Israel), KEK (Japan), Kyushu University (Japan), Nagoya University (Japan), National Centre for Nuclear Research (Poland), University of Bern (Switzerland), CERN (Switzerland), University of Geneva (Switzerland), University of Sheffield (United Kingdom) Rutgers University (United States), University of California (United States), University of Oregon (United States), University of Washington (United States).

The updated status of the Collaboration and experiment are available at: <https://twiki.cern.ch/twiki/bin/viewauth/FASER/WebHome>. FASER has submitted also a separate document⁴⁹ for the next ESPP update.

5.3.2. MATHUSLA

Brief presentation, unique features. The basic motivation for the MATHUSLA detector (MASSive Timing Hodoscope for Ultra-Stable neutral pArticles) [97] is the search for LLPs produced in $\sqrt{s} = 14$ TeV HL-LHC collisions, with lifetimes much greater than the size of the main detectors and up to the BBN constraint of ~ 0.1 s, with the peak sensitivity near $\beta c\tau \sim 100$ m. MATHUSLA also has a secondary physics case as a cosmic ray telescope.

This proposal has been the subject of several studies [86, 98–108], and the physics motivation from both a bottom-up and top-down point of view, including connections to naturalness, dark matter, baryogenesis and neutrino masses, has been explored in a comprehensive white paper [109]. The MATHUSLA Collaboration has also recently presented its Letter of Intent [110] to the LHCC. Given that some overlap exists between the MATHUSLA physics case and the PBC framework, the LHC Committee recommended MATHUSLA to be discussed within the PBC framework as well.

Location, beam requirements, beam time, timeline. The size of the detector and the corresponding location is not yet finalized. All sensitivity estimates in this document assume the MATHUSLA200 benchmark geometry from the Letter of Intent [110], which was also the original layout proposed in [97, 109]. This geometry assumes a very large (200×200 m²) area detector built on the surface, situated 100 m horizontally and vertically away from a LHC interaction point IP (either ATLAS or CMS IP), and a decay volume height of 20 m above the ground.

It is very unlikely that a detector with these large dimensions can be implemented at CERN, hence the sensitivity plots shown in this document should be properly rescaled once the final geometry will be finalized and the exact distance from the ATLAS/CMS IP points determined. An integrated luminosity of 3 ab^{-1} corresponding to the full HL-LHC period is assumed, with a hypothetical start of the data taking during Run 4. The timeline for the construction of the detector is under study.

Detector description, key requirements for detector. The MATHUSLA detector is essentially a large tracker, situated above an air-filled decay fiducial volume on the surface above ATLAS or CMS, that is able to robustly reconstruct displaced vertices (DVs) from the decay of neutral LLPs into two or more charged particles. The tracker should have on the order of five planes to provide robust tracking with \sim ns timing and cm spatial resolution. This is vital for rejecting cosmic ray (CR) and other backgrounds, and allows for the reconstruction of multi-pronged DV for LLPs with boost up to $\sim 10^3$, corresponding to minimum LLP mass of $\mathcal{O}(10 \text{ MeV})$ if the LLP is produced in exotic B -meson decays and $\mathcal{O}(0.1 - 1 \text{ GeV})$ for weak or TeV scale production [109]. Analyzing the geometry and multiplicity of the DV final states also allows the LLP decay mode and mass to be determined in many scenarios [102]. A layer of detectors in the floor is also considered, since this will improve LLP reconstruction and provide additional veto capabilities that may be necessary to reject upwards-going backgrounds like high-energy muons from the HL-LHC.

⁴⁹ FASER: ForwArD Search Experiment at the LHC, <https://indico.cern.ch/event/765096/contributions/>.

For the current MATHUSLA design, the focus is on proven and relatively cheap technologies to allow for MATHUSLA's construction in time for the HL-LHC upgrade. Therefore, the trackers are envisioned to be implemented with Resistive Plate Chambers (RPCs), which have been used for very large area experiments in the past [111, 112], or extruded scintillators which have also been used extensively [113, 114].

Assuming the baseline dimensions of $200 \times 200 \text{ m}^2$, with five active layers, this would correspond to $200\,000 \text{ m}^2$ of active detectors that have to provide time and space coordinates with $\sim \text{ns}$ time resolution and $\sim \text{cm}$ space resolution.

Open questions, feasibility studies. The main open questions for MATHUSLA are related to its large dimensions and to its capacity of controlling the backgrounds mostly coming from the tens of MHz of cosmic rays crossing the detector in all directions, with a total integrated rate of $\sim 10^{15}$ charged particle trajectories over the whole HL-LHC run.

- (1) *Cost:* The Collaboration has not provided an official estimate of the cost of the detector because of ongoing design optimizations. MATHUSLA requirements on resolution and rate are significantly lower compared to past experiments using similar detector technologies. The scale of the detector area is a further opportunity for cost optimization by employing mass production techniques. The detector size and location are currently being optimized to take into account land constraints and opportunities, with the hope to be able to reduce the size while keeping similar sensitivity. The detector design is modular for a staged implementation. The total cost will be driven by civil engineering and the large area tracking detectors. The Collaboration is investigating low-cost solutions with the challenging goal to keep the overall cost of the full size detector below 100 MCHF.
- (2) *Background:* As was argued in detail in [97], it is crucial for the projected sensitivities that MATHUSLA can search for LLP decays without backgrounds. The surface location shields MATHUSLA from ubiquitous QCD backgrounds from the LHC collision. It was quantitatively demonstrated that muon and neutrino backgrounds from the IP can be sufficiently rejected. Extremely stringent signal requirements and 4-dimensional DV reconstruction would limit the probability of cosmic rays to fake the hadronic or even leptonic LLP decays. Background estimates using a combination of detailed Monte Carlo studies with full detector simulation, the known cosmic ray spectrum, and empirical measurements at the LHC using a test stand detector, are currently in progress. The outcome of these studies will quantitatively determine whether the proposed background rejection strategies are sufficiently effective to reach the zero-background regime. However, to date, no quantitative analysis based on the full GEANT4 simulation of the detector with large Monte Carlo samples has been shown, and, as such, the assumption that MATHUSLA200 is a zero-background experiment is still to be demonstrated.

The Collaboration is currently studying a modular detector design, evaluating possible experimental sites at CERN and developing simulations of background and signal acceptance. Crucial to this endeavor is the data from the MATHUSLA test stand, a $\sim (3 \times 3 \times 5) \text{ m}^3$ MATHUSLA-type detector that is currently taking data on local cosmic rays and LHC muon backgrounds at CERN Point 1, allowing simulation frameworks to be calibrated and reconstruction strategies to be verified.

Precise timelines for the full detector proposal are still being established, but the aim is to have the full detector operating roughly by the time the HL-LHC goes online, around 2025 or

shortly thereafter. The MATHUSLA Collaboration has also prepared a separate stand-alone submission⁵⁰ to the ESPP update.

Status of the Collaboration. A snapshot of the MATHUSLA Collaboration is provided by the author list of the Letter of Intent [110]. It includes 64 authors, of which 48 are experimentalists and 16 are theorists. The institutes of the 48 experimentalists are the following: Universidad Mayor de San Andrés (Bolivia), University of Campinas (Brazil), Institute of High Energy Physics (Beijing, China) Tel Aviv University (Israel), Politecnico di Bari (Italy), INFN, sezione di Roma Tor Vergata (Italy), Università degli Studi di Roma La Sapienza (Italy), Benemérita Universidad Autónoma de Puebla (Mexico), Universidad Michoacana de San Nicolás de Hidalgo (Mexico), Universidad Autónoma de Chiapas (Mexico), CERN, Boston University (US), NYU (US), Ohio State University (US), Rutgers (US), SLAC (US), University of Arizona (US), University of Maryland (US), University of Washington (US).

5.3.3. CODEX-b

Brief presentation, unique features

The CODEX-b detector [115] is proposed as a new, shielded subdetector for LHCb to be placed in what is currently the LHCb data acquisition room. The purpose of the detector is to search for new, neutral LLPs which would penetrate the shield and decay in the detector volume. The largest gain in reach is for relatively light LLPs—i.e. $m \leq 10\text{GeV}$ —for which the backgrounds in ATLAS and CMS are prohibitive. The LLPs can be produced from hadron or Higgs decays, or as decay products from other, BSM states. Due to its proximity to the IP, CODEX-b is competitive with MATHUSLA200 in the low lifetime regime, despite its smaller acceptance and luminosity. The close distance to LHCb also means that CODEX-b can be interfaced with the LHCb trigger and reconstruction streams, as a true subdetector of the experiment.

Location, beam requirements, beam time, timeline

In more detail, the proposal is to house a tracking detector in the UXA hall roughly 25 m from the interaction point (IP8), behind the 3 m thick concrete UXA shield wall. The UXA shield would be supplemented with an additional lead or steel shield near the IP. The layout of the cavern and the proposed location of CODEX-b is shown in figure 10. The proposed location for the detector is currently occupied by the LHCb data acquisition system, but will be available from the beginning of Run 3. The size of the fiducial volume, and therefore the sensitivity, could be doubled if the DELPHI exhibit can be removed, but this is not essential. The necessary power supplies and services are already present in the cavern, and no further modifications to the cavern and/or beamline would be needed.

To reach the required sensitivity, CODEX-b has to integrate 300fb^{-1} . This is the dataset proposed for the LHCb phase-II upgrade to start in Run 5, which is still under discussion in the LHCC.

⁵⁰ MATHUSLA, <https://indico.cern.ch/event/765096/contributions/>.

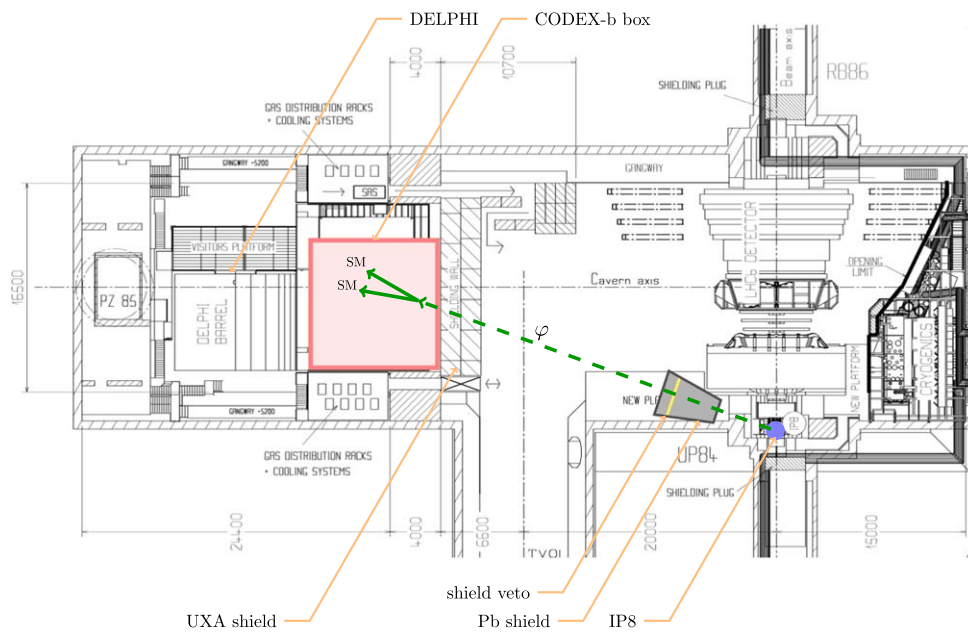


Figure 10. Layout of the LHCb experimental cavern UX85 at point 8 of the LHC [116], overlaid with the proposed CODEX-b location.

Detector description, key requirements for detector

The detector itself would consist of a $10 \times 10 \times 10 \text{ m}^3$ volume instrumented with RPC tracking layers or alternative off-the-shelf tracking technology. The shield consists of 25 nuclear interaction lengths of shielding near IP8—e.g. 4.5 m of Pb or steel. Combined with an additional 7 interaction lengths of shielding from the UXA wall, this should suffice to suppress primary and secondary K_L , neutron and other hadronic backgrounds [115], as verified through a preliminary GEANT4 simulation of the shielding response. An active muon veto with an efficiency of $\mathcal{O}(10^{-5})$ is embedded in the shield, in order to reject backgrounds from muon-induced secondaries in the downstream parts of the shield. The veto is located several meters within the shield to avoid a prohibitively large veto rate from charged primaries.

Open questions, feasibility studies

For CODEX-b to have the desired sensitivity, the LHCb high luminosity upgrade should be approved and an additional passive shield must be installed, as discussed above. One of the concerns related to this project is related to the approval of the LHCb high-luminosity upgrade which is still pending. The group behind the CODEX-b proposal will require additional funds and person-power, in order to further develop and eventually integrate this additional large sub-detector into the LHCb framework.

The CODEX-b detector geometry has been integrated into the LHCb simulation, with the help of the LHCb simulation team. This allows for a full simulation of collisions in IP8, including both the particles passing through the LHCb and CODEX-b detector volumes, and allows both realistic tracking studies to be performed and for studies of correlations between signals in CODEX-b and activity in LHCb. A baseline reconstruction algorithm is being

worked on, and a detailed report on the baseline geometry performance is foreseen for end of 2019.

In parallel, a two-scintillator setup has been used to perform a measurement of backgrounds in the DELPHI cavern during nominal LHC collisions at IP8. Measurements were taken at various points along the nominal CODEX-b geometry, and work is ongoing to relate these to the GEANT4 background estimates in the CODEX-b paper.

This data-driven background estimate is expected to be ready on a similar timescale as the nominal geometry performance report. As a consequence, the assumption of zero-background based on preliminary GEANT4 simulations and assumed in the compilation of the sensitivity curves in the following section, is still to be demonstrated.

Status of the collaboration

The CODEX-b Collaboration consists currently (December 2018) of 12 experimentalists and five theorists. A preliminary list of institutions is the following: Central China Normal University (Wuhan, Hubei, China); Henryk Niewodniczanski Institute of Nuclear Physics Polish Academy of Sciences (Krakow, Poland); LPNHE, Sorbonne Université Paris Diderot Sorbonne Paris Cité CNRS/IN2P3 (France); Clermont Université Université Blaise Pascal, CNRS/IN2P3, LPC (France); University of Birmingham (UK); University of Manchester (UK); University of Cincinnati (US); Syracuse University (US); Massachusetts Institute of Technology (US); Institute for Advanced Study (Princeton, US); Berkeley and Lawrence Berkeley National Lab (Berkeley, US); UC Santa Cruz (US); INFN, sezione di Bologna (Italy).

6. Proposals sensitive to New Physics in the multi-TeV mass range

The lack of an unambiguous evidence of NP so far could indicate that NP physics is at a very high mass scales, and therefore well beyond the reach of direct detection at the LHC or any other envisageable future high-energy collider but, perhaps, accessible via indirect effects. These can arise as modification in branching fractions, angular distributions, CP asymmetries in decays of strange, charm, beauty hadrons, or as a presence of measurable LFV decays in charged leptons or as presence of permanent EDMs in elementary particles containing quarks of the first (proton and deuteron) or second (charmed and strange baryons) generation.

(1) Ultra rare meson decays

Weak flavor-changing neutral current (FCNC) decays are very sensitive to contributions from heavy physics beyond the SM as they are both Cabibbo–Kobayashi–Maskawa (CKM) and loop-suppressed. In particular, the branching fractions (BRs) for the decays $K \rightarrow \pi \nu \bar{\nu}$ are among the observables in the quark-flavor sector most sensitive to NP. Because they are strongly suppressed and calculated very precisely in the SM, these BRs are potentially sensitive to mass scales of hundreds of TeV, surpassing the sensitivity of B decays in most SM extensions [117]. Observations of lepton-flavor-universality-violating phenomena are mounting in the B -sector. Measurements of the $K \rightarrow \pi \nu \bar{\nu}$ BRs are critical to interpreting the data from rare B decays, and may demonstrate that these effects are a manifestation of new degrees of freedom such as leptoquarks [118–120].

The *KLEVER* project aims at measuring the BR of the very rare decays $K_L \rightarrow \pi^0 \nu \bar{\nu}$ with 20% accuracy, assuming the SM branching fraction. It will complement the result that will be obtained in the next few years by the NA62 Collaboration on the charged mode, with an upgraded beam line and detector.

(2) LFV decays of charged leptons

LFV charged lepton decays are also an excellent probe of physics BSM: in fact within the SM with zero neutrino masses they are strictly forbidden, but many theories beyond the SM [121–124] predict a non zero branching fraction, depending on the mechanism of neutrino masses generation.

Although strong constraints exist in the muon sector, those involving the third generation are less stringent and need to be improved. Added impetus comes from the recent hints for the violation of lepton universality in B -meson decays, as this phenomenon, in general, implies LFV, with many theorists predicting effects just outside the current experimental bounds [125–128].

The *TauFV* proposal wants to search for LFV processes in τ and D -meson decays, exploiting the huge production of τ leptons and D meson occurring in the interactions of a high intensity 400 GeV proton beam with a target. *TauFV* aims at using $\sim 2\%$ of the total proton yield of the proposed BDF in the North Area.

(3) Searching for permanent EDMs

Permanent EDMs are forbidden by parity and time reversal symmetries and with the assumption of CPT invariance, they also violate CP invariance. For fundamental reasons of quantum mechanics an EDM (\vec{d}_X) needs to be proportional to the spin (\vec{s}) of a quantum mechanical particle X , $\vec{d}_X = \eta \cdot \mu_X \cdot \vec{s}$, where $\mu_X = \frac{e\hbar}{m_X}$ is the magneton associated with particle X of mass m_X and charge e . The constant η contains all relevant (new) physics. The dependence of \vec{d}_X on the inverse of the particle mass causes that sensitivities to New Physics of EDM search experiments are different for the same numerical values of established or future limits and it roughly scales with the mass of the tested particle. Typical mass limits corresponding to, e.g. electron EDMs are ≈ 5 TeV for two loop processes such as in multi Higgs scenarios, ≈ 60 TeV for one loop processes such as in supersymmetry and ≈ 1000 TeV in loop-free particle exchange such as for leptoquarks.

Two PBC proposals aim at studying permanent EDMs in proton/deuteron and in charmed and strange baryons: these are the *CPEDM* and the *LHC-FT* proposals, respectively.

In the following paragraphs a brief description of the *KLEVER*, *TauFV*, *CPEDM* and *LHC-FT* proposals is reported. Their physics reach, also in connection to a multi-TeV new physics scale, is discussed in section 10.

6.1. KLEVER

Brief presentation, unique features. The NA62 experiment at the CERN SPS is expected to measure $BR(K^+ \rightarrow \pi^+ \nu \bar{\nu})$ to within 10% by the end of LHC Run 3. In order to fully constrain the CKM matrix, or possibly, distinguish between different NP scenarios, it is necessary to measure $BR(K_L \rightarrow \pi^0 \nu \bar{\nu})$ as well. The KOTO experiment at J-PARC, should have enough data for the first observation of the $K_L \rightarrow \pi^0 \nu \bar{\nu}$ decay by the late 2020s⁵¹, but a next-generation experiment is needed in order to measure the BR.

As far as KOTO is concerned, a new detector and an upgraded beam line would be required to go to $\mathcal{O}(100)$ events sensitivity: an extension of the J-PARC hadron hall is currently being considered by the Japan Science Council with KOTO⁺⁺ as a priority.

⁵¹ T Yamanaka, presentation at the 26th J-PARC Program Advisory Committee, 18 July 2018, <https://kds.kek.jp/indico/event/28286/contribution/11/material/slides/1.pdf>.

The KLEVER experiment aims to measure $BR(K_L \rightarrow \pi^0 \nu \bar{\nu})$ to $\sim 20\%$ accuracy assuming the SM branching fraction, corresponding to the collection of 60 SM events with an S/B ratio of ~ 1 using a high-energy neutral beam at the CERN SPS starting in Run 4.

Relative to KOTO, which uses a neutral beam with a mean momentum of about 2 GeV, the boost from the high-energy beam in KLEVER facilitates the rejection of background channels such as $K_L \rightarrow \pi^0 \pi^0$ by detection of the additional photons in the final state. On the other hand, the layout poses particular challenges for the design of the small angle vetoes, which must reject photons from K_L decays escaping through the beam pipe amidst an intense background from soft photons and neutrons in the beam. Background from $\Lambda \rightarrow n \pi^0$ decays in the beam must also be kept under control.

Beam, beam time, timeline. KLEVER would make use of the 400 GeV SPS proton beam to produce a neutral secondary beam with a mean K_L momentum of 40 GeV, leading to a fiducial volume acceptance of 4%, and a K_L yield of $2 \times 10^{-5} K_L/\text{pot}$. With a selection efficiency of 5%, collection of 60 SM events would require a total primary flux of 5×10^{19} pot, corresponding to an intensity of 2×10^{13} ppp under NA62-like slow-extraction conditions. This is a six-fold increase in the primary intensity relative to NA62. The feasibility of an upgrade to provide this intensity on the T10 target is under study in the Conventional Beams working group [75]. Preliminary indications are positive: there is general progress on issues related to the slow extraction of the needed intensity to the North Area (including duty cycle optimization); a workable solution for T4-to-T10 bypass has been identified. The ventilation in the TCC8 cavern appears to be reasonably hermetic, obviating the need for potentially expensive upgrades. A four-collimator neutral beamline layout for ECN3 has been developed and simulation studies with FLUKA and GEANT4 are in progress to quantify the extent and composition of beam halo, muon backgrounds, and sweeping requirements.

KLEVER would aim to start data taking in LHC Run 4 (2026). Assuming a delivered proton intensity of 10^{19} pot yr^{-1} , collection of 60 SM events would require five years of data taking. To be ready for the 2026 start date, detector construction would have to begin by 2021 and be substantially concluded by 2025, leaving three years from the present for design consolidation and R&D.

Key requirements for detector. A schematic layout of the experiment is shown in figure 11. Most of the subdetector systems for KLEVER will have to be newly constructed. Early studies indicated that the NA48 liquid-krypton calorimeter (LKr) could be reused as the Main Electromagnetic Calorimeter (MEC), and indeed, the efficiency and energy resolution of the LKr appear to be satisfactory for KLEVER.

However, the LKr timing resolution would be a major liability. The LKr would measure the event time in KLEVER with 500 ps resolution, while the total rate of accidental vetoes from the SAC could be 100 MHz. The LKr time resolution might be improved via a comprehensive readout upgrade, but concerns about the service life of the LKr would remain, and the size of the inner bore would limit the beam solid angle (and hence kaon flux). The Collaboration is investigating the possibility of replacing the LKr with a shashlyk-based MEC patterned on the PANDA FS calorimeter (in turn, based on the KOPIO calorimeter [129]). This is a shashlyk design incorporating ‘spy tiles’ for longitudinal sampling of the shower development, resulting in additional information for γ/n separation. A first test of this concept was carried out with a prototype detector at Protvino in April 2018.

The upstream veto (UV), which rejects $K_L \rightarrow \pi^0 \pi^0$ decays upstream of the fiducial volume, would use the same shashlyk technology as the MEC. The active final collimator

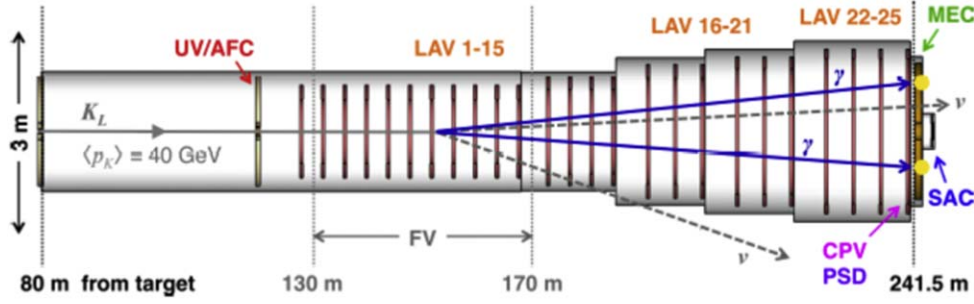


Figure 11. KLEVER experimental apparatus: upstream veto (UV), active final collimator (AFC), large-angle photon vetoes (LAV), main electromagnetic calorimeter (MEC), smallangle calorimeter (SAC), charged particle veto (CPV), pre-shower detector (PSD).

(AFC), inserted into the hole in the UV for passage of the beam, is a LYSO collar counter with angled inner surfaces. This provides the last stage of beam collimation while vetoing photons from K_L that decay in transit through the collimator itself. Because of the boost from the high-energy beam, it is sufficient for the large-angle photon vetoes (LAVs) to cover polar angles out to 100 mrad. The LAVs are lead/scintillating-tile detectors based on the CKM VVS [130]. Extensive experience with this type of detector (including in prototype tests for NA62) demonstrates that the low-energy photon detection efficiency will be sufficient for KLEVER [131, 132].

As far as the rejection of charged particles is concerned, simulations indicate that the needed rejection can be achieved with two staggered planes of charged-particle veto (CPV) each providing 99.5% detection efficiency, supplemented by the μ and π recognition capabilities of the MEC (assumed in this case to be equal to those of the LKr) and the current NA62 hadronic calorimeters and muon vetoes.

Finally, a pre-shower detector featuring a $0.5 X_0$ converter and two planes of tracking with $\sigma_{x,y} \sim 100 \mu\text{m}$ (assumed to be large-area MPGDs) would allow angular reconstruction of at least one γ from $K_L \rightarrow \pi^0\pi^0$ events with two lost γ 's to be reconstructed in 50% of cases.

Open questions, planned feasibility studies. Simulations of the experiment carried out with fast-simulation techniques (idealized geometry, parameterized detector response, etc) show that the target sensitivity is achievable (60 SM events with $S/B = 1$). Background channels considered at high simulation statistics include $K_L \rightarrow \pi^0\pi^0$ (including events with reconstructed photons from different π^0 s and events with overlapping photons on the MEC), $K_L \rightarrow 3\pi^0$ and $K_L \rightarrow \gamma\gamma$.

Background from $\Lambda \rightarrow n\pi^0$ and from decays with charged particles is assumed to be eliminated on the basis of studies with more limited statistics. An effort is underway to develop a comprehensive simulation and use it to validate the results obtained so far. Of particular note, backgrounds from radiative K_L decays, cascading hyperon decays, and beam-gas interactions remain to be studied, and the neutral-beam halo from more detailed FLUKA simulations needs to be incorporated into the simulation of the experiment. Preliminary studies indicate that the hit and event rates are similar to those in NA62, with the notable exception of the SAC, which will require an innovative readout solution. Offline computing resources required are similarly expected to be on the scale of NA62.

A PBC concern is related to the overall cost of the project if compared to the current strength of the Collaboration. The Collaboration is well aware that success in carrying out the KLEVER experimental program will require the involvement of new institutions and groups, with resources to contribute to the project, and initiatives to seek new collaborators are a major focus at present.

The proton sharing with existing or potential users in the North Area (as, e.g. SHiP), is also a concern: this will require a proper schedule and prioritization among the proposals.

Status of the collaboration. About 13 institutions currently participating in NA62 have expressed support for and interest in the KLEVER project. These are: University of Sofia (Bulgaria), Charles University (Czech Republic), Mainz (Germany), University and INFN Ferrara (Italy), University and INFN Firenze (Italy), University and INFN Naples (Italy), University and INFN Pisa (Italy), University and INFN Tor Vergata (Italy), University and INFN Torino (Italy), INR (Moscow, Russia), IHEP (Protvino, Russia), George Mason University (US).

Individuals from UK institutions participating in NA62 have indicated an interest in the KLEVER project and are exploring the possibility of joining. In addition 5 people from CERN EN-EA are currently dedicated to the study of the KLEVER beam line.

In addition to direct KLEVER input for the European Strategy update⁵², an Expression of Interest to the SPSC is in preparation and will serve as an opportunity to consolidate project membership.

6.2. TauFV

Brief presentation, unique features. The TauFV Collaboration aims at exploiting the high intensity of the BDF at CERN and install a detector, upstream of the proposed SHiP beam-dump target, which will have world-leading sensitivity to many LFV decay modes, for example probing for $\tau \rightarrow \mu\mu\mu$ decays down into the 10^{-10} regime. For the $\tau \rightarrow \mu\mu\mu$ mode, a limit of 2.1×10^{-8} at the 90% confidence level has been set by the Belle Collaboration [133]. Results of similar sensitivity have been obtained by BaBar [134] and LHCb [135]. The Belle-II experiment expects to reach a sensitivity of 1×10^{-9} [136], but may be able to go lower if all background is suppressed.

TauFV will be well suited to other LFV studies in tau decays, for example $\tau^- \rightarrow e^-e^+e^-$, $\tau^- \rightarrow \mu^-e^+e^-$, $\tau^- \rightarrow e^-\mu^+\mu^-$, $\tau^- \rightarrow \mu^+e^-e^-$ and $\tau^- \rightarrow \mu^+e^-e^-$. Particularly high sensitivity is expected for the latter two modes, where the initial level of contamination will be lower. Lepton number violation (LNV) searches will be performed with decays such as $\tau^- \rightarrow h^-h^-\ell^+$ ($h = \text{any hadron}$, $\ell = e$ or μ). The experiment will also have access to an enormous number of charm decays (e.g. 5×10^{15} D^0 mesons), which will allow a parallel program of LFV and LNV study with modes such as $D \rightarrow h\mu^-e^+$ and $D \rightarrow h\ell^-\ell^-$. World-leading measurements will be possible in the field of charm physics, many enabled by the excellent calorimetry of the experiment, including CP-violation measurements and searches for suppressed decays such as $D^0 \rightarrow \mu^+\mu^-$ and $D^0 \rightarrow \gamma\gamma$.

Location, beam, beam time, timeline. The baseline scenario is to use 2% of the protons currently intended for the SHiP experiment, which could be achieved with an integrated target thickness of 2 mm of tungsten. A five year period of operation would produce 4×10^{18}

⁵² KLEVER: An experiment to measure $BR(K_L \rightarrow \pi^0\nu\bar{\nu})$ at the CERN SPS, <https://indico.cern.ch/event/765096/contributions/>.

protons-on-target, which would result in $8 \times 10^{13} D_s^- \rightarrow \tau^- \bar{\nu}$ decays. This enormous yield is two orders of magnitude larger than the number of τ leptons so far produced at the LHCb interaction point, and five orders of magnitude larger than that produced at Belle.

The timescale for installing and operating TauFV is dictated both by the construction of the BDF, and by the development of the challenging sub-detector technology, in particular the front-end ASICs. The TauFV experimental hall could be prepared in 2026–27, in parallel with the installation of SHiP. If the project proceeds rapidly it would be possible to deploy the full detector at this time. Alternatively, a first-stage experiment, capable of demonstrating the possibility of performing high-precision flavor physics in this new environment, could be installed instead. The full scale experiment would then be assembled in LS4, currently foreseen for 2030. An attractive feature of TauFV is that the physics reach is not limited by the intensity of the available beam. Therefore, it is conceivable that future upgrades could be planned, integrating significantly more pot, depending on how both the detector technology and the physics landscape evolve.

From the beam optics point of view, several locations can provide the required beam conditions and the beam drift space to accommodate the detector along the new 200 m transfer line between the TDC2 switch-yard cavern and the BDF target station, without either affecting the location of the BDF experimental area or requiring significant changes to the beam-line configuration. The choice is instead driven by considerations related to the civil engineering in the vicinity of the existing installations, radiological protection, and access and transport requirements, both above ground and underground. Lateral space is required on both sides for shielding in order to limit the radiation exposure of the surrounding underground area to levels typical for the rest of the beam line. The currently preferred location is situated 100 m upstream of the BDF target bunker. An access and service complex for the transfer line is already foreseen at this location. This complex will be extended and reconfigured to include a bypass tunnel, the detector bunker, service cavern and the required surface infrastructure.

Key requirements for the detector. The target system of TauFV will consist of a set of thin tungsten blades, matched to an elliptical beam profile of vertical size ~ 1 mm, each separated by ~ 2 cm and distributed over a length of 10–20 cm (figure 12, left). This layout will ensure that interactions will be well spread both longitudinally and transversally, which is desirable for background rejection. Furthermore, the majority of the τ leptons will decay in free space, and there will be a low probability of a decay track passing through a downstream target.

The spectrometer design (figure 12, right) has an acceptance in polar angle between 20 and 260 mrad, and length of around 7 m. A Vertex Locator (VELO), comprising planes of silicon-pixel detectors broadly similar to the LHCb VELO, interleaves the target system, and continues downstream of it. Bending of charged tracks is provided by a dipole of integrated field of ~ 2.5 Tm, which is followed by a tracker, a TORCH detector [137, 138], a high performance ECAL and a muon system. All detector components will have fast-timing capabilities, good radiation hardness and high granularity. The TORCH detector provides time resolution for charged tracks of < 20 ps, which is a key weapon in the suppression of combinatoric background, and also brings hadron identification capabilities, which will enhance the charm-physics program of the experiment.

R&D is starting on the most critical elements of the detector, in particular the VELO and the ECAL. Here there is very close synergy with the requirements of Upgrade II of LHCb [139]. The VELO stations will be built from hybrid pixel sensors, and discussions have begun with the MediPix Collaboration concerning the requirements of the ASIC. A promising solution for the ECAL would be to employ crystal modules, based on YAG or GAGG crystal as a scintillator, and using the leading edge of the light pulse, or alternatively a silicon

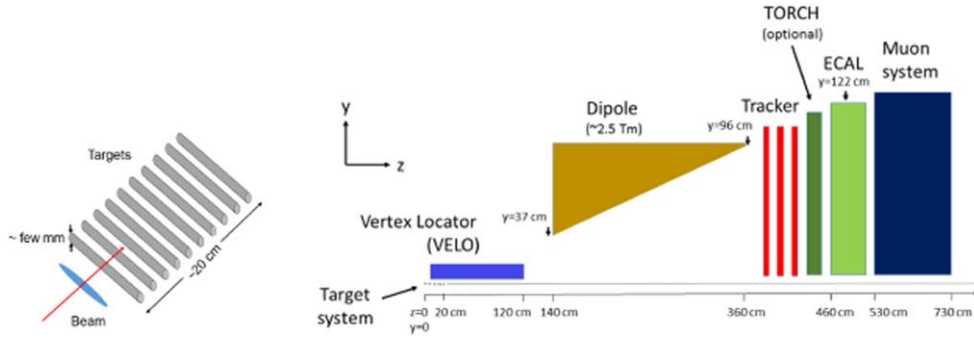


Figure 12. Schematic layout of the target system (left) and the spectrometer (right) of the TauFV experiment.

preshower, to provide the fast-timing information. Crystal samples have already been acquired, with the aim of constructing and evaluating a prototype module in 2019.

Physics reach and background considerations. Evaluation of the physics reach of the TauFV experiment has so far focused on the benchmark mode $\tau^- \rightarrow \mu^- \mu^+ \mu^-$. Studies are still ongoing, but preliminary results suggest that excellent control of combinatoric background will be achievable, mainly due to the distributed target system, which suppresses the likelihood of fake combinations, and the fast-timing provided by the TORCH and other sub-detectors. Hence, combinatorics will certainly be the sub-dominant source of background, and will not significantly impact upon the measurement down to signal branching ratios of 1×10^{-10} , and maybe lower. Background from same topology decays of D^+ and D^s mesons involving three leptons will be a greater concern, but will be controlled through good mass resolution, kinematic requirements involving the direction between the interaction and decay vertices, and the possibility to tag the soft photon from $D_s^* \rightarrow D_s \gamma$ decays, thereby rejecting backgrounds from D^+ mesons. Restrictions on the invariant mass of each di-muon pair can isolate ultra-pure regions of phase space, but at the expense of introducing model-dependence into the interpretation of the results. All these methods will be combined in a multivariate analysis to obtain maximum discrimination. Although final results are not yet available, it seems probable that sensitivity to branching ratios of a few 10^{-10} will be attainable. The physics reach in modes like $\tau^- \rightarrow e^+ \mu^- \mu^-$, which are afflicted by combinatoric background alone, will be even better by an order of magnitude.

The potential of TauFV in charm physics can be assessed by a direct comparison with LHCb, as the sources of background are the same, and are generally dominated by combinatorics, that TauFV can suppress effectively. The ECAL, optimized for soft photons, will give TauFV exciting possibilities in radiative decays. TauFV will therefore provide charm measurements of similar or higher precision to those of the proposed LHCb Upgrade II across a wide range of decay topologies, including modes that are complementary to the collider experiment.

Open questions, planned feasibility studies. The project is currently at a very early stage: no results from simulation are available, and the evaluation of the background is currently ongoing. This will be a mandatory step to address a definitive estimate of the physics reach. In order to pursue the proposed physics program, a strengthening of the Collaboration is also necessary.

Status of the Collaboration. The current TauFV Collaboration consists of nine physicists from the University of Bristol (UK), CERN, Imperial College London (UK), the University of Oxford (UK), the University of Zurich (Switzerland) and ETH Zurich (Switzerland). Before the end of this year these groups will complete the initial optimization of the layout and determine the physics reach for benchmark channels. In parallel, discussions will take place with additional potential collaborators.

6.3. CPEDM and LHC-FT electric dipole searches

6.3.1. Experimental landscape. There has been a substantial number of dedicated search experiments for permanent EDMs in a variety of systems over the past 60 years. All of them were well motivated and with a clear potential to discover new physics. They can be distinguished in four types depending on the particles studied. I.e. there are experiments on:

- (1) Free elementary particles, such as electron, muon, tau, but also approximately free elementary particles as the proton and the neutron;
- (2) Atoms, such as Hg, Xe, Tl, Cs;
- (3) Molecules such as YbF, ThO, BaF, HfF⁺;
- (4) Condensed matter samples, such as ferroelectric materials, liquid Xe.

Each of these lines of research has its own merits. Since a finite value of the not yet fully understood Θ_{QCD} parameter could cause EDM in hadrons, only an EDM found in a lepton would immediately indicate non-SM physics.

Any discovered EDM would call for further experiments to unravel the potentially different sources of the underlying new process of CP violation. Several hadronic EDMs could be used to demonstrate or disprove a Θ_{QCD} explanation, the combination with leptons will be indispensable to disentangling new physics. Because of the known CP-violation in the SM, permanent EDMs of fundamental particles are predicted which arise, e.g. for neutrons from three loop processes and for leptons from at least four loop processes. The SM EDM values are of order 10^{-32} ecm for neutrons and 10^{-40} ecm for electrons [140]. Such small values are orders of magnitude below present experimental possibilities and they therefore open large windows of opportunity for observing New Physics. For almost all particles speculative models exist which can provide for EDMs almost as large as the present experimental limits [141].

Motivation to carry out experiments to search for EDMs in one or another system therefore require judgment calls on the viability of such speculative models. Independent of this, the non-observation of any EDM has ruled out more speculative theories than any other known experimental approach⁵³. As one example of power of future EDM experiments, searches for EDMs on baryons and light nuclei, i.e. neutron, proton, deuteron and ³He, have particular potential to unravel different models of CP violation [142]. Below, we briefly present the main techniques currently used to search (directly or indirectly) for EDM in elementary particles as neutrons, protons, electrons and muons.

(1) Neutron EDM using ultra-cold neutrons

Experiments to search for the EDM of the free neutron (d_n) have been conducted since the 1950s [143]. A long chain of experiments with ever increasing sensitivity, first with neutron beams and later with stored ultracold neutrons (UCN), has yielded the present best limit of $|d_n| < 3 \times 10^{-26}$ ecm [144]. Presently there are at least five different

⁵³ N Ramsey, at 'Breit Symposium', Yale (1999).

sizeable efforts⁵⁴ aiming at improving the sensitivity to the neutron EDM in steps to 10^{-27} ecm and then to 10^{-28} ecm over the next 5–10 years. Several efforts (at PSI, ILL, LANL, TRIUMF) will use improved intensities of UCN stored in vacuum and at room temperature. One effort (at SNS) aims at conducting the measurement with UCN inside cold superfluid He (SFHe). The SFHe environment offers advantages [145] of potentially larger numbers of UCN exposed to larger electric fields, however, at the cost of considerable complication of the setup and handling. A first measurement in the cryogenic environment has still to be demonstrated. Beyond 10 years, some proposed or ongoing R&D efforts might succeed with cryogenic setups. Alternatively, also an experiment at a pulsed cold neutron beam of the ESS has been proposed [146].

(2) *Neutral atoms as probe of neutron and proton EDMs*

EDMs have also been searched for in neutral atoms. From EDM searches in diamagnetic atoms numerous limits on parameters describing physics within the SM or beyond could be extracted. The most recent table top experiment on ^{199}Hg has established $|d_{\text{Hg}}| < 7.4 \times 10^{-30}$ ecm (95% C.L.) [147]. From this value various other limits have been derived when assuming that there was for each case only one process that causes an EDM in ^{199}Hg . Amongst others a best neutron EDM limit of $|d_n| < 1.6 \times 10^{-26}$ ecm [148] and a proton EDM limit of $|d_p| < 2.0 \times 10^{-25}$ ecm [148] have been established as well as a limit on the QCD Θ parameter at $|\Theta_{\text{QCD}}| < 1.1 \times 10^{-10}$ [149].

(3) *Paramagnetic atoms and molecules as probe of an electron EDM*

EDM searches in paramagnetic atoms have yielded limits primarily on the electron EDM. Those early limits have been superseded since by searches in molecules and in molecular ions, where internal electric fields in these molecules give rise to some $10^5 \rightarrow 10^9$ fold enhancement for an electron EDM for example by using excited states of ThO in a molecular beam [150] or the ground state HfF^+ in an rf-particle trap [151]. Bounds could be established at $|d_e| < 1.1 \times 10^{-29}$ ecm and $|d_e| < 1.3 \times 10^{-28}$ ecm (90% C.L.), respectively, with these experiments exploiting significantly different techniques. Further improvements are expected soon from projects using these and also further molecules, such as YbF [152] and BaF [153]. It is highly realistic to expect that within the coming decade sensitivities better than 10^{-30} ecm will be achieved for the EDM on the electron.

(4) *Muon EDM*

The most sensitive EDM search experiments so far have been conducted on systems involving particles from the first particle generation. Yet limits on higher generation particles could be established as well. Along with measurements of the muon magnetic anomaly (muon g-2) EDM values could be obtained, the best limit currently being $|d_\mu| < 1.8 \times 10^{-19}$ ecm (95% C.L.) [154]. The series of muon g-2 experiments since the 1960s has exploited the strong motional magnetic fields muons experience when moving at high velocities (close to the speed of light) through static magnetic fields. This basic concept underlies a muon EDM experiment proposed for the Paul Scherrer Institute (PSI) [155]. As a major improvement in the experimental concept a radial electric field is installed in the storage volume to compensate the particle's g-2 value related spin precession. An EDM on the muon manifests itself as an out of orbit plane precession of the muon spin, which can be detected via the time evolution of spatial distribution of decay electrons.

At existing muon facilities a statistics limited sensitivity of $|d_\mu| \approx 7 \times 10^{-23}$ ecm can be achieved within 1 year of data taking. At this precision the viability of the technique to directly search for an EDM on even short-lived charged particles can be demonstrated.

⁵⁴ See, e.g. nedm2017 Workshop, Harrison Hot Springs, 15–20 October 2017.

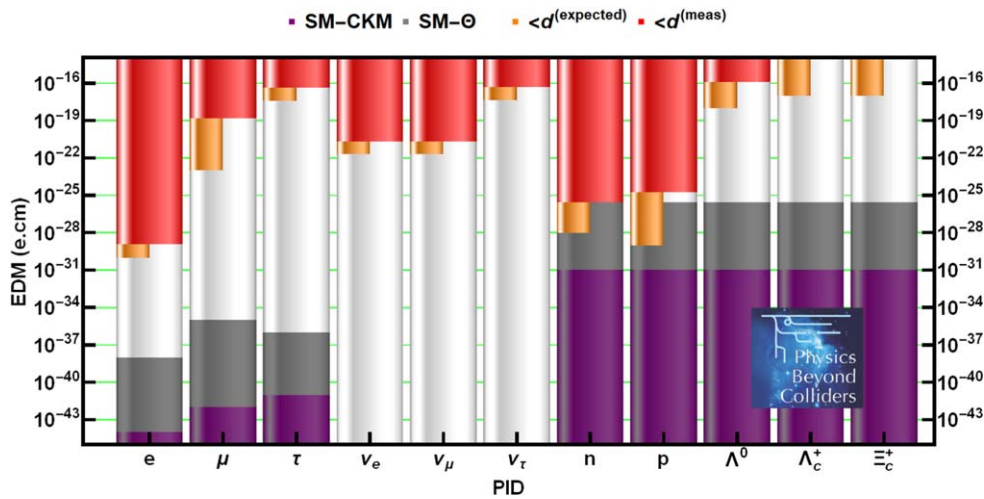


Figure 13. Overall status of EDM measurements: current limits on EDMs of fundamental particles are displayed as red bars from the top. From below come the SM estimates from CKM CP violation and Θ_{QCD} (assuming it takes the maximal value allowed by the neutron EDM). White regions indicate safe BSM discovery territory for the experiments.

Further, already at this sensitivity a number of SM extensions can be tested [155] which in particular account for the fact that the muon is a second generation particle.

Further limits on higher generation particles have been established. Figure 13 displays limits on the EDMs of fundamental particles. Muon and neutron limits have been deduced from measuring directly on these free particles, while e.g. the limit on the electron EDM results from the ACME experiment on ThO [150] assuming the electron EDM as the sole CP violating source.

The limits on the neutrino EDMs are together with limits on magnetic moments deduced from cross sections which would be affected by electromagnetic couplings. The experimental limits are displayed as red bars from the top. From below come the SM estimates from CKM CP violation and Θ_{QCD} , taken to be the maximal value consistent with the neutron EDM limits. White regions indicate safe BSM discovery territory for the experiments. The range of ongoing or proposed experimental projects is indicated in orange.

6.3.2. PBC proposals: CPEDM and LHC-FT. Improved sensitivities can in several cases be obtained with the projects proposed for CERN within this PBC study: the proton EDM is the topic of the CPEDM Collaboration, and the strange and charm baryons might be improved or measured for the first time at all [156, 157] with the experiment proposed by the LHC-FT group:

(1) *LHC-FT: measurement of EDMs in charmed and strange baryons*

Interest in hadronic EDM of second and even third generation quarks comes, e.g. from the fact that the indirect constraints on the charm EDM are rather weak, of order 4×10^{-17} ecm [158] only. As no finite EDM has been observed so far and no source of BSM CP violation is known yet, experimental efforts covering uncharted territory are

necessary. The charm quark as well as the muon might via unexpectedly large EDM give clues on specific flavor structure of new physics.

The experiment concept relies on a bent crystal to extract protons from the LHC beam halo. These protons will then hit a dense target and produce charged heavy and strange baryons that will then be channeled in bent crystals positioned in front of the detector. The intense electric field between the crystal atomic planes is able to induce a sizeable spin precession during the lifetime of the particle. The EDM, along with the magnetic dipole moment [159] can be determined by analyzing the angular distribution of the decay particles. Recently, the possibility to use the same technology for measuring the EDM (and MDM) of the tau lepton has been discussed in [160, 161].

The LHC interaction point IP8, where the LHCb detector [162, 163] sits, has been identified as a suitable location of the experiment. A main challenge is represented by the limited coverage of the detector in the very forward region, requiring a secondary crystal with a large bending exceeding 15 mrad. A W target of ≈ 2 cm thickness hit by a proton flux of $\approx 10^7$ protons s^{-1} is the upper limit for a parallel detector operation. R&D is ongoing to assess the feasibility of the secondary crystal along other challenges of the proposal, which include the compatibility with the machine, its operation mode, maximum reachable proton flux and the design of the absorber downstream the detector.

About 2.4×10^{14} protons on target could be reached in Run 3 with three years of data taking after the installation during an LHC technical stop, either with two weeks per year of a dedicated detector running at 10^8 proton s^{-1} or with a parallel detector operation at 10^7 proton s^{-1} . This would lead to EDM sensitivities of about 10^{-17} ecm for charm baryons. Extending the detector coverage down to 10 mrad along with an increase of the proton flux during LHC Run 4 and Run 5, either at LHCb or at a dedicated experiment would improve sensitivity by about one order of magnitude.

Figure 14 shows the EDM sensitivity for different baryons in two different scenarios, scenario 1 (S1) corresponds to data collected at the LHCb interaction point in a first phase at low luminosity (about 2×10^{14} pot); scenario 2 (S2) corresponds to data collected at a possible next-generation experiment at higher luminosity ($\sim 10^{17}$) and enhanced coverage.

(2) *CPEDM: measurement of proton and deuteron EDMs*

The same experimental concept as for muons, i.e. exploiting a magnetic storage ring and motional electromagnetic fields, underlies the proposed deuteron EDM experiment for CERN. The spin analysis in this case is achieved by a newly developed deuteron polarimeter. Numerous preparations including polarimetry and spin manipulation are already being studied by the JEDI Collaboration. The COSY experiment is an indispensable proof of principle at $\sim 10^{-24}$ ecm sensitivity for a ring experiment using a dedicated magnetic storage ring for deuterons (or protons) at CERN, which is needed to observe or establish a limit on the deuteron EDM at the level of 10^{-29} ecm.

For a deuteron experiment at CERN a new magnetic storage ring is required with some 80 m circumference to store polarized deuterons and observe the time evolution of their polarization. The precursor experiment at COSY is expected to develop all required detectors with sufficient sensitivity and to test the viability of the approach for hadrons. Both the muon and deuteron EDM experiment concepts take advantage of the fact that the magnetic anomaly is rather small and therefore magnetic spin precession in a magnetic storage ring can be compensated effectively by radial electrostatic fields.

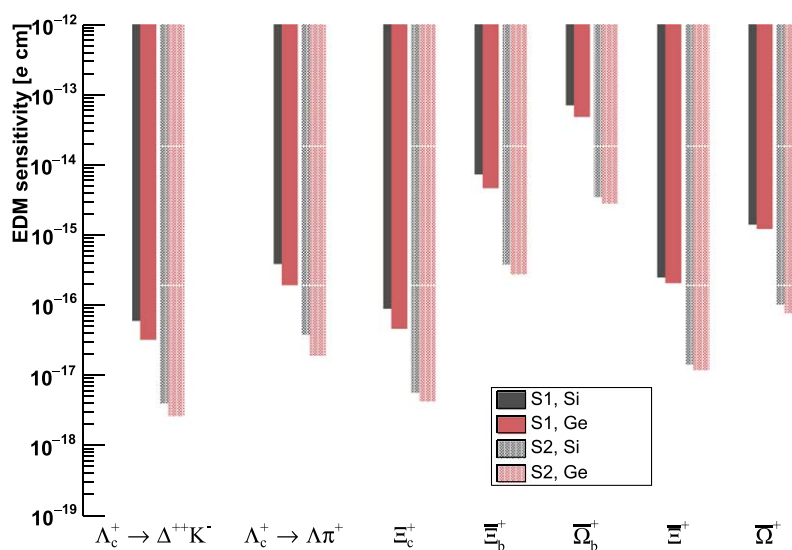


Figure 14. EDM sensitivities for different baryons in two different scenarios, scenario 1 (S1) corresponds to data collected at the LHCb interaction point in a first phase at low luminosity (about 2×10^{14} pot); scenario 2 (S2) corresponds to data collected at a possible next-generation experiment at higher luminosity ($\sim 10^{17}$) and enhanced coverage. Figure revisited from [157].

The proton EDM experiment proposed by the CPEDM Collaboration for CERN uses as in contrast a purely electrostatic dedicated storage ring of some 400–500 m circumference and with alternating field gradients, since the magnetic anomaly is much larger than for deuteron and muon. For sensitivity 10^{-29} ecm it exploits a proton beam of 233 MeV energy. The device needs provision for clockwise and counter-clockwise particle injection to minimize systematics. External magnetic fields at the experimental site need to be compensated to some 10 nT all over the particle storage volume and through the experimental running time. The substantial necessary expenses require a full structured program of stepwise testing of all essential concepts and necessary devices. The proton EDM project at CERN is a joint effort of the proton and deuteron EDM communities. It appears that a small size proof of principle experiment would be indispensable.

An experiment on the proton EDM tests to a large part the same speculative models as the neutron EDM, except for those constructed with isospin dependence. Therefore a proton EDM experiment will need to exceed the prospected future sensitivity values expected for neutron experiments in order to justify the expenditures. Here, one expects some 10^{-27} ecm by 2025 and 10^{-28} ecm by 2030. Note that, for the deuteron an EDM can arise from either a proton or a neutron EDM (or both) and in addition an EDM may be due to CP violating parts in the proton-neutron interaction of the deuteron binding. Both experiments, once they have proven sufficient sensitivity, are therefore strongly motivated and they have robust discovery potential. Yet, the speed of progress in the area of molecular EDM searches and the significantly lower costs of

table top experiments need to be weighted against those of the storage ring approaches. The CeNTREX experiment at Yale⁵⁵ aims for a 30 times improvement for the proton EDM (and 100 fold improvement on Θ_{QCD}) as compared to limits established for the proton to date⁵⁶.

7. Physics reach of PBC projects

In the following sections we review the physics reach of the experiments proposed in the PBC–BSM study group and the impact that CERN could have in the search for New Physics at mass scales different from the TeV scale in the next 10–20 years. Their physics reach is compared to the existing results and to the projections of experiments either operating at existing facilities or proposed to future facilities beyond those considered in this study. The results are presented following the scheme outlined in section 3 where the experiments were classified in terms of their sensitivity to New Physics in the sub-eV (section 4), MeV–GeV (section 5), and multi-TeV (section 6) mass scales.

8. Physics reach of PBC projects in the sub-eV mass range

Experiments searching for axions/ALPS in the sub-eV mass region discussed in the PBC–BSM study group exploit their possible coupling to photons, and, as such, are sensitive to the benchmark case BC9 discussed in section 3.1.

The photon regeneration experiment can be sensitive to milli-charged particles (benchmark case BC3) and hidden photons (benchmark case BC2), however no sensitivity estimate has been given for the first case BC3. For the hidden photons, their production in a LSW apparatus is not related to the presence of the static magnetic field; since one of the major improvements of the proposed experiment is related to the increase of the magnetic field amplitude, a smaller advancement over the present sensitivity to hidden photons is expected.

8.1. Axion portal with photon dominance (BC9)

8.1.1. Current bounds. The most updated review on the laboratory searches for axions and ALPs has been given in the recent paper by Irastorza and Redondo [39]. Figure 15 shows the current constraints for the axion-photon coupling $g_{a\gamma}$ versus axion mass m_a in the sub-eV mass range. The figure has been updated with the recent result of ADMX [164].

The figure follows a color scheme to present results obtained with different methods: black/gray for laboratory results, bluish colors for helioscope searches and bounds related to stellar physics, greenish for haloscopes or cosmology dependent arguments. Hinted regions, like the QCD axion, are in yellow/orange.

Laboratory limits (dark gray area in figure 15) are essentially due to the results of OSQAR (region below 1 meV), and PVLAS (region above 1 meV). OSQAR [165] is a CERN based light shining through a wall experiment based on a prototype LHC magnet. PVLAS [166] is a sensitive polarimeter employing two rotating 2.5 T permanent magnets and an ultra high finesse Fabry–Perot cavity to search for the magnetic birefringence of the vacuum [167]. A possible next generation magnetic polarimeter to study this effect is under discussion within the PBC Technology Group [168] under the name VMB@CERN.

⁵⁵ DeMille *et al* <https://physics.umass.edu/sites/default/files/attachments/page/20470/fie-kawall-centrex.pdf>.

⁵⁶ <https://demillegroup.yale.edu/research/centrex-search-electric-dipole-moment-edm-proton>.

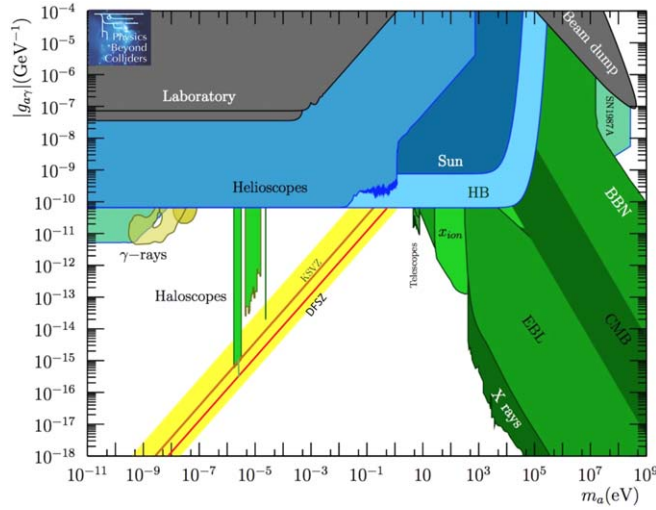


Figure 15. Current constraints for the axion photon coupling $g_{a\gamma}$ versus axion mass m_a . Revised from [39]. See text for details.

The bounds from helioscopes and haloscopes experiments are mostly driven by CAST [169] and ADMX [164, 170] results, respectively.

(1) **CAST**

CAST is an helioscope, searching from axions/ALPs with photon-coupling produced in the Sun through Primakoff conversion of plasma photons in the electrostatic field of charged particles.

The most efficient way to detect solar axions is through their reconversion into photons in the presence of a static electromagnetic field (usually magnetic dipole field) [164]. Reconverted photons are then detected by using low background x-ray devices. The achievable sensitivity in terms of the axion photon coupling constant is proportional to

$$\text{sens}(g_{a\gamma\gamma}) \propto \frac{b^{1/8}}{B^{1/2}L^{1/2}A^{1/4}t^{1/8}}, \tag{8.1}$$

where L is the length of the magnetic field of amplitude B , A is the area of the useful bore, b the background rate and t the integration time. Large volume magnets are therefore a primary ingredient for such a research.

By using a prototype LHC dipole magnet with 9 T magnetic field along 9.3 m length, CAST for the first time was able to explore solar axion in the QCD model range, in the mass region 0.1–1 eV. To maximize observing efficiency, the magnet was supported by a structure capable to track the Sun for a sizeable fraction of the day. The last CAST result [169] set the current best limit on the axion-photon coupling strength ($0.66 \times 10^{-10} \text{ GeV}^{-1}$ at 95% confidence level), thus competing with the most stringent limits from astrophysics on this coupling.

CAST has also searched for other axion production channels in the Sun, enabled by the axion-electron or the axion-nucleon couplings. The project is now over, and the magnet may be utilized for building a haloscope (project RADES [171]). Most of the CAST Collaboration will be entering IAXO. Among the key elements of the CAST apparatus were the use of x-ray focusing optics and very low background micromegas detector.

(2) **ADMX**

Axion or ALPs can be the main component of the dark matter halo of our galaxy and produce measurable signals in a suitable terrestrial detector. Such a detector usually exploits the long coherence length of these low mass particles, inside the galactic halo, in such a way to obtain detectability in spite of their very weak interactions with ordinary matter. Under the assumption that the searched for particle is the only constituent of the DM halo, limits on the coupling can be obtained in the absence of a detected signal. Strictly speaking, the limit is on the product between the coupling and the fraction of the local DM density in the case of a subdominant component. The oldest strategy to search for axions is the Sikivie or Primakoff haloscope [40], which has given almost all current limits for direct detection of dark matter in the sub eV range.

In a Sikivie type detector, a high Q tunable microwave resonator is immersed in a strong static magnetic field. DM axions can be converted into real photons via a Primakoff process and deposit energy into the resonant mode of the cavity. In the last two decades the Axion dark matter experiment—*ADMX*—has implemented this method for cavities in the GHz range. Under the assumption of dominant DM component for the axion, *ADMX* has excluded the KSVZ axion in the 1.91–3.69 μeV mass range [170], and very recently the DFSZ one in the 2.66–2.81 μeV range [164]. The apparatus is based on a large volume high Q tunable copper cavity, operated in the sub-K temperature range and read by a SQUID based detection chain. Coverage of masses up to 40 μeV (10 GHz) is envisioned for the near future by combining the outputs of multiple co-tuned cavity resonators in the current 8 T superconducting magnet.

For the stellar and cosmology limits shown in figure 15 the acronyms are as follows (see [172, 173]):

- (1) *HB, Sun, SN1987a*: limits from stellar evolution obtained by studying the ratio of horizontal branch (HB) to red giants in globular clusters (GCs) [174], by a combined fit of solar data (Sun) [175], and by the study of the SN1987A neutrino pulse duration [176];
- (2) *Telescopes, x-rays, γ -rays*: photons produced from axions inside galaxies show up as a peak in galactic spectra that must not exceed the observed background;
- (3) x_{ion} : the ionization of primordial hydrogen caused by the decay photons of axions must not contribute significantly to the optical depth after recombination;
- (4) *EBL*: photons produced in ALP decays when the Universe is transparent must not exceed the extragalactic background light;
- (5) *CMB*: axions decay photons must not cause spectral distortions in the CMB spectrum;
- (6) *BBN*: the decay of high mass ALPs produces electromagnetic and hadronic showers that must not spoil the agreement of big bang nucleosynthesis (BBN) with observations of primordial nuclei.

8.1.2. Experimental landscape and physics reach of PBC projects in the next 10 years.

Figure 16 shows the physics reach of the proposed PBC experiments, BabyIAXO, IAXO and JURA compared with other experiments currently proposed and/or planned in the world. Both IAXO and JURA projects could be operated on a $\mathcal{O}(10)$ year timescale. Table 4 shows the list of the relevant parameters of the IAXO project, together with the BabyIAXO setup and other past or competing experiments. Table 5 shows the key parameters for the JURA proposal.

The experiments planned or proposed in the world that could be able to produce results earlier or on the same timescale of the PBC projects are listed below.

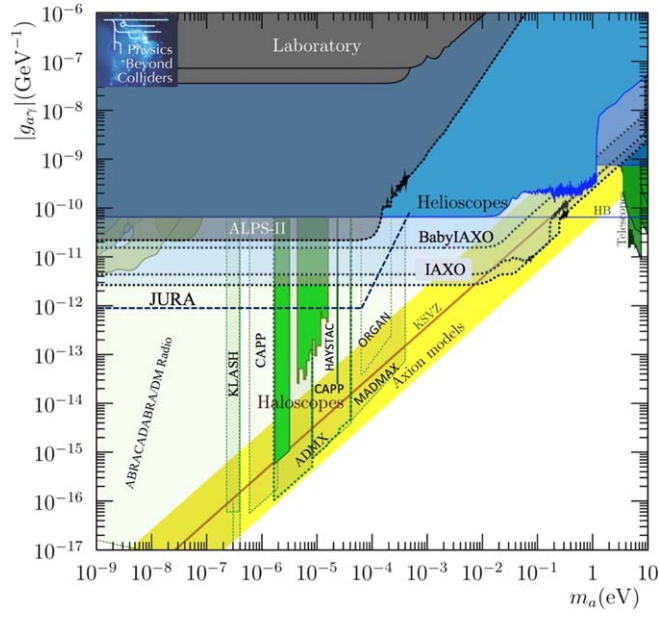


Figure 16. Physics reach of Baby-IAXO, IAXO and JURA compared with other experiments currently proposed and/or planned in the world. Revised from [39]. See text for details.

Table 4. List of the relevant parameters of the IAXO project, together with the Baby-IAXO setup and other past or competing experiments. For the meaning of the parameters see equation (8.1).

Experiment	Status	B (T)	L (m)	A (cm ²)	N (counts keV ⁻¹ cm ⁻² s ⁻¹)	t (years)
BNL E840 [177]	End	2.2	1.8	130		
SUMICO [178]	End	4	2.5	18		
CAST [169]	Running	9	9.3	30	10^{-6}	1.1
TASTE [179]	Proposal	3.5	12	2.8×10^3	5×10^{-7}	3
BabyIAXO	Design	2.5	10	2.8×10^3	1×10^{-7}	1
IAXO	Design	2.5	22	2.3×10^4	1×10^{-8}	3 + 3 (gas)

Table 5. Key parameters of the JURA proposal.

Parameter	Value
Magnetic field	13T × 426 m
Laser wavelength	1064 nm
Production cavity circulating power	2.5 MW
Amplification in regeneration cavity	10^5
Detector noise	10^{-4} s ⁻¹
Measuring time	4 weeks

8.1.3. LSW experiments.

(1) *ALPS II*

In a photon regeneration experiment axions are produced by an electromagnetic beam (laser or microwave) traversing an external dipolar magnetic field. These axions are then reconverted into photons after a wall and can be detected with very sensitive detector combatting only technical and thermal noise.

The pioneer experiment was conducted in Brookhaven by the BFRT Collaboration [45], and the two most recent results are those of the experiments ALPS [46] and OSQAR [47]. ALPS is DESY based and used a decommissioned HERA magnet. It is currently performing a major improvement to phase II, where a set of 10 + 10 HERA magnets will be coupled to two 100 m long Fabry–Perot cavities. ALPS II [48] will in fact take advantage of a resonant regeneration apparatus, thus expecting a major improvement over the current limit on LSW experiment given by OSQAR. ALPS II will represent the current state of the art LSW experiment, and for this reason its activities are monitored with interest by the PBC since they will give key elements to judge the proposal JURA.

8.1.4. Haloscopes.

(1) *HAYSTAC*

HAYSTAC is a high frequency version of the Sikivie detector, planned by a group that was Collaborating with ADMX. Its most notable feature is the use of a Josephson parametric amplifier with very low noise temperature, allowing the experiment to reach cosmological sensitivity in the mass region around 20 μeV . [180].

(2) *KLASH*

WISPDMMX and KLASH proposals aim at studying the low mass region (0.1–1 μeV), by employing large resonator and refurbished magnets from high energy physics experiments [181].

(3) *CAPP*

Activities on axion searches are also pushed forward by the South Korean Center for Axion and Precision Physics-CAPP. The initiative *CULTASK* [182] is a CAPP based standard haloscope whose strength is the development of very high field large bore magnets, with fields up to 35 T and above. A CAPP-CAST Collaboration [183] is also ongoing to use rectangular cavities embedded inside the CAST magnet, while the CAPP initiative ACTION [184] studies the use of toroidal geometry.

(4) *ORGAN*

ORGAN plans to study the higher mass region in the 50–200 μeV range, with specially designed resonant systems [185].

8.1.5. Other techniques with photon-coupling. The search for axions with masses above tens of μeV is very challenging when using resonant cavity detectors. Typically the useable cavity volume is reduced but also other factors like a decrease in the technically achievable resonant enhancement are a challenge. In view of this, new initiatives are being developed where the detectors are broadband and instrumenting large volumes. The explored coupling is still the one with the photon, and again there is the need for large volume of high static magnetic field.

(1) *BRASS and MADMAX*

By exploiting the axion induced electric field on a boundary immersed in a static magnetic field [186], the BRASS experiment will use a magnetized 8 m radius disk

immersed in a 1 T static magnetic field to study the mass region $10 \mu\text{eV}$ – 10meV simultaneously. At the moment it is at very preliminary stage. The same concept of radiating disk is at the heart of MADMAX experiment [187], where, however, a multiple disk configuration is used to obtain resonant enhancement, albeit with a relatively large width of the resonance. This Collaboration is already being developed and it is in the R&D phase.

(2) *DM Radio and ABRACADABRA*

Another method for ultra low mass dark matter axion detection is the use of a lumped element LC resonator inside a strong magnet, where an alternating current is induced by the axion field. Studies are underway to implement such idea within the ADMX magnet for a detector with sensitivity in the mass region below $1 \mu\text{eV}$. The *DM radio* experiment [188] is based on the same idea but uses a tunable LC resonator shielded by a superconducting structure and read by a SQUID. *ABRACADABRA* [189] is a 1m scale broadband detector based on a toroidal magnet equipped with with a superconducting pick up loop read by SQUID. Again, the best sensitivity is obtained for masses below $1 \mu\text{eV}$. All these efforts are just finalizing their R&D phase and should come out with first data in a few years.

9. Physics reach of PBC projects in the MeV–GeV mass range

As detailed in section 5, PBC examines the comprehensive physics case for 6 different proposals that aim to study the hidden sector in the MeV–GeV mass range exploiting the PS and SPS accelerator complex. In addition, this is compared to the physics reach in the same mass range of several proposed experiments at the LHC interaction points. In this section their physics reach is presented, compared against each other and put in the worldwide context. The presentation of the results follows the scheme outlined in section 2.1 where 11 benchmark cases were identified as theoretically well motivated target areas to explore. The 11 benchmark cases do not pretend to be exhaustive, but only to provide a common ground to compare different sensitivities from different experiments. These benchmark cases should be considered as the starting point towards a comprehensive investigation of hidden sector models in the MeV–GeV mass range that could be performed in the future.

The results are shown in the next sections as 90% CL exclusion limits and compared to the existing bounds and the physics reach of other similar initiatives proposed worldwide on the same timescale.

It is important to remark that the level of maturity in compiling these curves is highly non homogeneous among the PBC proposals. As a matter of fact, the physics reach of upgrades of existing experiments (as NA62⁺⁺ or NA64⁺⁺) can already rely on a deep understanding of the experimental effects and a realistic analysis of the levels of the backgrounds based on collected data. New, but already consolidated projects (as, e.g. LDMX and SHiP) can profit from detailed Monte Carlo simulations and a thorough level of understanding of possible background sources. More recent proposals, instead, are in the process of implementing a full simulation and for this study they have evaluated their physics reach mostly based on toy Monte Carlo or fast simulation. As a consequence, they should be taken with many caveats.

The 90% CL exclusion curves can be interpreted as 3σ discovery in case the backgrounds are maintained below a fraction of an event. In case of discovery in the visible channels, only experiments equipped with spectrometers providing mass measurements and particle identification will be able to understand the physics behind the signature.

Table 6. Current status of the understanding of the main backgrounds and experimental efficiencies considered by the PBC proposals in the evaluation of their physics reach.

Proposal	Background	Efficiency	Based on
At the PS:			
RedTop	Included	Included	Full simulation
At the SPS:			
KLEVER	$K_L \rightarrow \pi^0 \nu \bar{\nu}$, $K_L \rightarrow \pi^0 \pi^0$ bkg included	Included	Main backgrounds and efficiencies evaluated with fast simulation and partly validated with the full (NA62-based) Monte Carlo
LDMX	Background included	Included	Full GEANT4 simulation for 4 GeV beam
NA62 ⁺⁺	Zero background proven for fully reconstructed final states	Partially included	Analysis of $\sim 3 \times 10^{16}$ pot in dump mode
NA64 ⁺⁺ (<i>e</i>)	Included	Included	Background, efficiencies evaluated from data
NA64 ⁺⁺ (μ)	In progress	In progress	Test of the purity of the M2 line with COMPASS setup
NA64 ⁺⁺ ($K_{S,L}$, η , η')	To be done	Not included	—
AWAKE/NA64	To be done	Not included	—
SHiP	Zero background	Included	Full GEANT4 simulation, digitization and reconstruction ν -interactions based on 2×10^{20} pot μ -combinatorial and μ -interactions based on $\sim 10^{12}$ pot measurement of the muon flux at H4 performed in July 2018
At the LHC:			
CODEX-b	Zero background assumed (preliminary GEANT4 simulation)	Not included	Evaluation of background in progress with full MC
FASER	Zero background assumed	Not included	FLUKA simulation and <i>in situ</i> measurements
MATHUSLA200	Zero background assumed	Not included	FLUKA, Pythia and MadGraph simulation for ν - μ - fluxes from the LHC IP and cosmic rays background.
MilliQan	Included	Included	Full GEANT4 simulation of the detector

The experiments are described in detail in sections 5 and 6. The relevant facts pertaining the current situation on the level of maturity of each project are collected below and summarized in table 6. These considerations should be taken into account when comparing sensitivity curves across the proposals.

PBC proposals on a 5 year timescale

(1) $NA64^{++}(e)$

The $NA64^{++}(e)$ sensitivity curves assume to collect 5×10^{12} eot at the current H4 line where the existing NA64 experiment has already collected $\mathcal{O}(10^{12})$ eot. The projection is based on the knowledge of the experimental efficiencies and background levels measured in the current run and assumes an upgrade of the detector that must be able to cope with the increased $\times(5 - 10)$ beam intensity.

(2) $NA64^{++}(\mu)$

The $NA64^{++}(\mu)$ sensitivity curves assume an integrated yield of 5×10^{13} muons-on-target (mot) that can be collected in ~ 1.5 years. This data taking is supposed to start during Run 3 (Phase I) and finalized in Run 4 (Phase II). The status of the proposal, along with a thorough evaluation of the beam purity and the main background sources, is summarized in a recent Addendum⁵⁷ sent to the SPSC.

(3) $NA62^{++}$

The $NA62^{++}$ sensitivity curves assume collecting $\mathcal{O}(10^{18})$ pot in dump mode by 2023. The backgrounds and experimental efficiencies have been partially included in the curves: their estimate is based on $\sim 3 \times 10^{16}$ pot dataset already collected in a few days of operation in dump mode during the recent 2016–2018 run.

(4) $FASER 150 fb^{-1}$

FASER in its initial phase will be a small detector of 10 cm radius and 1.5 m length. It is planned to be installed during LS2 in T112 480 m downstream of the ATLAS IP and shielded by 90 m of rock. The sensitivity curves assume 100% detection and reconstruction efficiency and zero background. While a full simulation of the detector is still do be done, a preliminary study with FLUKA has shown that possible backgrounds of high-energy (>100 GeV) particles and radiation levels at the FASER location are very low. Moreover, an emulsion detector and a battery-operated radiation monitor installed at the FASER site in June 2018 is helping to validate and complement the current background estimates.

PBC proposals on a ~ 10 – 15 timescale

(1) *REDTOP*

The REDTOP sensitivity curves assume a dataset of 2×10^{17} pot that can be collected in two years of run at the PS, one year at the energy corresponding to the η threshold of 1.7–1.9 GeV and one year at the η' threshold, 3.5 GeV. Detector efficiency and backgrounds have been evaluated with the full Monte Carlo and included in the results. The fact that the detector, including the optical TPC, could be ready in order to take data during Run 3, as claimed by the Collaboration, is instead an open question. REDTOP's main physics goal is to search for BSM physics in ultra-rare η and η' decays⁵⁸. As part of that physics program, REDTOP can also explore hidden sector physics in a similar parameter space as the $NA62^{++}$ and SeaQuest experiments, but using a very different

⁵⁷ CERN-SPSC-2018-024/SPSC-P-348-ADD-3.

⁵⁸ See <http://redtop.fnal.gov/the-physics/>.

experimental technique (the η/η' decays) with respect to beam dump methods and thus with different systematic uncertainties and background sources.

(2) *SHiP*

An extensive simulation campaign was performed to optimize the design of the muon shield as well as develop a selection that reduces all possible sources of background to <0.1 events over the experiment lifetime. The backgrounds considered were: neutrinos produced through the initial collision that undergo deep inelastic scattering anywhere in the SHiP facility producing V^0 s; muons deflected by the shield that undergo deep inelastic scattering in the experimental hall or anywhere within the decay volume producing V^0 s; muons in coincidence from the same spill (combinatorial muons) escaping the shield; cosmic muons interacting anywhere in the decay volume or with experimental hall. The rate and momentum spectrum of the muon halo obtained with the full simulation is being calibrated using data from a dedicated 1 month long run performed in July 2018 where a smaller replica of the SHiP target was exposed to $\sim 5 \times 10^{11}$ 400 GeV protons.

All samples relied on GEANT4 to simulate the entire SHiP target, muon shield, detector, and experimental hall (walls, ceiling, floor). In addition, neutrino interactions were simulated through GENIE. A comprehensive study of background sources and other experimental effects is reported in the SHiP document submitted in 2018 to the SPSC⁵⁹.

(3) *KLEVER*

The results obtained in this study are based on the fast simulation described in section 6.1. Particle production in the target and propagation of the neutral beam through the beamline elements has been studied with a detailed FLUKA simulation and parameterized for the fast simulation. An effort is underway to develop a comprehensive simulation based on the NA62 Monte Carlo and reconstruction framework with the new detectors added and input from the FLUKA simulation of the neutral beam. A preliminary version of this simulation was used to validate the acceptance calculation for signal events.

(4) *LDMX*

A thorough investigation of all the possible background sources and experimental effects has been performed by the LDMX Collaboration [78] for a 4 GeV electron beam, with on average 1 electron per bunch and 46 MHz repetition rate. These are the baseline conditions for LDMX at the DASEL facility on LCLS-II at SLAC. LDMX @ eSPS should be operated with a 16 GeV electron beam energy, a higher repetition rate, and higher e^- multiplicity per bunch. The evaluation of the background in this operation mode is still to be done but no major showstopper is expected.

(5) *CODEX-b*

The CODEX-b detector geometry has been integrated into the LHCb simulation, with the help of the LHCb simulation team. This allows for a full simulation of collisions in IP8, including both the particles passing through the LHCb and CODEX-b detector volumes, and allows both realistic tracking studies and studies of correlations between signals in CODEX-b and activity in LHCb to be performed. In parallel a measurement of the backgrounds in the DELPHI cavern during nominal LHC operation at IP8 has been carried out in summer 2018 in order to calibrate the GEANT4 simulation. A lot of work is ongoing but, as to date, the assumption of zero-background assumed in the compilation of the sensitivity curves in the following sections is still to be proven.

⁵⁹ *SHiP Experiment—Progress Report*, CERN-SPSC-2019-010, SPSC-SR-248.

(6) *MATHUSLA200*

The assumption of zero background for a large (200×200) m² surface detector that is crossed by tens of MHz of cosmic rays in all directions is a strong assumption that has to be proven. The surface location shields MATHUSLA from ubiquitous QCD backgrounds from the LHC collision, and it was quantitatively demonstrated that muon and neutrino backgrounds from the LHC IP can be sufficiently rejected. Background estimates using a combination of detailed Monte Carlo studies with full detector simulation, the known cosmic ray spectrum, and empirical measurements at the LHC using a test stand detector, are currently in progress. However no quantitative analysis based on the full GEANT4 simulation of the detector geometry has been shown.

(7) *FASER2*

If FASER is successful, a larger version of the detector, with an active volume of 1 m radius and 5 m length could be installed during LS3 and integrate 3 ab^{-1} during the HL-LHC era. However this installation would require non negligible engineering, as the extension of the TI12 or the widening the adjacent staging area UJ12. This makes FASER2 at the moment less certain. All the considerations related to background estimates done for FASER apply to FASER2, with the additional caveat that an increase of background is expected during the HL-LHC operation.

9.1. *Vector portal*

In the case of a vector mediator or *dark photon*, several constraints have been set depending on the assumption that the mediator can decay directly to dark matter (DM) particles (χ) (*invisible decays*) or has a mass below the $2 \cdot m_\chi$ threshold and therefore can decay only to SM particles (*visible decays*).

9.1.1. Minimal dark photon model (BC1). In the minimal dark photon model, the SM is augmented by a single new state A' . DM is assumed to be either heavy or contained in a different sector. In that case, once produced, the dark photon decays back to the SM states. The parameter space of this model is then $(m_{A'}, \epsilon)$ where $m_{A'}$ is the mass of the dark photon and ϵ the coupling parameter of the Dark Photon with the standard photon.

Current bounds

Visible decays of vector mediators are mostly constrained from searches for di-electron or di-muon resonances [190–192] and from the re-interpretation of data from fixed target or neutrino experiments in the low (< 1 GeV) mass region [193–195], NA48/2 [191], A1 [192] and BaBar [190] experiments put the strongest bounds for $\epsilon > 10^{-3}$ in the 0.01–10 GeV mass range. They search for a bump in the e^+e^- or $\mu^+\mu^-$ invariant mass distribution over a smooth background. These experiments consider a variety of dark photon production mechanisms, such as meson decays (NA48/2 [191]), bremsstrahlung (A1 [192]), and annihilation (BaBar [190], KLOE [196–199], LHCb [200]). These results are complemented by those from beam dump experiments, such as E141 [193] and E137 [194, 201] at SLAC, E774 at Fermilab [195], CHARM [202, 203] and NuCal [204]. The KOTO experiment has also set recently a limit on the $BR(K_L \rightarrow \pi^0 X) < 2.4 \times 10^{-9}$ (90% CL) [205] that could partially fill of the hole of the E949 coverage around $m = m_{\pi^0}$.

Existing limits in the plane mixing strength versus mass of the dark photon are shown in figure 17. In the following we briefly detail the contributions by classifying them as a function of the experimental technique used.

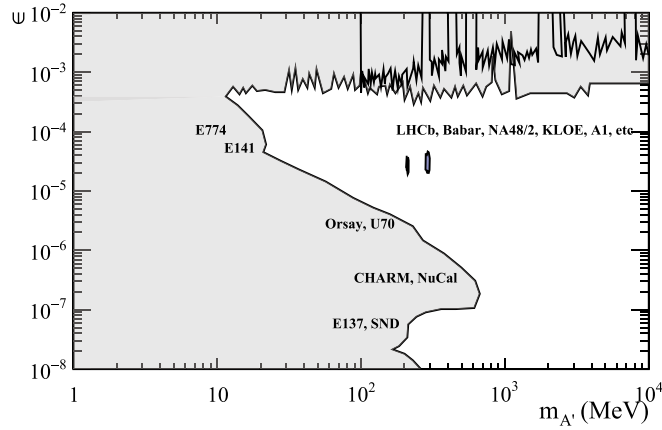


Figure 17. Current limits for dark photon in visible decays in the plane mixing strength ϵ versus mass of the dark photon $m_{A'}$.

1. Searches for dilepton resonances:

- (1) *NA48/2 @ CERN*: searches for dark photon decays to e^+e^- final state in the decay chain $\pi^0 \rightarrow \gamma A'$ using $\sim 2 \times 10^7$ fully reconstructed $\pi^0 \rightarrow \gamma e^+e^-$ decays collected in 2003–2004 [191].
- (2) *BaBar @ KEK*: searches for a dark photon in the reaction $e^+ + e^- \rightarrow \gamma + A'$, $A' \rightarrow e^+e^-$, $\mu^+\mu^-$ using 514 fb^{-1} of data [190].
- (3) *KLOE @ DAFNE*: searches for dark photon in visible final states using a large variety of production modes, such as meson decay ($\phi \rightarrow \eta A'$), and annihilation ($e^+ + e^- \rightarrow \gamma + A'$) [196–199].
- (4) *LHCb*: inclusive di-muon search in pp collisions at $\sqrt{s} = 13 \text{ TeV}$ performed with the current Run 2 LHCb data above the di-muon threshold [200].

2. Reinterpretation of data of fixed target experiments:

- (1) *E137 @ SLAC (electron beam dump)*: E137 was an experiment conducted at SLAC in 1980–1982 where a 20 GeV electron beam was dumped on a target. Dark matter interacting with electrons (e.g. via a dark photon) could have been produced in the electron-target collisions and scattered off electrons in the E137 detector, producing the striking, zero-background signature of a high-energy electromagnetic shower that points back to the beam dump [194, 201].
- (2) *CHARM @ CERN (proton beam dump)*: the CHARM Collaboration performed a search for ALPs decaying to photon, electron or muon pairs using the 400 GeV, 2.4×10^{18} protons-on-target (pot) dumped on a thick copper target distant 480 m from the 35 m long decay volume [202].
- (3) *E141 @ SLAC (electron beam dump)*: the E141 Collaboration searched for high-energy positron signals from a hypothetical $X^0 \rightarrow e^+e^-$ decay, produced in the interactions of 2×10^{15} 9 GeV electrons dumped on a 10 and 12 cm long W -target [193].
- (4) *E774 @ Fermilab (electron beam dump)*: the E774 Collaboration used 5.2×10^9 eot from an electron beam of 275 GeV at FNAL. A hypothetical X^0 particle could have been produced by bremsstrahlung in the dump and then decays to e^+e^- pairs in the ~ 2 m long decay volume [195].

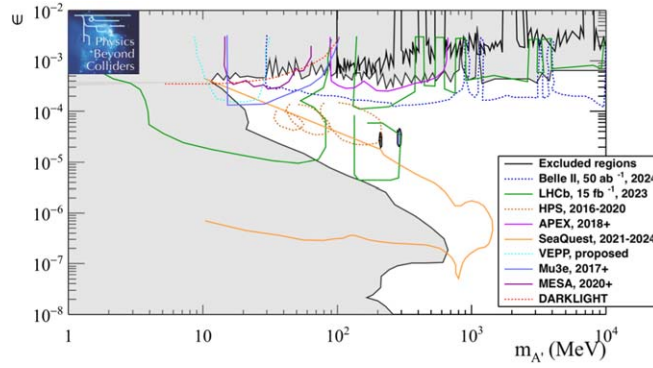


Figure 18. Future upper limits at 90% CL for dark photon in visible decays in the plane mixing strength ϵ versus mass $m_{A'}$ from experiments and proposals not related to the PBC activity.

Future experimental landscape

Several experiments and proposals not considered in the PBC activity will search for dark photons in decays to visible final states using different types of beams and experimental techniques. The projections of their sensitivity in the near future are shown in figure 18. The status of these projects is briefly reported in the following.

- (1) *Belle-II @ KEK*: will search for visible dark photon decays $A' \rightarrow e^+e^-, \mu^+\mu^-$ where A' is produced in the process $e^+ + e^- \rightarrow A' + \gamma$. Projections are based on 50 ab^{-1} . Timeline: data taking started in 2018, expected about 50 ab^{-1} by 2025 [206].
- (2) *LHCb @ CERN*: LHCb will search for dark photon in visible final states both using the inclusive di-muon production [207] and the $D^{*0} \rightarrow D^0 e^+ e^-$ decays [208]. The D^{*0} search will cover dark photon masses from the di-electron mass threshold up to 1.9 GeV. The D^{*0} search requires the upgrade of the current LHCb trigger system, currently scheduled during 2019–2020. The projections are based on 15 fb^{-1} , 3 years data taking with $5 \text{ fb}^{-1}/\text{yr}^{-1}$ with an upgraded detector after Long Shutdown 2.
- (3) *HPS @ JLAB*: electron beam-dump at CEBAF electron beam (2.2–6.6 GeV, up to 500 nA), search for visible ($A' \rightarrow e^+e^-$) dark photon (prompt and displaced) decays produced via bremsstrahlung production in a thin W target. The experiment makes use of the 200 nA electron beam available in Hall-B at Jefferson Lab. Of the 180 PAC-days⁶⁰ granted, HPS collected data for 1.7 PAC-days in 2015 (engineering run) at 1.06 GeV beam energy and 5.4 PAC-days for a physics run in 2016 at 2.3 GeV. Results of the 2015 analysis are reported in [209]. A 28 PAC-days data taking at 4.55 GeV beam energy is expected in Summer 2019 [210].
- (4) *APEX @ JLAB*: electron beam dump at CEBAF electron beam, search for visible dark photon decays. Status: planned one-month physics run in 2018–2019 [211, 212].
- (5) *SeaQuest @ FNAL*: will search for visible dark photon decays $A' \rightarrow e^+e^-$ at the 120 GeV Main Injector beamline at FNAL. SeaQuest plans to install a refurbished electromagnetic calorimeter (ECAL) from the PHENIX detector at Brookhaven National Laboratory within the next few years. The Collaboration plans to submit an official proposal to the Fermilab physics advisory committee in 2019 to install the ECAL at the end of the next polarization target run in 2021 and acquire $\sim 10^{18}$ (10^{20}) pot by 2024

⁶⁰ 1 PAC-day = 2 calendar days.

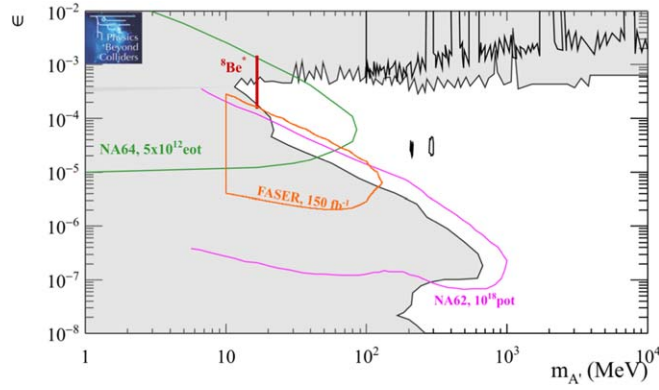


Figure 19. PBC projects on ~ 5 year timescale: upper limits at 90% CL for dark photon in visible decays in the plane mixing strength ϵ versus mass $m_{A'}$. The vertical red line shows the allowed range of e - X couplings of a new gauge boson X coupled to electrons that could explain the ${}^8\text{Be}$ anomaly [73, 74].

(2030s). The 10^{20} pot yield could be collected as a result of the Fermilab Proton Improvement Plan [105, 213].

- (6) *VEPP3 at BINP*: missing mass method and visible decay searches at BINP at Novosibirsk. Dark photons are produced by colliding a 500 MeV positron beam on an internal gaseous hydrogen target, and both visible and invisible (via the missing mass mode) final state are identified. Timeline: First run is anticipated for 2019–2020 [214].
- (7) *Mu3e @ PSI*: Search for $\mu \rightarrow eee$ decay at PSI. Phase I: sensitivity 2×10^{-15} with the existing muon line, from proton cyclotron of 2.4 mA protons at 590 MeV. Phase II: sensitivity of 10^{-16} with upgraded muon line.
- (8) *MAGIX at MESA (Mainz, Germany)*: is a step beyond the traditional visible dark photon decay searches with a dipole spectrometer at the 105 MeV polarized electron beam at A1/MAMI. The MESA accelerator has $E_{\text{max}} = 155$ MeV energy, and up to 1 mA current. The MAGIX detector is a twin arm dipole spectrometer placed around a gas target. Production mechanism similar to HPS and identification through a di-electron resonance. The possibility of a beam dump setup similar to BDX is under study. Timeline: Proposal in 2017 with targeted operations in 2021–2022 and 2 years of data taking [215].

Physics reach of PBC projects on 5 and 10–15 year timescales

Figure 19 shows the 90% CL exclusion limits for searches for dark photons decaying to visible final states performed by PBC proposals that might produce results on ~ 5 year timescale: NA64 $^{++}(e)$, NA62 $^{++}$ and FASER with 150 fb^{-1} . These projects will be competing with other initiatives in the same timescale, as for example SeaQuest, HPS and LHCb, as shown in figure 18.

The physics reach of PBC projects on a 10–15 year timescale is shown in figure 20. On this timescale several projects could be ready and operated, such as REDTOP, SHiP, FASER2, MATHUSLA200, AWAKE, and LDMX. The sensitivity for dark photons decaying in visible final states will be dominated by SHiP, while FASER2, LDMX and AWAKE will be directly competing with SeaQuest, LHCb, HPS, and others as shown in figure 18. MATHUSLA200 in this scenario is however not competitive, mostly due to the fact that the dark photon is produced in the forward direction.

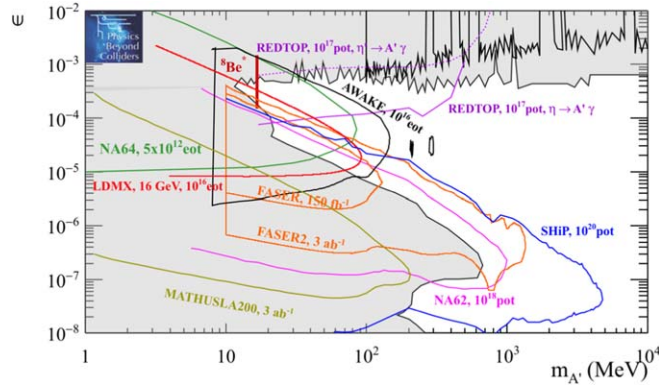


Figure 20. Future upper limits at 90% CL for dark photon in visible decays in the plane mixing strength ϵ versus mass $m_{A'}$ for PBC projects on a ~ 10 – 15 year timescale. The vertical red line shows the allowed range of e – X couplings of a new gauge boson X coupled to electrons that could explain the ${}^8\text{Be}$ anomaly [73, 74].

9.1.2. Dark photon decaying to invisible final states (BC2). This is the model where minimally coupled viable WIMP dark matter model can be constructed with a dark photon as light mediator. Preferred values of the dark coupling $\alpha_D = g^2 D/4\pi$ are such that the decay of A' occurs predominantly into DM $\chi\bar{\chi}$ states. These states can further rescatter on electrons and nuclei due to ϵ -proportional interaction between SM and DM states mediated by the mixed AA' propagator. The parameter space for this model is $(m_{A'}, \epsilon; m_\chi; \alpha_D)$ with further model-dependence associated with the properties of the dark matter candidate χ (boson or fermion).

The sensitivity plots for this benchmark case can be shown in two ways:

- (a) the plane ϵ versus $m_{A'}$ where $\alpha_D^2 \gg \epsilon\alpha_D$ and $m_{A'} > 2m_\chi$;
- (b) the plane y versus m_χ plot where the ‘yield’ variable y , $y = \alpha_D \epsilon^2 (m_\chi/m_{A'})^4$, is argued to contain a combination of parameters relevant for the freeze-out and DM–SM particles scattering cross section. Here α_D is the dark fine structure constant that describes the interactions between dark photon and dark matter. The coupling of the dark photon to SM particles happens via the *millicharge* ϵe . The choice adopted by the PBC is $\alpha_D = 0.1$ and $m_{A'}/m_\chi = 3$.

In case (b), the yield variable y can be put in direct connection to the DM thermal relic abundance. In fact, the direct DM annihilation responsible of the thermal relic abundance, is driven by the same couplings that define the direct DM scattering, leading to rather well defined predictions:

$$\langle \sigma \cdot v \rangle \sim \frac{y}{m_\chi},$$

where v is the velocity. The measured dark matter abundance imposes a minimum bound on this cross-section, $\langle \sigma \cdot v \rangle > \langle \sigma \cdot v \rangle_{\text{relic}}$. This lower bound can be translated in turn into a lower bound on the strength of the SM-mediator and DM-mediator couplings, and, as a consequence, opens up the possibility to link results obtained at accelerator-based experiments to those coming from DM direct detection experiments, depending on the nature of the DM candidate. Two cases considered in this study are Elastic Scalar and Pseudo-Dirac fermion dark matter.

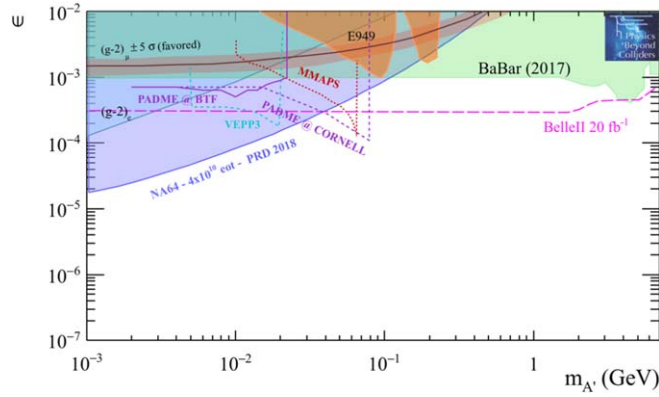


Figure 21. Current limits (filled areas) and experimental landscape for projects not PBC related (solid or dashed lines) for dark photon in invisible decays in the plane mixing strength ϵ versus dark photon mass $m_{A'}$.

Current bounds and future experimental landscape

In case of dark photons with invisible decays, the strongest limits on the coupling strength of DM with light vector mediator for DM and mediator masses in the MeV–GeV range are provided by the NA64 experiment [70], and from a recent result on mono-photon search from BaBar [216]. Limits in the low mass range come from a re-interpretation by theorists of old results from the liquid scintillator near detector (LSND) [217] and E137 [201] experiments, and as such, should be taken with many caveats. A re-analysis of electron-scattering data from direct detection experiments has led to constraints in the sub-GeV DM region [218, 219]

(a) *Plane ϵ versus $m_{A'}$* Figure 21 shows the current 90% CL upper limits in the plane ϵ versus $m_{A'}$ from BaBar [216], E787/E949 [220, 221] and NA64 [70] as filled areas and future perspectives from projects not PBC related as solid or dashed curves. The region preferred by the $(g - 2)_\mu$ puzzle [222] is also shown in the plot. Most of the future projections come from experiments using the missing momentum/missing mass techniques, as explained below.

- (1) *Belle II @ KEK:* search for dark photons in the process $e^+ + e^- \rightarrow A' + \gamma$, $A' \rightarrow$ invisible relies on a L1 trigger sensitive to mono-energetic ISR photon with energy $E = (E_{CM}^2 - M_{A'}^2)/2E_{cm}$. A trigger threshold as low as 1.2 GeV is anticipated to be applied for the 2018–2019 dataset, corresponding to $\sim 20 \text{ fb}^{-1}$ of data. [206].
- (2) *MMAPS @ Cornell:* MMAPS aims at searching for dark photons in the process $e^+ + e^- \rightarrow A' + \gamma$ using the interactions of a 5.3 GeV positron beam extracted from the Cornell synchrotron with a fixed Be target. The measure of the outgoing photon kinematics with a CsI calorimeter allows to infer the A' mass. This method provides sensitivity to all possible decay modes. The main limitations arise from the detector resolution and QED backgrounds, such as $e^+ + e^- \rightarrow \gamma + \gamma$ or $e^+ + e^- \rightarrow e^+ + e^- \gamma$ where charged final particle(s) sometimes escape undetected.
Timeline: proposal stage, no starting date (>2020).
- (3) *PADME @ LNF:* missing momentum searches at the Beam Test Facility (BTF) in LNF. The principle is similar to the MMAPS experiment, using a 550 MeV positron beam on a diamond target. In addition to invisible A' decays, PADME is studying its sensitivity to di-photon decays of ALPs and dark Higgs decays. Timeline: Expected to collect 10^{13} positron on target by end of 2019.

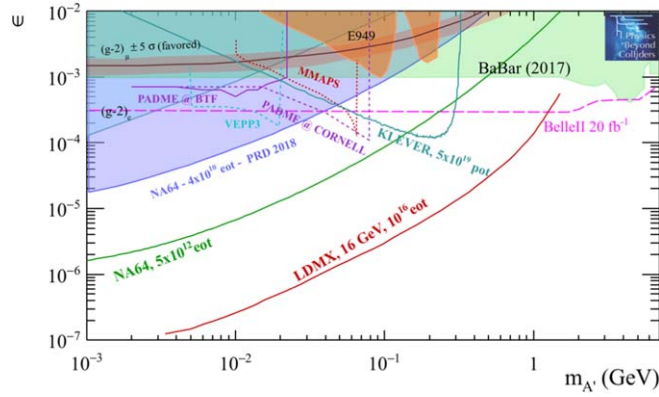


Figure 22. Dark photon decaying to invisible final states. Prospects for PBC projects on a timescale of 5 years (NA64⁺⁺(e), green line) and 10–15 years (LDMX, red line and KLEVER, cyan line) compared to the current bounds (solid areas) and future experimental landscape (other solid and dashed lines) as explained in figure 21.

We do expect NA62 will be able to produce results in the next few years as a by-product of the $K^+ \rightarrow \pi^+ \nu \bar{\nu}$ analysis, but no sensitivity curves have been provided by the Collaboration so far.

Figure 22 show the projections from the PBC experiments. NA64⁺⁺(e) with 5×10^{12} eot will be able to explore a large part of the parameter space on a 5 year timescale. KLEVER could further push the search for dark photons in the invisible final states in the mass region between 100 and 200 MeV as a by-product of the analysis of the $K_L \rightarrow \pi^0 \nu \bar{\nu}$ rare decay. The ultimate sensitivity can be reached by LDMX, either at the DASEL facility with 8 GeV electron beam and even further at the eSPS facility with 16 GeV electron beam at CERN.

(b) *Plane y versus m_χ* The current bounds and future perspectives in the plane y versus DM mass are shown in figure 23 for two different hypotheses on the dark matter nature: Elastic Scalar and Pseudo-Dirac fermion.

In this plot, the lower limits for the thermal relic targets are also shown, under that hypothesis that a single DM candidate is responsible for the whole DM abundance. Under the hypothesis of an elastic scalar DM candidate, limits from direct detection DM experiments, as CRESST-II [223], XENON 10/100 [224, 225] and Super-CDMS [226] can be used, which is not the case for a DM as Pseudo-Dirac fermion hypothesis.

In contrast, results from accelerator-based experiments, are largely independent of the assumptions on the specific DM nature as in this case it is produced in relativistic regime and the strength of the interactions with light mediators and SM particles is only fixed by thermal freeze-out.

Future initiatives that could explore still uncovered parameter space in the plane y versus DM mass for DM masses below 1 GeV are all those that have sensitivity in the plane ϵ versus dark photon mass and, in addition, experiments exploiting DM scattering with nucleons and/or electrons, both accelerator-based and from direct detection searches. Among the accelerator-based experiments, there are BDX at JLab [227], MiniBooNE at FNAL [228] and COHERENT at ORNL [229], as explained below.

- (1) *BDX at JLab (electron beam-dump)*: the Beam Dump eXperiment (BDX) is aiming to detect light dark matter produced in the interaction of an intense electron beam with the dump. The experiment is sensitive to elastic DM scattering $e^- + \chi \rightarrow e^- + \chi$ in the

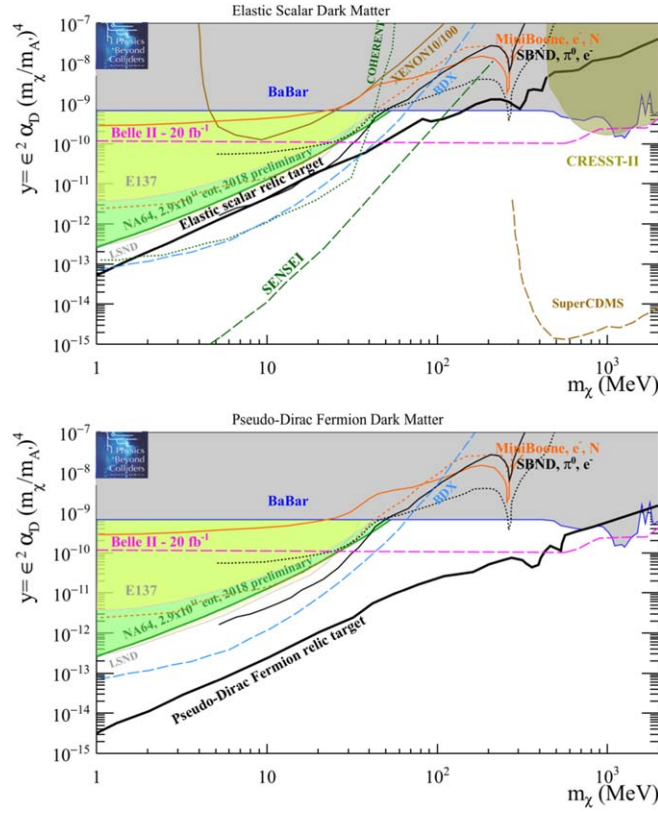


Figure 23. Current limits (filled areas) and experimental landscape for projects not PBC related (solid, dashed, and dotted lines) for dark photon decaying to light dark matter in the plane of the ‘yield’ variable (see text) versus dark matter mass m_χ , assuming DM as an Elastic Scalar particle (top) or Pseudo-Dirac Fermion (bottom). In the limit computation we assume a Dark coupling constant value $\alpha_D = 0.1$ and a ratio between the dark photon A' and LDM χ masses $m_{A'}/m_\chi = 3$.

detector after production in $e^- + Z \rightarrow e^- + Z(+A', A' \rightarrow \chi\chi)$. A detector placed ~ 20 m downstream of the Hall-A beam-dump at Jefferson lab is expected to identify a dark matter scattering by measuring a electromagnetic shower produced by the DM interaction with atomic electrons of the detector. The BDX detector is composed by a \sim GeV electromagnetic calorimeter surrounded by two layers of active plastic scintillator vetos. The calorimeter re-uses ~ 800 CsI(Tl) crystals formerly used in the BaBar EM Cal, upgraded with SiPM-readout and triggerless data acquisition. The experiment makes use of the high energy (~ 10 GeV) and high intensity ($\sim 100 \mu\text{A}$) electron beam available in Hall-A running in parallel (parasitically) with the scheduled hadron physics program. BDX has been approved with the maximum scientific rating (A) by the JLab PAC and granted with 285 PAC-days of data taking, corresponding to an integrated yield of 10^{22} eot. The BDX Collaboration is currently seeking for funds to build the new experimental hall that will host the BDX detector. The experiment is expected to be deployed and take data in 2–3 years from now [227].

- (2) *MiniBooNE @ FNAL (proton beam dump)*: neutrino detector at the 8 GeV Booster Neutrino Beamline at FNAL. MiniBooNE is a 800 ton mineral oil Cherenkov detector situated 490 m downstream of the beam dump. The DM is searched for via the chain $p + p \rightarrow X + \pi^0/\eta$, $\pi^0/\eta \rightarrow \gamma + A'$ and $A' \rightarrow \chi\chi$. The results are based on 1.8×10^{20} pot and have been published for DM-nucleon and electron-elastic scattering [228].
- (3) *COHERENT (proton beam dump)*: the COHERENT Collaboration aims to measure Coherent Elastic Neutrino-Nucleus Scattering using the high-quality pion-decay-at-rest neutrino source at the Spallation Neutron Source in Oak Ridge, Tennessee. The SNS provides an intense flux of neutrinos in the energy range of few tens-of-MeV. The beam has a sharply-pulsed timing structure that is beneficial for background rejection. The current experimental apparatus includes $\mathcal{O}(10\text{ kg})$ NaI(Tl) and CsI(Tl) detectors, and a 35 kg single-phase LAr scintillation detector. The same apparatus can be used to search for dark matter mainly produced via the process $\pi^0/\eta \rightarrow \gamma + A'$ with $A' \rightarrow \chi\chi^*$, where the π^0/η are produced out of collisions from the primary proton beam. The DM candidates are identified through coherent scattering leading to a detectable nuclear recoil. Timeline: currently taking data, upgrade after 2019 [229]⁶¹.
- (4) *SBN @ FNAL (proton beam-dump)*: the SBN program consists of three LAr-based detectors of 112 ton (SBND), 89 ton (microBooNE), and 476 ton (ICARUS-T600) situated at 110 m, 470 m and 600 m downstream the beam dump, respectively, of the 8 GeV primary proton beam of the Booster Neutrino Beamline at FNAL. Dark matter could be primarily produced via pion decays created in the collisions of the protons with the dump and scatter in LAr TPC detectors. SBND is expected to yield the most sensitive results and could improve upon MiniBooNE by more than an order of magnitude with 6×10^{20} pot. Projections shown in figure 23 are based on 2×10^{20} pot.

Several experiments designed to perform direct detection DM searches will be able to put bounds.

- (1) *SENSEI*: is a direct detection experiment that will be able to explore DM candidates with masses in the MeV–GeV range, by detecting the signal released in DM-electron scattering interactions in a fully depleted silicon CCD. For the first time, it has been demonstrated that the charge in each pixel of a CCD—in a detector consisting of millions of pixels—can be measured with sub-electron noise. A 1 g detector is already operating in the NUMI access tunnel. A larger project (100 g) can be deployed at a deeper site on a 1–2 year timescale if funding is obtained [230].
- (2) *CRESST-II*: uses cryogenic detectors to search for nuclear recoil events induced by elastic scattering of DM particles in CaWO₄ crystals. Because of its low-energy threshold, the sensitivity to DM was extended in the sub-GeV region. Current bounds are derived from a dataset corresponding to 52 kg live days [223].
- (3) *XENON 10/100*: DM-electron scattering searches have already illustrated their potential, probing down to $m_\chi > 5\text{ MeV}$ [218, 219] using XENON10 data [224] sensitive to single electrons and down to $m_\chi > 35\text{ MeV}$ [219] using XENON100 data [225].

Physics reach of PBC projects on 5 and 10–15 years timescales PBC projects able to put bounds on the y versus m_χ plane are NA64⁺⁺(e) on a 5 year timescale and LDMX and SHiP on a 10–15 year timescale, as shown in figure 24. NA64⁺⁺(e) and LDMX will use the missing energy/missing momentum techniques, respectively. SHiP, instead, will exploit the

⁶¹ See also <https://sites.duke.edu/coherent/>.

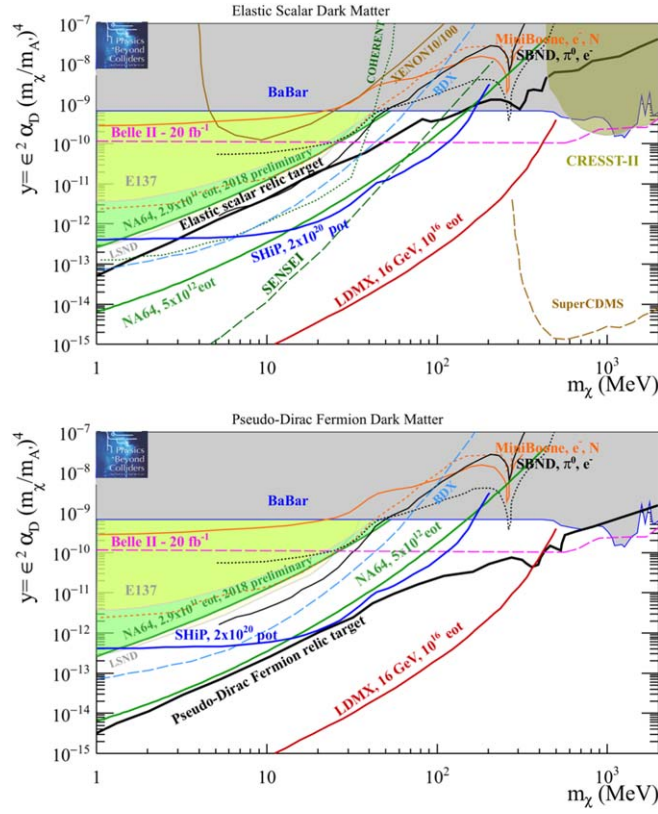


Figure 24. Dark photon decaying to DM elastic scalar (top) or Pseudo-Dirac fermion (bottom) particle. Prospects for PBC projects on a timescale of 5 years (NA64⁺⁺, green line) and 10–15 years (LDMX, red line and SHiP, blue line) are compared to the current bounds (solid areas) and future experimental landscape (other solid and dashed lines). In the limit computation we assume a dark coupling constant value $\alpha_D = 0.1$ and a ratio between the dark photon A' and LDM χ masses $m_{A'}/m_\chi = 3$.

elastic scattering of DM candidates with the electrons in the medium of the emulsion-based neutrino detector. As such, SHiP is fully complementary to the other two.

9.1.3. Milli-charged particles (BC3). Milli-charged particles (mCP) can be seen as a specific limit of the vector portal when $m_{A'}$ goes to zero and the parameter space simplifies to the mass (m_χ) and effective charge ($|Q| = |\epsilon g_D e|$) of milli-charged particles. The suggested choice of parameter space is $(m_\chi, Q_\chi/e)$ and χ can be taken to be a fermion. The searches for millicharged particles can be performed either through missing energy techniques or through minimum ionizing (milli-charged) signals.

A recent review [231] showed the potential of the existing data from MiniBooNE [232] and the LSND [233], and the soon to be released data from MicroBooNE, the ongoing SBN program [234], the Deep Underground Neutrino Experiment (DUNE) [235], beyond the standard electron beam-dump experiments [236, 237] to probe the milli-charged particles model. In the following sections we stick on experimental published bounds and official projections of current experiments and future proposals.

Current bounds and future experimental landscape The most stringent current experimental bounds on millicharged particles arise from the SLAC milliQ experiment [236], the EDGES experiment [238] and from colliders [237].

(1) *SLAC milliQ experiment*

A dedicated search for mQ's has been carried out at SLAC in the late 90s. This search was sensitive to particles with electric charge in the range $(10^{-1}-10^{-5})e$ and masses between 0.1 and 1000 MeV. The experiment, located near the positron-production target of the SLC beam, looked for extremely feebly ionization and/or excitation signals in scintillators counters (down to a single scintillation photon) that might arise from millicharged particles surviving the 110 m sandstone filling the distance between the detector and the positron source [236].

(2) *Colliders*

In the mass region above 100 MeV the strongest direct bounds arise from colliders, mainly from the constraint from the invisible width of the Z, as well as direct searches for fractionally charged particles at LEP [237].

(3) *EDGES experiment*

The unexpected strength of 21 cm absorption signal measured by the Experiment to Detect the Global Epoch of Reionization (EDGES) could be naturally explained [239, 240] if even only a fraction (less than 0.4%) of the dark matter due to CMB constraints [241]⁶² is in form of milli-charged particles. Data from [238], interpretation from [241].

(4) *SuperNovae 1987A bounds*

The number of neutrinos detected on Earth during the explosion of the SN 1987A agree roughly with the theoretical expectations. This allows us to use the generic stellar energy-loss argument that if other particles were contributing to the cooling of the proto neutron star these would have reduced the neutrino fluxes and duration of the neutrino signal.

(5) *milliQan*

Future experimental bounds outside the PBC projects will be set by the milliQan experiment. milliQan has been proposed to be sited in the PX56 Observation and Drainage gallery above the CMS underground experimental cavern (UXC). It consists of one or more scintillator detector layers of roughly 1 m^3 each. The experimental signature would consist of a few photo-electrons arising from the small ionization produced by the mCPs that travel without interacting through material after escaping the CMS detector. milliQan plans to integrate $\sim 150\text{ fb}^{-1}$ during Run 3 and 3 ab^{-1} in the HL-LHC era [245].

(6) *FerMINI*

The FerMINI project [246] is a milliQan-type detector proposed to be installed downstream of the proton target of a neutrino experiment, either in MINOS near detector hall and/or the proposed DUNE near detector hall, both at Fermilab. FerMINI can achieve unprecedented sensitivity for milli-charged particles with mass in the MeV–GeV range and fractional charge Q_χ/e in the $10^{-4}-10^{-1}$ range.

PBC projects on 5 and 10–15 years timescale Three PBC projects have sensitivity to search for milli-charged particles, as shown in figure 25: NA64⁺⁺(e) and NA64⁺⁺(μ) on 5–10 year timescale and LDMX on a ~ 10 to 15 year timescale. NA64⁺⁺(e) with 5×10^{12} eot collected during Run 3 can explore the region with masses between 100 and 1000 MeV

⁶² Even with subcomponent DM, it is likely excluded by direct detection [242, 243]. However this constraint is somewhat uncertain, as it is possible that supernovae evacuate the DM from the disc, and this would nullify the direct detection constraint [244].

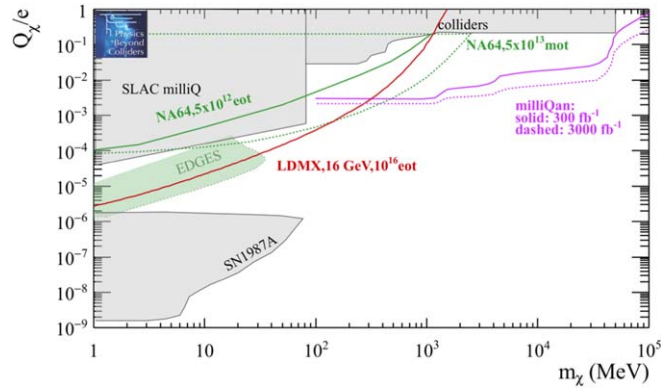


Figure 25. BC3: milli-charged particles. Current bounds (filled areas), experimental landscape and physics reach of PBC projects on 5 years time scale (NA64⁺⁺(*e*) and NA64⁺⁺(*μ*)), and on 10–15 years time scale (LDMX @ eSPS).

and fractional charge $Q/e = 10^{-3} - 10^{-1}$; NA64⁺⁺(*μ*) with 5×10^{13} mot can improve over NA64⁺⁺(*e*) by pushing down the limit of the fractional charge by almost an order of magnitude. LDMX, with an electron beam of 16 GeV momentum and a collected yield of 10^{16} eot will further improve the search in particular in the intermediate (100–1000 MeV) mass region.

9.2. Scalar portal

9.2.1. Dark scalar mixing with the Higgs (BC4 and BC5). A light scalar particle mixing with the Higgs with angle θ can be a mediator between DM and SM particles. The Langrangian to be added to the SM one is of the form:

$$\mathcal{L}_{\text{scalar}} = \mathcal{L}_{\text{SM}} + \mathcal{L}_{\text{DS}} - (\mu S + \lambda S^2) H^\dagger H. \quad (9.1)$$

The minimal scenario (BC4) assumes for simplicity that $\lambda = 0$ and all production and decay processes of the dark scalars are controlled by the same parameter $\mu = \sin\theta$. Therefore, the parameter space for this model is (θ, m_S) . A more general approach (BC5) consists in having both λ and μ being different from zero: in this case, the parameter space is $\{\lambda, \theta, m_S\}$, and λ is assumed to dominate the production via e.g. $h \rightarrow SS$, $B \rightarrow K^{(*)}SS$, $B^0 \rightarrow SS$ etc. In the following we will assume the branching fraction $BR(h \rightarrow SS) \sim 10^{-2}$ in order to be complementary to the LHC searches for the Higgs to invisible channels.

A key feature of the scalar portal is that its production is often proportional to one of the larger Yukawa couplings, y_ν , in the case of the EW penguin, while its decay is controlled by one of the smaller Yukawa’s or the induced gluon coupling. This means that it is natural for dark scalars to be both long-lived and be produced at a relatively large rate, which makes them an excellent target for the proposals discussed in this study.

Current bounds and future experimental landscape Figure 26 shows the current bounds on the mixing parameter $\sin^2\theta$ versus the mass of the dark scalar m_S . Bounds on this scenario come from recast of data from old beam dump experiments [247, 248], bump hunt in visible *B* meson decays [249–251] and cosmological and astrophysical arguments, as explained below.

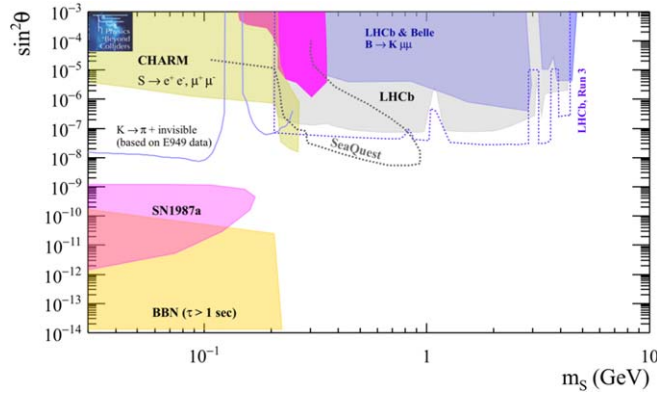


Figure 26. BC4: Dark scalar mixing with the Higgs. Current limits (filled areas) and experimental landscape (solid and dotted curves) for searches for dark scalar in the plane coupling strength ($\sin^2 \theta$) versus dark scalar mass m_s .

(1) *CHARM*

The CHARM Collaboration has put bounds on light ALPs using a 400 GeV proton beam impinging on a copper target [202]. Figure 26 shows the reinterpretation of the CHARM data from [248] as yellow shaded region.

(2) *Visible Meson Decays*

A visibly decaying scalar mediator can contribute to the processes $B^+ \rightarrow K^+ \mu^+ \mu^-$ and $B^0 \rightarrow K^{*0} \mu^+ \mu^-$, which are tightly constrained by LHCb [249, 250] and Belle [251] measurements. In the same parameter space, we also show bounds computed by us⁶³ based on the measurement of the $K^+ \rightarrow \pi^+ \nu \bar{\nu}$ branching fraction from E949 experiment [252].

(3) *BBN*

A sufficiently light ($M < 10$ MeV), weakly coupled scalar particle with a thermal number density can decay appreciably during BBN and spoil the successful predictions of light element yields accumulated in the early universe.

(4) *Supernovae*

A light, weakly coupled scalar mediator can be produced on shell during a supernova (SN) explosion and significantly contribute to its energy loss, thereby shortening the duration of the observable neutrino pulse emitted during core collapse. The most significant constraint arises from SN1987a which has been used to constrain the parameter space for axions and ALPs [253–256].

Searches in the near (~ 5 years) future will be performed by: SeaQuest at FNAL [105], using the same dataset for the search for a dark photon into $e^+ e^-$ final state as explained in section 9.1; LHCb will update the bump hunt in $B \rightarrow K \ell^+ \ell^-$ decays with an integrated luminosity of $\sim 15 \text{fb}^{-1}$ which is expected to be collected during Run 3. NA62 in kaon-mode will be able to explore the mass range below the kaon mass, as a side product of the measurement at $\mathcal{O}(10\%)$ accuracy of the rare decay $K^+ \rightarrow \pi^+ \nu \bar{\nu}$, by interpreting it as $K^+ \rightarrow \pi^+ S$. The NA62 search should be able to push down the limit currently set by the E949 experiment by, at least, an order of magnitude, even if official projections have not yet been made by the Collaboration.

⁶³ M Moulson, KLEVER Collaboration.

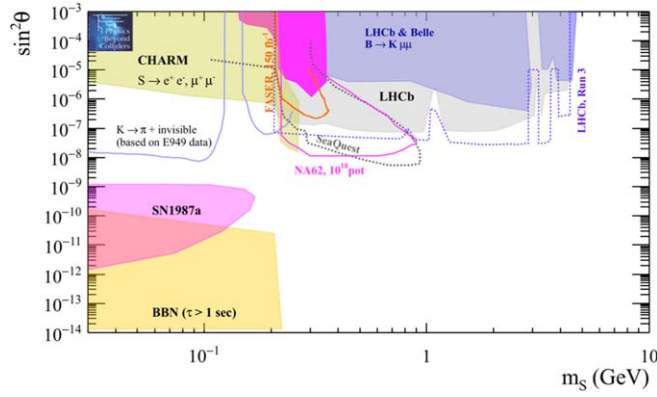


Figure 27. BC4: prospects on 5 year timescale for PBC projects for the dark scalar mixing with the Higgs in the plane mixing angle $\sin^2\theta$ versus dark scalar mass m_s . The two PBC projects that can provide results on 5 year timescale are NA62⁺⁺ and FASER.

Physics reach of PBC projects on 5 and 10–15 year timescale Figure 27 shows the sensitivity of FASER during its first phase of data taking during Run 3, and NA62⁺⁺ in dump mode with 10^{18} pot collected in about 100 days of data taking during Run 3. These results could be obtained on a ~ 5 year timescale. NA62⁺⁺ in dump mode should be able to improve the limit between the di-muon mass and ~ 1 GeV range and will compete with SeaQuest on the same timescale; FASER, in its first phase, is instead not competitive.

On a longer timescale (10–15 years) the explored parameter space will be significantly extended by bigger PBC projects, as SHiP with 2×10^{20} pot, KLEVER with 5×10^{19} pot delivered, REDTOP with 10^{17} pot collected at the η threshold, MATHUSLA200 and FASER2 with 3 ab^{-1} , running parasitically at the ATLAS or CMS interaction points, and CODEX-b with 300 fb^{-1} , if the LHCb phase-II upgrade will be approved during the HL-LHC era. Above the di-muon threshold SHiP, FASER2, MATHUSLA200 and CODEX-b have comparable sensitivity. Below the kaon mass, KLEVER will be able to close the gap between the recasted limit from the data of the E949 experiment (and possible future result from NA62) and the Super Novae bound. REDTOP with 10^{17} pot at the η threshold instead is not competitive with respect to the others. This is shown in figure 28.

The extended version of the minimal Higgs-Dark Scalar model, with both couplings μ and λ different from zero, allows to cover a larger fraction of the parameters space, as shown in figure 29, due to the new contributions arising from a virtual (as in the $B \rightarrow KSS$ mode) or real (as in the case $h \rightarrow SS$) Higgs in the chain. Also in this case the larger impact is provided by the bigger experiments, MATHUSLA200, SHiP, FASER2 and CODEX-b which will be able to explore the region well above the GeV mass scale in a fully uncharted range of couplings. The experiments at a central location near the LHC interaction points, MATHUSLA and CODEX-b, will have sensitivity all the way up to ~ 60 GeV, if the assumption of zero background is valid.

9.3. Neutrino portal

All fermions in the SM with the exception of neutrinos are known to exist with both left handed and right-handed chirality. A particularly strong motivation for the existence of

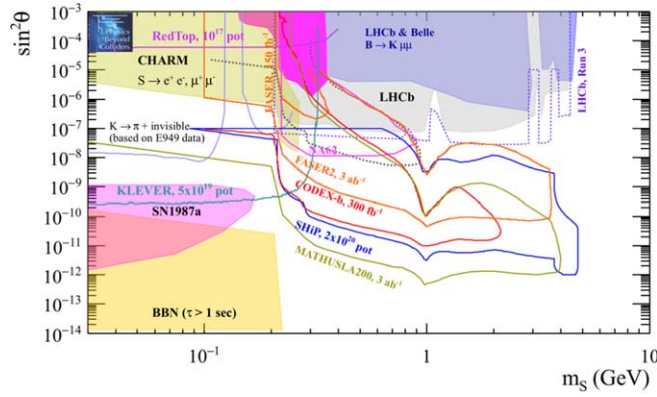


Figure 28. BC4: prospects on 10–15 year timescale for PBC projects for the Dark Scalar mixing with the Higgs in the plane mixing angle $\sin^2\theta$ versus dark scalar mass m_S .

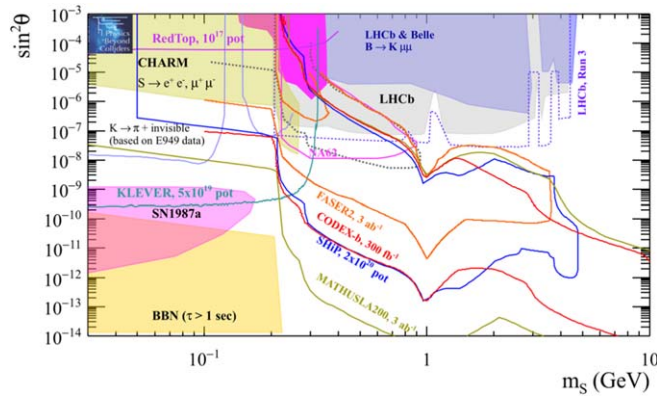


Figure 29. BC5: prospects on 10–15 year timescale for PBC projects for the dark scalar mixing with the Higgs in the plane mixing angle $\sin^2\theta$ versus dark scalar mass m_S under the hypothesis that both parameters λ and μ are different from zero. The sensitivity curves have been obtained assuming $BR(h \rightarrow SS) = 10^{-2}$. The NA62⁺⁺ and KLEVER curves correspond still to the case of $\lambda = 0$, and, hence, should be considered conservative.

right-handed neutrinos ν_R or HNLs comes from the fact that they can explain the smallness of neutrino masses [257–262] via the type I seesaw mechanism.

Another motivation for the existence of the ν_R comes from cosmology. Couplings between ν_R generally violate CP , and the interactions of the ν_R in the early universe can potentially generate a matter-antimatter asymmetry in the primordial plasma. At temperatures above $T_{\text{sphaleron}} = 130 \text{ GeV}$ [263] this asymmetry can be converted into a net baryon number by weak sphalerons [264]. This process called *leptogenesis* can either occur during the ‘freeze-out’ and decay of the ν_R [265] (‘freeze-out scenario’) or during their production [11, 266, 267] (‘freeze-in scenario’). It is one of the most promising explanations for the baryon asymmetry of the Universe (BAU), which is believed to be the origin of baryonic matter in the present day universe, see [268] for a discussion.

HNLs have been studied in connection to large scale structure formation [269], BBN [270], CMB, diffuse extragalactic background radiation, and supernovae [271]. In general, the scale of the HNL masses is entirely unknown; different choices can have a wide range of implications for particle physics, astrophysics and cosmology, see e.g. [272] for an overview. In the neutrino minimal standard model (ν MSM) [11] two HNLs are expected to be in the range MeV–GeV while a third HNL is a DM candidate and can have a mass as low as a few keV. This model is particularly interesting from a phenomenological viewpoint because it is feasible for masses of as low as 10MeV [273], which are well within reach of accelerator-based experiments.

Moreover, the decay width of the HNLs is suppressed by both the small mixing angle and G_F^2 , while the latter factor drops out in their production. As for the dark scalar, this means that the HNL's are naturally long lived, but have a relatively unsuppressed production rate, which makes them ideal targets for the PBC proposals.

Current bounds on HNLs: general considerations Mixing of heavy neutrinos with both ν_e and ν_μ can be probed searching for bumps in the missing-mass distribution of pion and kaon leptonic decays, eg. $K^+ \rightarrow \ell^+ \nu_\ell$, ($\ell = e, \mu$). These bounds are very robust because they assume only that a heavy neutrino exists and mixes with ν_e and/or ν_μ . Another strategy to search for heavy neutrinos mixed with ν_e, ν_μ and ν_τ , is via searches of their decay products. If the HNLs exist, they would be produced in every process containing active neutrinos with a branching fraction proportional to the mixing parameters $|U_{e,\mu,\tau}|^2$. Then the HNLs would decay via charged current (CC) and neutral current (NC) interactions into active neutrinos and other visible final states, as pions, muons and electrons. In beam-dump experiments, the HNLs would be produced in meson decays. Other ways to constrain the couplings of HNLs in a relatively high mass regime is using possible Z^0 decays into heavy neutrinos from LEP data [274]. In this case, only large values of the mixing angle can be explored.

The bounds obtained from searches for HNLs with visible decays are in general less robust than the ones from searches that use the missing mass technique. In fact, the bounds obtained with HNLs in visible decays would be largely weakened if the HNLs have other dominant decay modes into invisible particles.

In the following we will consider only benchmark scenarios in which a HNL couples to one SM generation at the time. This choice is driven by simplicity and allows us to ease the comparison with bounds provided by past experiments that in most cases were sensitive to one flavor coupling only. Other combinations of ratios of couplings are certainly possible but they are beyond the present study.

Strong constraints on couplings for HNLs with masses below the kaon mass are set by past experiments, in particular PS191 [275], CHARM [276], NuTeV [277], E949 [278], PIENU [279], TRIUMF-248 [280] and NA3 [281]. An interesting search has been also performed recently by the NA62 Collaboration [282].

A significant improvement in the entire mass range below the B -meson mass could be achieved by SHiP, as will be shown in the following. The same mass range could also be probed by a FASER2 [85], CODEX-b [115] and MATHUSLA200 [97]. Above the B -meson mass, displaced vertex searches at high energy hadron [86, 283–287] or lepton [284, 288] colliders would be more sensitive, see e.g., [287] for a summary. Neutrinos that are heavy enough to decay promptly can leave distinct lepton number and flavor violating signatures in high energy collisions, see [289, 290] for a recent review.

9.3.1. Neutrino portal with electron-flavor dominance (BC6). In this section we consider the case in which HNLs couple only to first SM generation and the sensitivity plots are shown in the plane $\{|U_e|^2, m_N\}$.

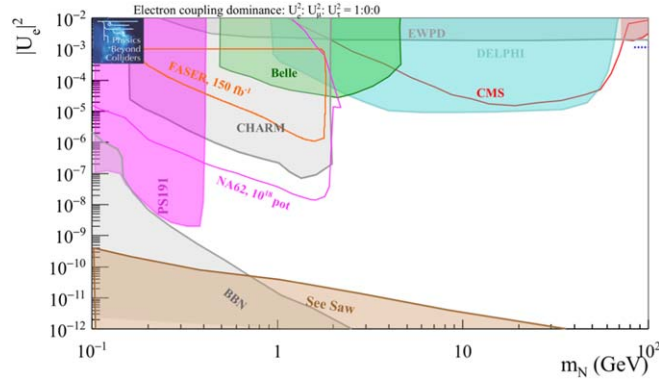


Figure 30. BC6: sensitivity to heavy neutral leptons with coupling to the first lepton generation only. Current bounds (filled areas) and near (~ 5 years) future physics reach of two PBC projects, FASER and NA62⁺⁺ (solid lines). See text for details.

Current bounds, experimental landscape and PBC projects on 5 year timescale

Current bounds and the future experimental landscape in the next ~ 5 years, including some PBC projects, are shown in figure 30 for the case of HNLs with couplings only to the first lepton generation and masses in the MeV–GeV range.

Existing bounds, shown as filled colored areas, for masses below the charm mass arise mostly from beam dump experiments (PS191 [275] and CHARM [276]) while those above the charm mass from LEP data, dominated by the DELPHI result [274], from Belle [291] and more recently from CMS [292]. The allowed range of couplings is bounded from below by the BBN constraint [270], and the see-saw limit [293].

- (1) *PS 191 @ CERN*: the PS191 CERN experiment was specifically designed to search for neutrino decays in a low-energy neutrino beam. The apparatus consisted of 10 m long nearly empty decay volume instrumented by flash chambers, calorimeter and scintillator hodoscope [275].
- (2) *CHARM @ CERN*: a search for heavy neutrinos was performed by the CHARM Collaboration by dumping $\mathcal{O}(2 \cdot 10^{18})$ 400 GeV protons on a thick Copper beam dump and looking for visible decays with electrons in the final state in the 35 m long decay volume with a spectrometer of $3 \times 3 \text{ m}^2$ cross section [276].
- (3) *Belle @ KEK*: Belle performed a search for heavy neutrinos with 772 M of $B\bar{B}$ pairs using leptonic and semileptonic B mesons decays, $B \rightarrow X\ell\nu_R$, where $\ell = e, \mu$ and X was a charmed meson $D^{(*)}$, a light meson (π, ρ, η , etc.) or nothing (purely leptonic decays), in a range of masses between the kaon and the B mass [291].
- (4) *LEP data*: the most stringent limits above the B meson mass have been put by DELPHI [274]. HNLs have been searched for using data collected by the DELPHI detector corresponding to 3.3×10^6 hadronic Z^0 decays at LEP1.
- (5) *CMS @ LHC*: CMS searched for HNLs in three prompt charged leptons sample in any combination of electrons and muons collected at a center-of-mass energy of 13 TeV and corresponding to an integrated luminosity of 35.9 fb^{-1} . The search is performed in the HNL mass range between 1 GeV and 1.2 TeV [292].
- (6) *BBN constraint*: a HNL with parameters to the left of the BBN line would live sufficiently long in the early Universe to result in an overproduction of primordial Helium-4 [270].

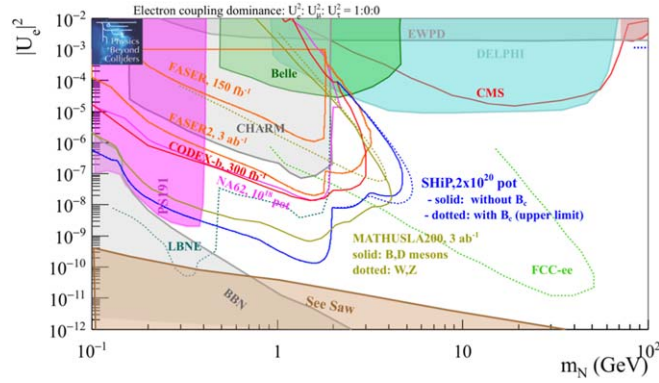


Figure 31. BC6: sensitivity to heavy neutral leptons with coupling to the first lepton generation only. Current bounds (filled areas) and 10–15 years prospects for PBC projects (SHiP, MATHUSLA200, CODEX-b and FASER2) (solid lines). Projections for a LBNE near detector with 5×10^{21} pot and from FCC-ee with 10^{12} Z^0 decays are also shown.

(7) *See-saw limit*: below the see-saw limit, the mixing of the HNL with active neutrinos becomes too weak to produce the observed pattern of neutrino flavor oscillations [293].

Only two PBC projects with a ~ 5 year timescale can contribute to this benchmark case: FASER with 150 fb^{-1} , which unfortunately is not competitive with the current bounds set by CHARM, and more interestingly, NA62⁺⁺ that can push down the CHARM limits by about one order of magnitude in the same mass range by collecting $\sim 10^{18}$ pot in dump mode. The NA62⁺⁺ projections correspond to the 90% CL exclusion limits in case all the final states with at least two charged tracks are considered [294]. In the projections the zero background hypothesis is assumed. Studies performed with the already acquired 3×10^{16} pot dataset in dump mode show that the background can be reduced to zero with the current setup for fully reconstructed final states, while for open final states the addition of an Upstream Veto in front of the decay volume is required. The addition of this detector is currently under study by the Collaboration.

Physics reach of PBC projects on 10–15 year timescale On a 10–15 year timescale many PBC projects can contribute to this benchmark case, as shown in figure 31: MATHUSLA200, FASER2, CODEX-b and SHiP. For MATHUSLA200 we show separately the contributions from heavy mesons and gauge bosons decays. The SHiP sensitivity curve is obtained without (solid curve) and with (dashed curve) a particular assumption for the contribution from B_c . This is because the $\sigma(B_c)/\sigma(B)$ fraction at the SPS energies is not reliably known. We therefore show an upper sensitivity limit provided by assuming the fraction measured at the LHC energy.

Also in this case the plot shows the 90% CL exclusion limits under the hypothesis of zero background. This hypothesis is a strong assumption that has been properly validated only by SHiP so far, using a full GEANT4 simulation of the detector, including digitization and reconstruction, and large samples of Monte Carlo data. The background evaluation for MATHUSLA200, CODEX-b and FASER2 is still work in progress and will be carried on in the coming years. Figure 31 shows also projections from the LBNE *near detector* as 5-year sensitivity corresponding to an exposure of 5×10^{21} protons on target for a detector length of

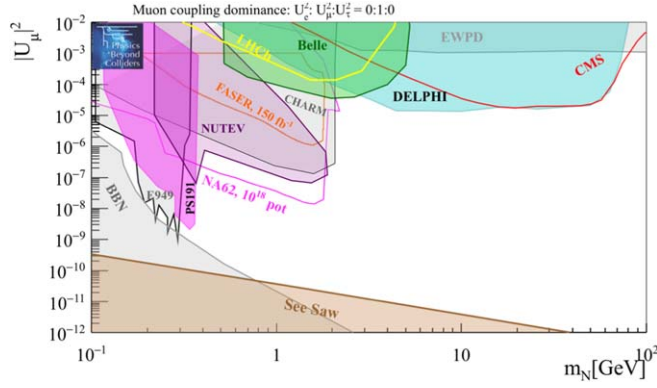


Figure 32. BC7: sensitivity to heavy neutral leptons with coupling to the second lepton generation only. Current bounds (filled areas) and near (~ 5 years) physics reach of two PBC projects, FASER and NA62⁺⁺ (solid lines). See text for details.

30 m and assuming a normal hierarchy of neutrinos masses [295] and from *FCC-ee* with 10^{12} Z^0 decays and HNLs decaying between 10 and 100 cm from the interaction vertex [296].

9.3.2. Neutrino portal with muon-flavor dominance (BC7). In this section we consider the case in which HNLs couple only to second SM generation and the sensitivity plots are shown in the plane $\{|U_{\mu}|^2, m_N\}$.

Current bounds, experimental landscape and PBC projects on 5 year timescale Current bounds and the future experimental landscape in the next ~ 5 years, including some PBC projects, are shown in figure 32 for the case of HNL with couplings only to the second lepton generation and masses in the MeV–GeV range.

Also in this case the allowed range of couplings is bounded from below by the BBN constraint [270], and the see-saw limit [293]. Existing experimental limits are shown as filled colored areas: for masses below the charm mass they arise mostly from the same beam dump experiments contributing to the sensitivity for electron-flavor dominance (PS191 [275] and CHARM [276], as explained in the previous subsection) with the addition of NuTeV [277], and E949 [278]:

- (1) *NuTeV @ Fermilab*: a search for HNLs decaying in muonic final states has been performed at the neutrino detector NuTeV at Fermilab in 1996–1997, using 2×10^{18} 800 GeV protons interacting with a Beryllium-oxide target and a proton dump. [277].
- (2) *E949 @ BNL*: Evidence of a heavy neutrino, in the process $K^+ \rightarrow \mu^+ \nu_R$ was searched for by the E949 Collaboration using 1.7×10^{12} stopped kaons.

Above the charm mass, current bounds are set by DELPHI [274], Belle [291], CMS [292] with the same analysis used to set bounds for electron-dominance, and by LHCb with a dedicated analysis to search for prompt and displaced $\pi^- \mu^+ \mu^+$ vertices in $B^+ \rightarrow \pi^- \mu^+ \mu^+$ LNV decays [297].

In this scenario, NA62⁺⁺ in dump mode will be able to perform this search with competitive physics reach in a time scale of ~ 5 years.

Physics reach of PBC projects on 10–15 year timescale Figure 33 shows the 90% CL exclusion limits from MATHUSLA200, FASER2, CODEX-b and SHiP in a 10–15 years time scale. Also in this case the curves are obtained under the assumption of zero background, for which the same considerations drawn in the previous subsection hold.

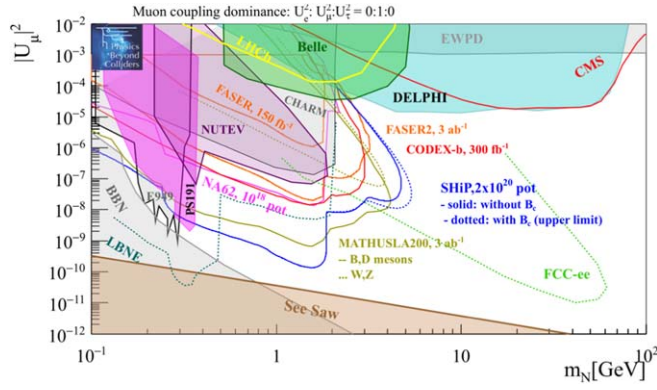


Figure 33. BC7: sensitivity to heavy neutral leptons with coupling to the second lepton generation only. Current bounds (filled areas) and 10–15 years prospects for PBC projects (SHiP, MATHUSLA200, CODEX-b and FASER2) (dotted and solid lines). Projections for the LBNE near detector with 5×10^{21} pot and FCC-ee with 10^{12} Z^0 decays are also shown.

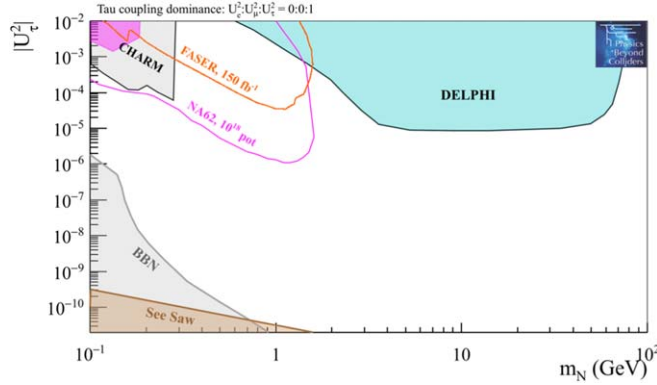


Figure 34. BC8: sensitivity to heavy neutral leptons with coupling to the third lepton generation only. Current bounds (filled areas) and near (~ 5 years) future physics reach of two PBC projects, FASER and $NA62^{++}$ (solid curves). See text for details.

9.3.3. Neutrino portal with tau-flavor dominance (BC8). In this section we consider the case in which HNLs couple only to third SM generation and the sensitivity plots are shown in the plane $\{|U_\tau|^2, m_N\}$.

Current bounds and experimental landscape Current bounds and future experimental landscape in the next ~ 5 years, including some PBC projects, are shown in figure 34 for the case of HNL coupling only to the third lepton generation and masses in the MeV–GeV range. Also in this case the allowed range of couplings is bounded from below by the BBN constraints [270], and the see-saw limit [293].

Main bounds in this benchmark case arise from CHARM [298], NOMAD [299], and again the same data from DELPHI [274] used for the other two benchmark cases (BC6 and BC7).

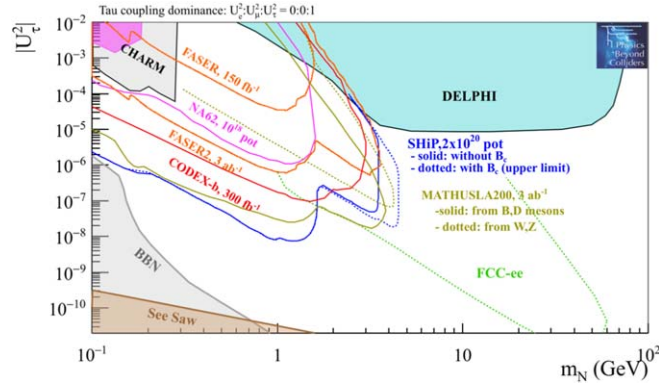


Figure 35. BC8: sensitivity to heavy neutral leptons with coupling to the third lepton generation only. Current bounds (filled areas) and 10–15 years prospects for PBC projects (SHiP, MATHUSLA200, CODEX-b and FASER2) (solid and dotted curves). Projections from FCC-ee with 10^{12} Z^0 decays are also shown.

- (1) *CHARM*: limits on the square mixing strength $|U_{\tau}|^2$ in a mass range 10–290 MeV were set by re-interpreting the null result of a search for events produced by the decay of neutral particles into two electrons performed by the CHARM experiment using the neutrino flux produced by $\mathcal{O}(2 \times 10^{18})$ 400 GeV protons on a solid copper target [298].
- (2) *NOMAD*: a search for heavy neutrinos was performed using 4.1×10^{19} 450 GeV protons on target at the WANF facility at CERN in 1996–1998. The HNLs were searched in the process $D_s \rightarrow \tau \nu_R$ followed by the decay $\nu_R \rightarrow \nu_{\tau} e^+ e^-$ in the NOMAD detector. This allowed to derive an upper limit on the mixing strength between the heavy neutrino and the tau neutrino in the ν_R mass range from 10 to 190 MeV [299].

Physics reach of PBC projects on 5 and 10–15 year timescale Among the PBC projects the only two contributing on a 5 year timescale are, again, FASER with 150 fb^{-1} and NA62⁺⁺, as shown in figure 34. Figure 35 shows the 90% CL exclusion limits from MATHUSLA200, FASER2, CODEX-b and SHiP in a 10–15 years time scale. The physics reach from FCC(ee) with 10^{12} Z^0 is also shown.

9.4. Axion portal

The discovery of the Higgs boson shows clearly that elementary scalar bosons exist in Nature. Therefore it is timely and well-motivated to search for further light scalar or pseudoscalar particles. Pseudo-scalar particles can arise as pseudo-Nambu–Goldstone bosons of a spontaneously broken $U(1)$ symmetry at a scale f_A . The principal example of very light pseudo-Goldstone bosons is the axion [35–37, 300] introduced to solve the strong CP problem in QCD. Natural extensions of the axion paradigm bring a wide range of interesting pseudoscalar particles which typically have very similar interactions as the axion, but without a strict relation between the mass and the coupling, the Axion-Like Particles or ALPs.

ALPs also provide an interesting connection to the puzzle of dark matter, because they can mediate the interactions between the DM particle and SM states and allow for additional annihilation channels relevant for the thermal freeze-out of DM. In fact in presence of an additional pseudoscalar particle that mediates the interactions of DM with the SM sector [301, 302], constraints from direct detection experiments [303–306] and invisible Higgs width [307, 308] on the scalar portal can be easily evaded [301, 302].

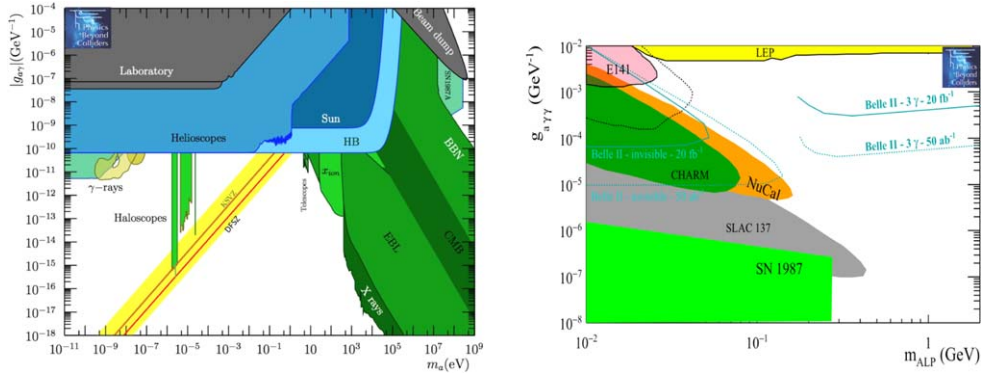


Figure 36. Left panel: current limits on axion with photon coupling in the plane coupling ($g_{a\gamma\gamma}$) versus mass (m_a). Right panel: zoom in the range of masses interesting for accelerator-based experiments (note the different units for the mass ranges in the two panels). The plot in the left panel is revised from [39]. In the right panel, current bounds are shown as filled colored areas. A possible sensitivity from Belle-II from a phenomenological study [311] is also shown.

Moreover, if the pseudoscalar mass is in the sub-GeV range it can furthermore evade detection at the LHC, as, e.g. in monojet searches [309]. Another advantage of a very light pseudoscalar a is that it allows for the possibility that DM can obtain the correct relic density from thermal freeze-out even if it is very weakly coupled to SM particles. This is due to the fact that, provided the pseudo-scalar mass is less than twice the mass of the DM particle χ , the annihilation process $\chi\bar{\chi} \rightarrow aa$, followed by decays of the pseudoscalars into SM particles, allows for a highly efficient annihilation of DM particles. The only important constraint is that such pseudoscalar particles must decay before BBN. As explained in section 2.1, ALPs can mediate interactions between DM and the SM sector via three different couplings: photon-, gluon-, and fermion-coupling.

9.4.1. Axion portal with photon-coupling (BC9). Assuming a single ALP state a , and the predominant coupling to photons, all phenomenology (production, decay, oscillation in the magnetic field) can be determined as functions of the ($m_a; g_{a\gamma\gamma} = f_\gamma^{-1}$) parameter space.

Current bounds and near future experimental landscape The current bounds for ALPs with photon coupling are shown in figure 36, left. A zoom on the region of interest for experiments at accelerators is shown in the right panel and covers a range of masses between MeV and GeV. We note that this is also the mass region of interest in models where ALPs serve as mediators to a DM sector.

Searches for ALPs with photon coupling have been performed using monophoton searches at LEP, $e^+e^- \rightarrow \gamma^* \rightarrow a\gamma$, mono-photon searches at BaBar ($e^+e^- \rightarrow \gamma a, a \rightarrow$ invisible), radiative Υ decays ($\Upsilon(nS) \rightarrow \gamma^* \rightarrow \gamma a$), radiative Z-boson decays, and electron- and proton beam dump experiments, where the ALPs are produced mainly via the Primakoff effect, i.e. the conversion of a photon into an ALP in the vicinity of a nucleus [310].

- (1) *E141 @ SLAC (electron beam dump)*: primarily searched for LLPs decaying into the e^+e^- final state [193] but the addition of a photon converter in front of the detector for certain period of data taking opened the possibility to be sensitive also to photons from an ALP decay. Reinterpretation of the E141 results was performed in [312, 313], leading to somehow more conservative bound with respect previous interpretations [314].

- (2) *E137 @ SLAC (electron beam dump)*: dedicated search for ALPs coupling only to photons [194]. However the exclusion limits presented in the paper did not contain the turnover towards large couplings due to the exponential suppression of the number of ALPs that reach the detector, this has been added in [311].
- (3) *CHARM (proton beam dump)*: a search for a ALP in 400 GeV proton interactions with a thick copper target was performed with the CHARM detector [202]. The target was placed 480 m apart from the 35 m long decay volume and the hypothetical decay $a \rightarrow \gamma\gamma$ has been sought using a fine-grained calorimeter of 9 m² active area.
- (4) *NuCal (proton beam dump)*: the production and decay of a light scalar and pseudoscalar particle has been investigated in a proton-iron beam dump experiment at the 70 GeV Serpukhov accelerator [204].
- (5) *LEP*: limits from LEP data in the ALP mass range MeV–GeV arise from a reinterpretation [315] of the LEP $Z^0 \rightarrow \gamma\gamma$ data [316–319] where one of the two neutral clusters was considered the result of a merging of two highly collimated photons from the ALP decay in the process $Z^0 \rightarrow a\gamma$, $a \rightarrow \gamma\gamma$. Mono-photon searches, i.e. searches for highly-energetic photons in association with missing energy resulting from the process $e^+e^- \rightarrow \gamma + a(a \rightarrow \text{invisible})$ have been performed as well [320] but they are not sensitive to ALPs with mass in the sub-GeV range [311].
- (6) *Bound from Astrophysics*: Supernova 1987A. Weakly coupled particles such as axions or ALPs with masses up to about 100 MeV can be copiously produced in the hot core of a supernova. Because of their weak couplings these particles stream out of the core and thereby constitute a new energy loss mechanism. In the absence of such new particles the main cooling mechanism is due to neutrino emission. The corresponding neutrino signal has been observed in the case of SN 1987A, placing a bound on possible exotic energy loss mechanisms, which should not exceed the energy loss via neutrino emission [311].

We note that mono-photon searches have also been carried out at the LHC (for the most recent analyses see e.g. [321]), but their sensitivity does not significantly improve on the bound from LEP.

Near future bounds will come from Belle-II where the ALP can be searched in the invisible and 3γ decay modes. A phenomenological study has been performed in [311] where the authors consider ALP decays into dark matter (invisible) and two (resolved) photons. The bounds have been shown in figure 36. However the $a \rightarrow \text{invisible}$ sensitivity heavily relies on the possibility to use the single-photon trigger with a low threshold (1.8 GeV), that is not guaranteed during the nominal Belle-II luminosity regime.

PBC projects on 5 and 10–15 years timescale Three PBC experiments can perform searches of ALPs with photon coupling on a 5 year timescale: NA62⁺⁺ in dump mode and FASER, will look for visible ALP decays, $a \rightarrow \gamma\gamma$, while NA62⁺⁺(e) will be able to perform a search into visible and invisible decays. The contour plots are shown in figure 37. On a longer timescale the big PBC projects can enter in the game further extending the physics reach in a still uncharted parameter space. In this respect SHiP and LDMX will be fully complementary, the first covering larger masses and smaller coupling, the latter filling the uncovered phase space between the old beam-dump experiments and the colliders, in the 10–300 MeV mass range.

9.4.2. Axion portal with fermion-coupling (BC10). Assuming a single ALP state a , and the predominant coupling to fermions, all phenomenology (production and decay) can be determined as functions of $(m_a; g_Y = 2vf_\ell^{-1}, 2vf_q^{-1})$, with v the vev of the Higgs. Furthermore, for the sake of simplicity, we take $f_q = f_\ell$. Details about approximations and

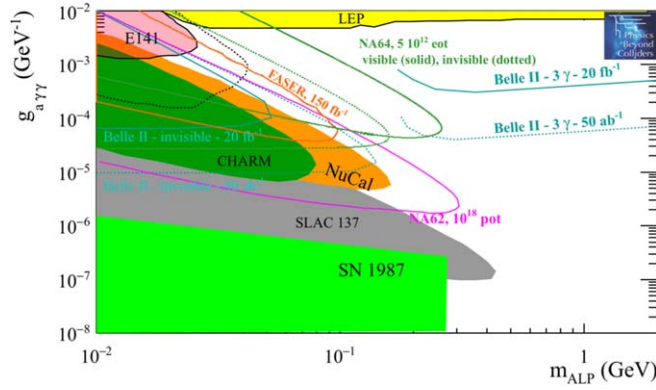


Figure 37. BC9: ALPs with photon coupling. Current bounds (filled areas) and prospects for PBC projects on 5 years timescale (solid lines) in the plane coupling $g_{a\gamma\gamma}$ versus mass m_{ALP} . The results from a phenomenological study for Belle-II [311] are also shown.

assumptions in computing sensitivities for this benchmark case are reported in appendices A and B.

The effective Yukawa coupling ALP-SM fermions is proportional to the mass of the SM fermions. Hence: a possible ALP with fermion coupling is mostly originated from meson decays and only very rarely from electrons. Heavy mesons can be produced in e^+e^- colliders, pp colliders and in the interactions of a proton beam with a target.

Searches for ALPs with fermion coupling are being pursued at the LHC, namely in the analysis of rare B decays as for example $B^+ \rightarrow K^{*0} \mu^+ \mu^-$ [250]. The geometry of the LHC experiments, on the other hand, is such that a search can be performed only if the ALP decays more or less instantaneously, hence has large couplings. For ALPs with smaller couplings and longer lifetimes these searches are much less effective even though ALPs may still be produced in abundance.

Beam-dump experiments in contrast are particularly sensitive to long-lived and very weakly coupled light new states, which can travel through the hadron absorber before decaying. Several constraints already exist, mostly coming from old beam dump experiments as CHARM [202], NuCal [204], and E613 [322]. Other constraints are derived from K and B mesons experiments, as explained below.

Current bounds and near future prospects, including PBC projects The current status of the exclusion limits for ALPS with fermion coupling in the MeV–GeV range is shown in figure 39, as filled colored areas.

Most of the current bounds arise from a re-interpretation of experimental results from CHARM [202], E949 [221, 323], KTeV [324] performed by theorists [325, 326]. As such, these bounds should be taken with many caveats. A few searches are instead coming directly from experiments, as for example BaBar [327] and LHCb [249, 250].

- (1) $K^+ \rightarrow \pi^+ + X$: the $K_{\mu 2}$ experiment has studied the momentum distribution of charge pions produced in the decay $K^+ \rightarrow \pi^+$ [328]. In presence of a light pseudoscalar, the decay channel $K^+ \rightarrow \pi^+ a$ would lead to a bump in the spectrum.
- (2) $K^+ \rightarrow \pi^+ + invisible$: reinterpretation of the E949 results [221, 323] as an upper bound on the process $K^+ \rightarrow \pi^+ a$ performed in [325], and cross-checked by the KLEVER Collaboration. The curve assumes that the ALP escapes the decay volume.

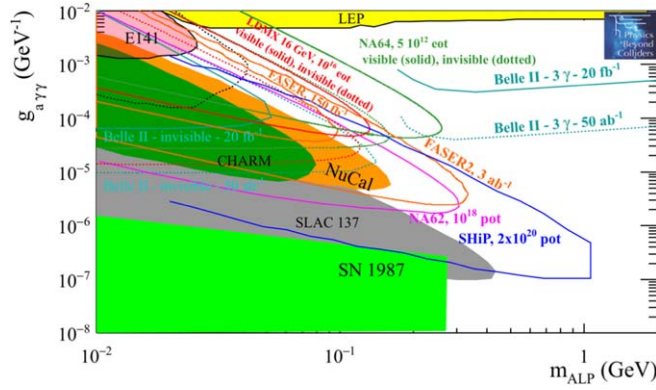


Figure 38. BC9: ALPs with photon coupling. Current bounds (filled areas) and prospects for PBC projects on 10–15 years timescale (solid lines) in the plane coupling $g_{a\gamma\gamma}$ versus mass m_{ALP} . The results from a phenomenological study for Belle-II [311] are also shown.

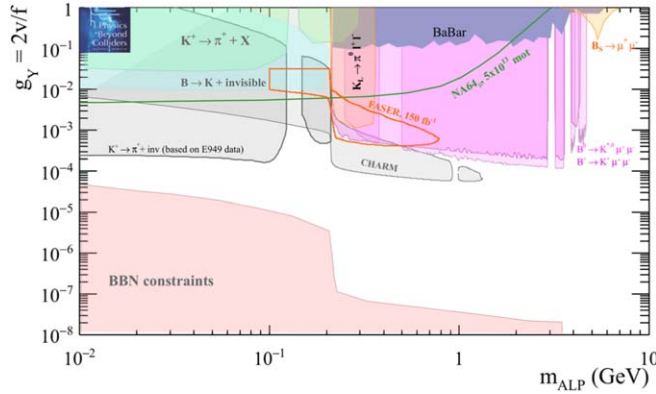


Figure 39. BC10: ALPs with fermion coupling. Current bounds (filled areas) and near (~ 5 years) prospects for PBC projects (solid lines). CHARM and LHCb filled areas have been adapted to PBC prescriptions by F Kahlhoefer, following [326]. The E949 area has been computed by the KLEVER Collaboration and M Papucci based on E949 data. All other exclusion regions have been properly re-computed by M Papucci, following [325].

- (3) $B^0 \rightarrow K_S + invisible$: This search is the analogous as the $K^+ \rightarrow \pi^+ + invisible$ search. The strongest bounds come from CLEO [329].
- (4) $K_L \rightarrow \pi^0 \ell^+ \ell^-$: in the mass range $210 < m < 420$ MeV the pseudoscalar will decay predominantly to muon pairs. The KTeV/E749 Collaboration has set an upper limit on the $K_L \rightarrow \pi^0 \ell^+ \ell^-$ decay [324] and this result has been converted into an upper limit for the branching fraction of the decay $K_L \rightarrow \pi^0 a$ under the hypothesis that the ALP decays instantaneously [325].
- (5) *Radiative Υ decays*: pseudo-scalar particles have been sought by the BaBar Collaboration in radiative Υ decays $\Upsilon \rightarrow a \gamma$, with $a \rightarrow \mu^+ \mu^-$ for $a < 2m_\tau$ [327] and $a \rightarrow \tau^+ \tau^-$ for m_a above threshold [330].

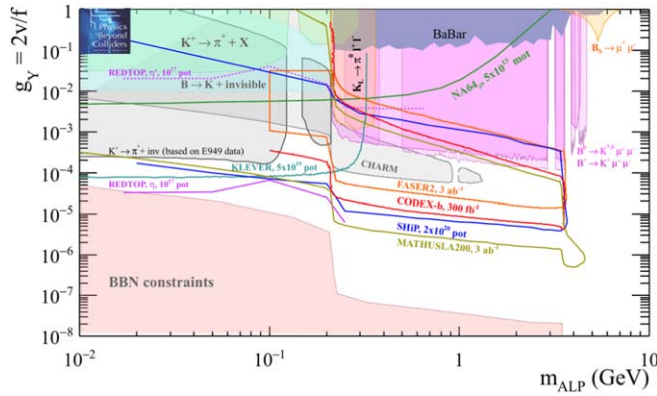


Figure 40. BC10: ALPs with fermion coupling. Current bounds (filled areas) and medium-far (~ 10 to 15 years) prospects for PBC projects (solid lines) for ALPs with fermion coupling. CHARM and LHCb filled areas have been adapted to PBC prescriptions by F Kahlhoefer, following [326]. E949 area has been computed by the KLEVER Collaboration and M Papucci based on E949 data. All other exclusion regions have been properly re-computed by M Papucci, following [325].

- (6) $B \rightarrow K\mu^+\mu^-$: the measurement of the branching fraction of the $B^+ \rightarrow K^+\mu^+\mu^-$ decay as a function of the di-muon mass performed by LHCb [331] has been interpreted in [325] as an upper bound for the process $B^+ \rightarrow K^+a$, $a \rightarrow \mu^+\mu^-$ in each $\mu^+\mu^-$ mass bin, under the hypothesis that a decays instantaneously. Dedicated searches have been instead performed by the Collaboration, allowing also for displaced di-muon vertices in the $B^0 \rightarrow K^{0*}\mu^+\mu^-$ and $B^+ \rightarrow K^+\mu^+\mu^-$ processes, and the results reported in [250] and [249], respectively⁶⁴.

9.4.3. *Axion portal with gluon-coupling (BC11).* Near (~ 5 years) and medium-far (10-15 years) prospects for PBC experiments are shown as solid lines in figures 39 and 40, respectively. This benchmark case considers a scenario in which the ALP a only couples to the gluon field at a scale $\Lambda = 1$ T eV. One can write down the corresponding low-energy Lagrangian at the tree level as

$$\mathcal{L} = \mathcal{L}_{\text{SM}} + \mathcal{L}_{\text{DS}} + a \frac{g_s^2}{8f_G} G_{\mu\nu}^b \tilde{G}^{b\mu\nu}. \tag{9.2}$$

Because the ALP mixes with the neutral pseudoscalar mesons, it is produced in any process that produces such mesons. Moreover it can be produced also in B mesons decays, as explained in section 2.1.4. Details about approximations and assumptions assumed in computing sensitivities for this benchmark case are reported in appendices A and B.

Figure 41 shows the current bounds (as colored filled areas) and the prospects for PBC projects (solid lines) both on 5 year (FASER) and 10–15 year (CODEX-b, MATHUSLA200, FASER2) timescale. Below the three pion threshold, the CODEX-b and MATHUSLA200 reach for this benchmark is conditional upon the eventual detectors being sensitive to the diphoton final state. Production from K and B decays depend on UV completion and the results shown assume $\approx [\log \Lambda_{\text{UV}}^2/m_t^2 \pm \mathcal{O}(1)] \Rightarrow 1$. The CODEX-b curve has been obtained

⁶⁴ These data have been adapted to the model prescriptions used in this study by Kahlhoefer.

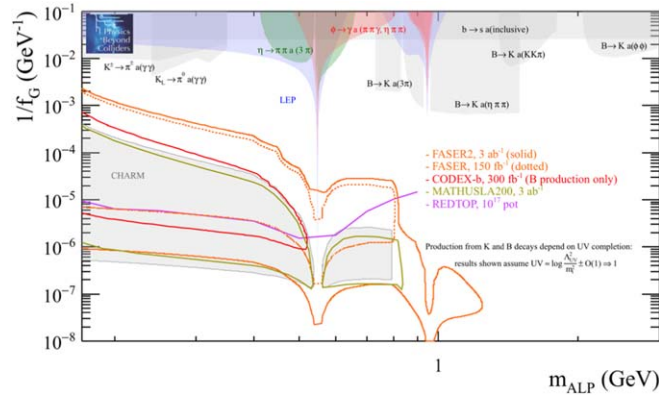


Figure 41. Current bounds (as colored filled areas) and the prospects for PBC projects (solid lines) both on 5 year (FASER) and 10–15 year (CODEX-b, MATHUSLA200, FASER2) timescale. The CHARM gray filled area has been computed by Kling, recasting the search for long-lived particles decaying to two photons performed at CHARM [202]. Other colored filled areas are kindly provided by Mike Williams and revisited from [332]. The gray areas depend on the UV completion and the results shown assume $\approx[\log\Lambda_{UV}^2/m_t^2 \pm \mathcal{O}(1)] \Rightarrow 1$. The CODEX-b curve has been obtained considering B -decays only, hence it is conservative. Both NA62⁺⁺ and SHiP are sensitive to this benchmark case too, the curves are currently being compiled.

considering B -decays only, hence it is conservative. NA62⁺⁺ and SHiP are also expected to be sensitive to this benchmark case but they did not provide the sensitivity curves on the timescale of this paper.

Current bounds arise from flavor physics, old beam-dump experiments and LEP data. A comprehensive reinterpretation of these data has been performed in [332] in the $m_\pi < m_a < 3$ GeV mass region, namely:

- (1) Data from LEP [333, 334] and old beam dump experiments, E137 [194] and NuCal [204], have been used to recast limit on the $a\gamma\gamma$ vertex and translated into a limit in the $BR(a \rightarrow \gamma\gamma)$;
- (2) The limits on the branching fractions of the decays $\phi \rightarrow \pi\pi\gamma\gamma$ and $\eta' \rightarrow \pi^+\pi^-\pi^+\pi^-\pi^0$ [335] are used to set a limit on the rate of the processes $\phi \rightarrow \gamma a(\pi\pi\gamma)$ and $\eta' \rightarrow \pi^+\pi^-\pi^+\pi^-\pi^0$, assuming that the full rate is due to ALPs;
- (3) Decays driven by the $b \rightarrow sa$ penguin diagram are considered and a recast of results is performed while analyzing:
 - the $m_{\eta\pi\pi}$ spectrum of the decay $B^\pm \rightarrow K^\pm\eta\pi^+\pi^-$, interpreted as $B^\pm \rightarrow K^\pm a(\eta\pi^+\pi^-)$, from [336];
 - the m_{K^*K} spectrum of the decay $B^\pm \rightarrow K^\pm K^* K_S \pi^\mp$, interpreted as $B^\pm = K^\pm a(K^* K_S \pi^\mp)$, from [336];
 - the measurement of the two decay rates, $BR(B^0 \rightarrow K^0\phi\phi)$ [337] and $BR(B^\pm \rightarrow K^\pm\omega(3\pi))$ [338], to put a constraints on the processes $B^0 \rightarrow K^0 a(\phi\phi)$ and $B^\pm \rightarrow K^\pm a(\pi^+\pi^-\pi^0)$, respectively.
- (4) Measurements on processes driven by the $s \rightarrow d$ penguin diagram, as $K^\pm \rightarrow \pi^\pm\gamma\gamma$ [339] and $K_L \rightarrow \pi^0\gamma\gamma$ [340], are used to recast limits on ALPs.

For cases (2) and (3) listed above, at one loop, the *agg* vertex generates an axial-vector *att* coupling [341] which enhances the rate for $B \rightarrow K^{(*)}a$ decays [31, 342–344]. Following [332] the UV-dependent factor contained in the loop, $\approx [\log \Lambda_{UV}^2/m_t^2 \pm \mathcal{O}(1)]$, is approximated to unity (which corresponds to a UV scale $\sim \text{TeV}$).

10. Physics reach of PBC projects in the multi-TeV mass range

The PBC projects have sensitivity to physics BSM at and above the TeV mass scale. Since the center of mass energy in the collisions for the PBC experiments is small compared to the LHC experiments, this sensitivity comes through modifications of known particle properties through virtual exchanges of New Physics particles. In some cases, when new physics violates exact or approximate symmetries of the SM (such as CP symmetry, and/or lepton flavor), the SM backgrounds are very low. As a result precision measurements can be sensitive to NP in the multi-TeV range.

10.1. Measurement of EDMs as probe of NP in the multi TeV scale

Measurements of, and constraints on, EDMs of elementary particles and atoms are a very powerful way of probing theories of New Physics. One of the key puzzles of the SM, the smallness of CP -violation in the QCD sector, originates from the tight bounds on neutron and atomic EDMs. The axion solution to this strong CP problem implies the existence of heavy Peccei–Quinn sectors at high-energy scales that cannot be directly accessed in high-energy experiments, and so an alternative approach is needed to understand the solution to this problem. New physics at the weak scale (or more generically, TeV scale and beyond) can also induce EDMs. Famously, the Kobayashi–Maskawa CP violation mechanism does not induce neutron or proton EDMs above $10^{-32}e$ cm, which is firmly outside the reach of current and next generation EDM experiments. This opens up the possibility of exploring the TeV frontier with EDMs by increasing the experimental sensitivity. One of the long-term proposals to measure EDMs is the proton (and other charged nuclei) storage ring where EDMs can be probed to unprecedented precision.

If new CP -violating physics is heavy, for the purpose of the EDM description, one can encapsulate its effect in form of the SM effective operators. For example, the following operators can be interpreted as up- and down-quark EDMs $d_{u(d)}$:

$$\mathcal{L} = \frac{v \times \sin(\phi^{(u)})}{\Lambda_u^2} \times \frac{ie}{2} \bar{u} F_{\mu\nu} \sigma_{\mu\nu} \gamma_5 u + \frac{v \times \sin(\phi^{(d)})}{\Lambda_d^2} \times \frac{ie}{2} \bar{d} F_{\mu\nu} \sigma_{\mu\nu} \gamma_5 d + \dots \quad (10.1)$$

The insertion of the SM vacuum expectation $v = 246 \text{ GeV}$ is necessitated by the $SU(2) \times U(1)$ gauge invariance. Possible small Yukawa couplings, loop factors etc have been subsumed into energy scale coefficients Λ_u and Λ_d . $\phi^{(d)}$ and $\phi^{(u)}$ indicate CP -violating phases.

There is, of course, a wide variety of possible dimension six operators, and more independent EDM measurements and constraints are required to limit them all. Non-perturbative methods can be used to relate proton/neutron EDMs to the quark EDM and other CP -odd operator coefficients. Suppressing u, d flavor dependence, and taking for simplicity $d_p \sim \mathcal{O}(d_q)$, one arrives at the maximum expected sensitivity of the proton EDM being reinterpreted as the sensitivity to Λ ,

$$\frac{|\sin(\phi^{(q)})|}{\Lambda_q^2} \sim \frac{1}{(7 \times 10^5 h \text{ TeV})^2} \times \left(\frac{d_p}{10^{-29} e \text{ cm}} \right)^{1/2}. \quad (10.2)$$

It is likely that operators in (10.1) are proportional to small Yukawa couplings and a loop factor, so that the sensitivity to the actual energy scales of new physics are several orders of magnitude lower than this estimate indicates. Even then, the suggested target of $10^{-29} e \text{ cm}$ for d_p will cover models with CP-violation in the multi-100 TeV range, thereby exploring, for example, the scalar quark mass range which would be expected if the measured value of the Higgs mass, $m_h \simeq 125 \text{ GeV}$, is interpreted within simple SUSY models.

10.2. Experiments sensitive to flavor violation

Of particular interest for the PBC program is the search for flavor violation which is almost entirely absent in the SM, but introduced in many beyond the SM scenarios, including theories with supersymmetry. Two PBC experiments aim to explore the sensitivity of flavor-violating processes to TeV scale physics, TauFV and KLEVER.

10.2.1. TauFV. In case of the TauFV experiment, the physics goal is to observe and measure, or alternatively set the upper bound on, the several LFV τ or D -meson decays. To estimate the sensitivity to a multi-TeV New Physics scale, the LFV process $\tau^\pm \rightarrow \mu^\pm \mu^\pm \mu^\mp$ is considered. This process is almost entirely forbidden in the SM, and any attempt to measure this small branching will automatically probe the New Physics that violates approximate τ and μ flavor conservation.

To quantify the New Physics reach, one can introduce a series of effective operators that mediate such transitions. For this particular decay process, at lowest order, one can have

$$\mathcal{L} = \frac{e^{i\phi}}{\Lambda_{\mu\tau}^2} \times (\bar{\mu} \gamma_\alpha \mu)(\bar{\tau} \gamma_\alpha \tau) + (\text{h.c.}) + \text{other Lorentz structures}. \quad (10.3)$$

In this expression, all coupling constants have been subsumed into the definition of the energy scale $\Lambda_{\mu\tau}$, apart from a possible phase ϕ .

The resulting branching ratio for the $\tau \rightarrow 3\mu$ decay in the $m_\mu \ll m_\tau$ limit is given by

$$\Gamma_{\tau \rightarrow 3\mu} = \frac{m_\tau^5}{256\pi^3 \Lambda_{\mu\tau}^4}. \quad (10.4)$$

Given the stated goal of the TauFV experiment (in the absence of positive signal) is to reach the exclusion level of $\text{BR}_{\tau \rightarrow 3\mu} \sim 10^{-10}$, one can translate the above formula to the $\Lambda_{\mu\tau}$ sensitivity,

$$\Lambda_{\mu\tau} > 55 \text{ TeV} \times \left(\frac{10^{-10}}{\text{Br}_{\tau \rightarrow 3\mu}} \right)^{1/4}. \quad (10.5)$$

10.2.2. KLEVER. The KLEVER proposal seeks to complement the NA62 experiment by measuring $K_L \rightarrow \pi^0 + \text{missing energy}$. In the SM, the missing energy is carried by neutrinos, $K_L \rightarrow \pi^0 \nu \bar{\nu}$, and the corresponding branching ratio is predicted to be $\text{BR}_{\text{SM}} = (3.4 \pm 0.6) \times 10^{-11}$ [345].

The branching ratios for the decays $K \rightarrow \pi \nu \bar{\nu}$ are among the observables in the quark-flavor sector most sensitive to NP. Because the SM decay amplitudes are strongly suppressed by the GIM mechanism and the CKM hierarchy and dominated by short-distance physics, the

SM rates are small and predicted very precisely, making the $K \rightarrow \pi\nu\bar{\nu}$ BRs potentially sensitive to NP at mass scales of hundreds of TeV, in general surpassing the sensitivity of B decays in SM extensions [117]. Observations of lepton-flavor-universality-violating phenomena are mounting in the B sector. Most explanations for such phenomena predict strong third-generation couplings and thus significant changes to the $K \rightarrow \pi\nu\bar{\nu}$ BRs through couplings to final states with tau neutrinos [119].

The BR for the decay $K_L \rightarrow \pi^0\nu\bar{\nu}$ has never been measured. The current experimental result, $\text{BR}(K^+ \rightarrow \pi^+\nu\bar{\nu}) = 1.73^{+1.15}_{-1.05} \times 10^{-10}$, obtained at Brookhaven from K^+ decays at rest with seven candidate events [221], together with considerations of isospin symmetry [346], leads to the model-independent bound $\text{BR}(K_L \rightarrow \pi^0\nu\bar{\nu}) < 1.4 \times 10^{-9}$. This limit has to be compared to the direct limit set by the KOTO experiment, $\text{BR}(K_L \rightarrow \pi^0\nu\bar{\nu}) < 3.0 \times 10^{-9}$ at 90% CL [205]. Because the amplitude for $K^+ \rightarrow \pi^+\nu\bar{\nu}$ has both real and imaginary parts while the amplitude for $K_L \rightarrow \pi^0\nu\bar{\nu}$ is purely imaginary, the decays have different sensitivity to new sources of CP violation.

In general, the measurement of the $\text{BR}(K_L \rightarrow \pi^0\nu\bar{\nu})$ is sensitive to additional sources of flavor violation coming from NP at, or above, the TeV scale. Parametrizing the effective Lagrangian for new physics in terms of effective operators as before, and taking one flavor of neutrinos for simplicity,

$$\mathcal{L} = \frac{e^{i\phi}}{\Lambda_{ds}^2} \times (\bar{\nu}\gamma_\alpha(1 - \gamma_5)\nu)(\bar{d}\gamma_\alpha(1 - \gamma_5)s) + (\text{h.c.}) + \text{other Lorentz structures}, \quad (10.6)$$

one can quantify the sensitivity of KLEVER to NP. The decay $K_L \rightarrow \pi^0\nu\bar{\nu}$ is CP -violating, and therefore the amplitude is proportional to $\sin(\phi)$, ϕ being the phase of NP contributions. In contrast, the $K^+ \rightarrow \pi^+\nu\bar{\nu}$ branching fraction is phase-independent, so it can also be used as a probe of TeV physics independently from $K_L \rightarrow \pi^0\nu\bar{\nu}$. Should NA62 discover deviations from the SM, a KLEVER-type of measurement would be required to further investigate their origins.

If the sensitivity of KLEVER can reach the SM branching ratio level, it would also entail sensitivity to New Physics at approximately

$$\frac{|\sin \phi|}{\Lambda_{ds}^2} \sim \frac{1}{(500 \text{ TeV})^2}. \quad (10.7)$$

Figure 42, reproduced from [347], illustrates a general scheme for the expected correlation between the charged and neutral decays under various scenarios.

If the NP has a CKM-like structure of flavor interactions, the K_L and K^+ BRs will lie along the band of correlation shown in green. In models with only left-handed or only right-handed couplings to the quark currents (e.g. models with modified Z couplings or littlest-Higgs models with T parity), because of constraints from ϵ'_K , the BRs must lie along one of the branches shown in blue. If the NP has an arbitrary flavor structure and both left-handed and right-handed couplings (e.g. in Randall–Sundrum models), there is little correlation, as illustrated in red.

In a recent breakthrough, the RBC-UKQCD Collaboration obtained the first result for $\text{Re } \epsilon'_K/\epsilon_K$ from a lattice calculation thought to have reliable systematics: $\text{Re } \epsilon'_K/\epsilon_K = (1.38 \pm 5.15 \pm 4.59) \times 10^{-4}$, 2.1σ less than the experimental value [348]. Estimates from large- N_c dual QCD support the lattice result [349].

With this result for $\text{Re } \epsilon'_K/\epsilon_K$, the correlation between ϵ_K and $\text{BR}(K_L \rightarrow \pi^0\nu\bar{\nu})$ has been examined in various SM extensions at energy scales Λ in the neighborhood of 1–10 TeV by several authors, in many cases, with constraints from ϵ'_K , Δm_K , and $\text{BR}(K_L \rightarrow \mu\mu)$

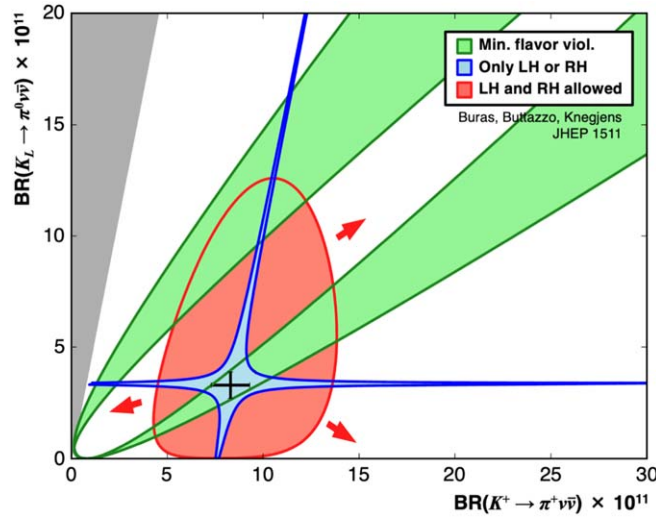


Figure 42. Scheme for BSM modifications of $K \rightarrow \pi \nu \bar{\nu}$ BRs. Reproduced from [347].

considered as well. The results of these studies are summarized in table 7. In general, an observed value of ϵ_K that is larger than expected in the SM implies a suppression of $\text{BR}(K_L \rightarrow \pi^0 \nu \bar{\nu})$ to below the SM value. However, it is possible to construct models in which ϵ_K and $\text{BR}(K_L \rightarrow \pi^0 \nu \bar{\nu})$ are simultaneously enhanced. With moderate parameter tuning (e.g., cancellation among SM and NP interference terms to the 10%–20% level), $\text{BR}(K_L \rightarrow \pi^0 \nu \bar{\nu})$ may be enhanced by up to an order of magnitude.

The KLEVER experiment aims to use a high-energy neutral beam at the CERN SPS to achieve 60-event sensitivity for the decay $K_L \rightarrow \pi^0 \nu \bar{\nu}$ at the SM BR with an S/B ratio of 1. At the SM BR, this would correspond to a relative uncertainty of about 20%, demonstrating a discrepancy with 5σ significance if the observed rate is a bit more than twice or less than one-quarter of the SM rate, or with 3σ significance if the observed rate is less than half of the SM rate. These scenarios are consistent with the rates predicted for many different SM extensions, as seen in table 7.

10.3. B physics anomalies and $\text{BR}(K \rightarrow \pi \nu \bar{\nu})$

A number of anomalies have been observed, some of which are 3σ deviations from SM predictions, in semi-leptonic B decays [64, 65]. The upcoming analysis of the full LHC Run II data set, together with the large B -pair data set collected by CMS in 2018 via the data parking technique (more than 10^{10} B -pairs collected), as well as future data from Belle-II, will go a long way towards clarifying the status of these anomalies: are they evidence for new physics, or just statistic fluctuations? Taken together the anomalies hint at a violation of Lepton Flavor Universality. PBC experiments such as NA62 and KLEVER can therefore shed complementary light on explanations for these anomalies. Explanations for the B anomalies include models with flavor violation only in the third generation [119], theories with an additional Z' [358], and theories with leptoquarks [359].

In most such models the decay $K_L \rightarrow \pi^0 \nu \bar{\nu}$, as probed by KLEVER, could be as sensitive to the physics responsible to the anomalies as $K^+ \rightarrow \pi^+ \nu \bar{\nu}$. The key question then is to which level of precision can one measure these branching ratios relative to the SM expectation and

Table 7. Effects on BRs for $K \rightarrow \pi\nu\bar{\nu}$ decays in various SM extensions, with constraints from other kaon observables, including in particular $\text{Re } \epsilon'_K / \epsilon_K$.

Model	Λ (TeV)	Effect on $\text{BR}(K^+ \rightarrow \pi^+\nu\bar{\nu})$	Effect on $\text{BR}(K_L \rightarrow \pi^0\nu\bar{\nu})$	References
Leptoquarks, most models	1–20	Very large enhancements; mainly ruled out		[350]
Leptoquarks, U_1	1–20	+10% to +60%	+100% to +800%	[350]
Vector-like quarks	1–10	–90% to +60%	–100% to +30%	[351]
Vector-like quarks + Z'	10	–80% to +400%	–100% to 0%	[351]
Simplified modified Z , no tuning	1	–100% to +80%	–100% to –50%	[352]
General modified Z , cancellation to 20%	1	–100% to +400%	–100% to +500%	[352]
SUSY, chargino Z penguin	4–6 TeV		–100% to –40%	[353]
SUSY, gluino Z penguin	3–5.5 TeV	0% to +60%	–20% to +60%	[354]
SUSY, gluino Z penguin	10	Small effect	0% to +300%	[355]
SUSY, gluino box, tuning to 10%	1.5–3	$\pm 10\%$	$\pm 20\%$	[356]
LHT	1	$\pm 20\%$	–10% to –100%	[357]

the timescale within which such sensitivity can be reached. With the sensitivities discussed for the PBC program, both NA62 and KLEVER can shed light on many of the possible explanations for the anomalies.

11. Conclusions and outlook

In the past decade, one of the major accomplishments of particle physics has been the discovery of the Higgs boson that has successfully completed the experimental validation of the SM. Beyond this outstanding achievement, a wealth of experimental results has been produced by the ATLAS, CMS and LHCb Collaborations during Run 1 and Run 2 of the LHC: these Collaborations have explored in depth the paradigm of NP at the TeV scale, required to solve the hierarchy problem in case of the presence of an intermediate scale between the EW and the Planck scales. The search for NP has been performed so far both via direct searches and through precision measurements in flavor: tremendous progress has been achieved in understanding the SM structure in the last decades.

This progress is expected to continue for the next two decades: the upgrade of the LHCb experiment in 2019–2020 will allow a dataset of 50 fb^{-1} to be collected in about five years of operation. Major upgrades of the ATLAS and CMS detectors are also scheduled in 2023–2026 with the ultimate aim to reach an integrated luminosity of about 3000 fb^{-1} by around 2035.

Away from the LHC, Belle-II is expected to collect an integrated luminosity of 50 ab^{-1} by 2024. This will provide a dataset that is about a factor of 50 times larger than that collected by BaBar and Belle in the recent past. The Mu2E experiment at FNAL, and the Mu3e and the upgrade of MEG experiments at the PSI in the next decade will advance tremendously in the investigation of NP in charged LFV processes, nicely completing and complementing the quest of NP performed at the LHC experiments and at the *B*-factory.

However, the absence, so far, of unambiguous signal of NP from direct searches at the LHC, indirect searches in flavor physics and direct detection dark matter experiments, along with the absence of a clear guidance from the theory about the NP scale, imposes today, more than ever, to broadening the experimental effort in the quest for NP and exploring different ranges of interaction strengths and masses with respect to what is already covered by existing or planned initiatives.

The CERN laboratory could offer an unprecedented variety of high-intensity, high-energy beams and scientific infrastructures that could be exploited to this endeavour. This effort would nicely complement and further broaden the already rich physics program ongoing at the LHC and HL-LHC.

The proposals presented in the PBC–BSM context can search for NP in a fully complementary range of masses and couplings with respect to those investigated at the LHC: new particles with masses in the sub-eV range and very weakly coupled to the SM particles, can be explored by the IAXO and JURA proposals or through the investigation of oscillating EDMs in protons or deuterons in a electrostatic ring (CPEDM); MeV–GeV hidden-sector physics can be explored by a multitude of experiments at the PS beam lines (REDTOP proposal), SPS beam lines (NA62⁺⁺, NA64⁺⁺, SHiP, KLEVER, LDMX, and NA64/AWAKE proposals) and at the LHC interaction points (FASER, CODEX-b, MATHUSLA200, and milliQan proposals). The multi-TeV mass range ($\sim 100 \text{ TeV}$) can be indirectly explored both via ultra-rare or forbidden decays (KLEVER and TauFV) and through the search for a permanent EDM in protons/deuterons (CPEDM) or in strange/charmed baryons (LHC-FT).

The Collaborations behind these proposals are backed up by a lively phenomenological and theoretical community, and represent a fertile ground where New Physics models can be developed, discussed, and further improved. These proposals will possibly compete with similar proposals planned in the world (as, for example, at Jefferson Lab, FNAL, J-PARC, KEK, Mainz, PSI, etc) and complement the current effort in the search for NP in other domains (as, for example, DM direct searches at Gran Sasso Laboratory, SNOLAB or elsewhere). They will further enrich the ongoing effort at the LHC to discover NP at the TeV scale, increasing the impact that CERN could have in the next 10-20 years on the international landscape.

Acknowledgments

We are grateful to the colleagues of the Beam Dump Facility, Conventional Beams, AWAKE and eSPS Physics Beyond Colliders working groups for useful discussions and synergies. We warmly thank F Kahlhoefer and M Williams for help with recasting some old experimental results related to ALPs with fermion and gluon couplings. We are grateful to Dean Robinson and Harikrishnan Ramani for help with computing the CODEX-b reach, and to Marat Freytsis for helpful discussions related to the penguin calculations for the benchmark cases BC10 and BC11. Individual authors of this report have received financial support from ERC Ideas Consolidator Grant No. 771642 SELDOM (European Union); MINECO and GVA (Spain).

Appendix A. ALPS: prescription for treating the FCNC processes

The prescription for treating the FCNC processes for ALPS production and consequent decay described below assume a certain number of approximations. For an in-depth study of ALP production and decay, see the recent work [332] where the non-perturbative aspects of the problem are treated using the data-driven approach, derived from meson production, interaction and decay.

A.1. ALPs with fermion coupling (BC10)

There is a certain degree of UV dependence associated with the production through B -meson decays, and the PBC recommends following the prescription in [31]. Concretely, the effective $b - s - a$ vertex upon integrating out the W and t is taken to be

$$\mathcal{L} \supset \frac{a}{f_q} \bar{s}_L b_R \times \frac{\sqrt{2} G_F m_t^2 m_b V_{ts}^* V_{tb}}{8\pi^2} \times c_{fnc}^{(BC10)} + (\text{h.c.}). \quad (\text{A.1})$$

and coefficient $c_{fnc}^{(BC10)}$ is chosen to be

$$c_{fnc}^{(BC10)} = \log \left(\frac{\Lambda_{UV}^2}{m_t^2} \right). \quad (\text{A.2})$$

where the threshold (model dependent finite pieces) cannot be determined without UV completion and are dropped. The generalization to $\bar{d}_L s_R a$ interactions is done by taking $V_{ts}^* V_{tb} \rightarrow V_{td}^* V_{ts}$.

Taking $\Lambda_{UV} = 1$ TeV and again following [31], the branching ratios are

$$\text{Br}(B \rightarrow Ka) \approx 1.5 \times 10^{-5} \times \left(\frac{100 \text{ TeV}}{f_q} \right)^2 \times (\mathcal{F}_K(m_a))^2 \lambda_{Ka}^{1/2} \quad (\text{A.3})$$

$$\text{Br}(B \rightarrow K^*a) \approx 1.8 \times 10^{-5} \times \left(\frac{100 \text{ TeV}}{f_q} \right)^2 \times (\mathcal{F}_{K^*}(m_a))^2 \lambda_{K^*a}^{3/2} \quad (\text{A.4})$$

with form-factors extracted from B -physics literature:

$$\mathcal{F}_K(m_a) = \frac{1}{1 - m_a^2/(38 \text{ GeV}^2)} \quad (\text{A.5})$$

$$\mathcal{F}_{K^*}(m_a) = \frac{3.65}{1 - m_a^2/(28 \text{ GeV}^2)} - \frac{2.65}{1 - m_a^2/(37 \text{ GeV}^2)} \quad (\text{A.6})$$

$$\lambda_{ij} = \left(1 - \frac{(m_i + m_j)^2}{m_B^2} \right) \left(1 - \frac{(m_i - m_j)^2}{m_B^2} \right). \quad (\text{A.7})$$

For the inclusive rate, we assume

$$\text{Br}(B \rightarrow X_s a) \approx 5 \times (\text{Br}(B \rightarrow Ka) + \text{Br}(B \rightarrow K^*a)), \quad (\text{A.8})$$

following arguments presented in [332].

A.2. ALPs with gluon coupling (BC11)

In this benchmark case, the ALP can be produced directly in the hadronization process or through a B -meson decay. Concretely, 1-loop operator mixing generates the effective coupling of already considered in BC10:

$$\mathcal{L} \supset \delta c_{qq} \frac{\partial_\mu a}{f_G} \sum_\beta \bar{q}_\beta \gamma_\mu \gamma_5 q_\beta, \quad (\text{A.9})$$

where δc_{qq} is generated through a gluon loop. The corresponding log-enhanced coefficient can be found in [341].

A full calculation would require specifying a UV model, especially since the log-enhanced coefficient is not parametrically large. For concreteness we follow the choice in [332] by (1) dropping all logs and (2) setting δc_{qq} equal to the coefficient of the leading log of the diagram which generates (A.9). In formulas this corresponds to

$$\mathcal{L} \supset \frac{a}{f_q} \bar{s}_L b_R \times \frac{\sqrt{2} G_F m_t^2 m_b V_{ts}^* V_{tb}}{8\pi^2} \times c_{fnc}^{(BC11)} + (\text{h.c.}). \quad (\text{A.10})$$

Our choice for $c_{fnc}^{(BC11)}$ is

$$c_{fnc}^{(BC11)} \simeq \alpha_s^2(m_t). \quad (\text{A.11})$$

We note here that there is a significant UV-completion dependence, and further work would be required to properly estimate the preferred range for $c^{(BC11)}$.

With this convention, again following [31], the branching fractions are

$$\text{Br}(B \rightarrow Ka) \approx 6.6 \times 10^{-10} \times \left(\frac{100 \text{ TeV}}{f_G} \right)^2 \times (\mathcal{F}_K(m_a))^2 \lambda_{Ka}^{1/2} \quad (\text{A.12})$$

$$\text{Br}(B \rightarrow K^*a) \approx 7.9 \times 10^{-10} \times \left(\frac{100 \text{ TeV}}{f_G} \right)^2 \times (\mathcal{F}_{K^*}(m_a))^2 \lambda_{K^*a}^{3/2}. \quad (\text{A.13})$$

Again, the uncertainty in the amplitude could result in as much as $\mathcal{O}(10)$ changes in the width, with more accurate calculation of RG effects and threshold corrections in UV complete models.

A.3. Approximation for ALP lifetime

For computing the ALP lifetime the PBC has taken the following approximations, depending on the mass range considered.

- *Region 1*, $m_a < 3m_\pi$, *photon decay* $a \rightarrow \gamma\gamma$. In this case the decay is dominated by the two-photon contribution.

$$\Gamma_{\text{tot}}(m_a < 3m_\pi) \approx \Gamma_{\gamma\gamma} = \frac{m_a^3}{f_G^2} \times \frac{\pi\alpha^2}{4} \times \left(\frac{4m_d + m_u}{3(m_u + m_d)} - \frac{m_a^2}{m_a^2 - m_\pi^2} \frac{m_d - m_u}{2(m_u + m_d)} \right)^2 \quad (\text{A.14})$$

$$= \frac{m_a^3}{f_G^2} \times \frac{\pi\alpha^2}{4} \times \left(1.0 - 0.18 \times \frac{m_a^2}{m_a^2 - m_\pi^2} \right)^2. \quad (\text{A.15})$$

Notice that the $\frac{4m_d + m_u}{3(m_u + m_d)}$ ratio in (A.14), to good accuracy, is 1 for the physical point of $m_u/m_d \simeq 0.48$. The second term in the bracket comes from the mixing with π^0 meson, see [341]. This formula can be further improved by including contributions from mixing with η (and η').

- *Region 2*, $3m_\pi < m_a < 2m_\pi + m_\eta$, *$a \rightarrow 3\pi$ decay*. In this region, two new decay modes, $\pi^+\pi^-\pi^0$ and $3\pi^0$, open up. Within 2-flavor chiral perturbation theory, these decays were treated in [341]. The results are chirally suppressed, $\Gamma_{a \rightarrow 3\pi} \propto m_a m_\pi^2 / (F_\pi f_G)^2$. Using formulae from [341], we adopt it to normalization used in these notes

$$\Gamma_{\text{tot}} = \Gamma_{\gamma\gamma} + \Gamma_{a \rightarrow 3\pi}; \quad \Gamma_{a \rightarrow 3\pi} = \frac{\pi}{3 \times 128} \frac{m_a m_\pi^4}{F_\pi^2 f_G^2} \left(\frac{m_a^2}{m_a^2 - m_\pi^2} \frac{m_d - m_u}{m_u + m_d} \right)^2 \times I(m_\pi^2/m_a^2),$$

$$I(y) = \int_{4y}^{(1-\sqrt{y})^2} \sqrt{1 - \frac{4y}{x}} \sqrt{(1-x-y)^2 - 4xy} \times [12(x-y)^2 + 2]. \quad (\text{A.16})$$

One can check that $\Gamma_{a \rightarrow 3\pi}$ is comparable to $\Gamma_{\gamma\gamma}$. Asymptotically⁶⁵, at large m_a , $I \rightarrow 2$. Given the experience with η decays [360], the validity of the leading chiral order answer is within a factor of ~ 3 , and can be improved by including next orders in the chiral expansion. In this mass region, $a \rightarrow \eta^* \rightarrow 3\pi$ mediated decay is also important, especially near $m_a = m_\eta$.

⁶⁵ This formula is valid in the regime of $f_G \gg F_\pi$, $\theta_\pi \ll 1$.

- *Region 3*, $2m_\pi + m_\eta < m_a < 1.5 \text{ GeV}$, *multiple hadronic decays*. Above the $2m_\pi + m_\eta \sim 830 \text{ MeV}$ threshold many new hadronic contributions open up, ($\eta\pi\pi$, $\rho\pi$, also $f_0\pi$ etc) so that the result is much larger than chiral perturbation theory answer for $a \rightarrow 3\pi$. One could use hadronic resonance models to have a phenomenological description of a decays, but for sake of simplicity we suggest an interpolating formula for the a decay. The following formula

$$\Gamma_{\text{tot}}(m_1 < m_a < m_2) \approx A(m_a - B)^3; \quad A = \frac{\Gamma_2(1-r)^3}{(m_2 - m_1)^3}; \quad B = \frac{m_1 - rm_2}{1-r}; \quad r = (\Gamma_1/\Gamma_2)^{1/3} \quad (\text{A.17})$$

interpolates in the region from $m_1 = 2m_\pi + m_\eta$ to $m_2 = 1.5 \text{ GeV}$ where $\Gamma_1 = \Gamma_\gamma(m_1) + \Gamma_{3\pi}(m_1)$ and $\Gamma_2 = \Gamma_{gg}(m_a = 1.5 \text{ GeV})$ is the inclusive decay to gluons (see below). This interpolation captures the rapidly growing decay rate by introducing $\propto m_a^3$ scaling. $m_a = 1.5 \text{ GeV}$ is chosen to be the lower boundary of the perturbative description, and this choice bears significant uncertainty.

- *Region 4*, $m_a > 1.5 \text{ GeV}$, *perturbative description*. At $m_a \sim 1.1 - 1.5 \text{ GeV}$, many new additional hadronic decays of a open up, $\pi_0 f_0(980)$, πa_0 , ηf_0 , $\rho\rho$, KK^* etc, quickly driving up the value for Γ_{tot} . Asymptotically, the sum of all hadronic states approaches the perturbative $a \rightarrow \text{gluons}$ answer. PBC recommends using the perturbative formula of a decays to gluons as a proxy for hadronic decays above 1.5 GeV :

$$\Gamma_{\text{tot}}(m_a > 1.5 \text{ GeV}) \approx \Gamma_{gg} = \frac{m_a^3}{f_G^2} \times \frac{\pi\alpha_s^2(m_a)}{2}, \quad (\text{A.18})$$

This is an order-of-magnitude estimate, that cannot be improved using perturbation theory, and may only be improved with non-perturbative methods.

- *Resonance regions*, $m_a \sim m_\eta$, $m_a \sim m_{\eta'}$. In addition to the above expressions, one needs to add strong resonant contributions when m_a becomes close to m_η and $m_{\eta'}$. If the continuum—resonance interference is neglected, this is achieved via the following formulae

$$\Gamma_{a-\eta, \text{res}} = (2\pi^2 \cos \theta_p)^2 \times \frac{F_\pi^2}{f_G^2} \times \frac{m_a^4 \Gamma_\eta(m_a)}{(m_a^2 - m_\eta^2)^2 + m_\eta^2 \Gamma_\eta^2(m_a)}, \quad (\text{A.19})$$

$$\Gamma_{a-\eta', \text{res}} = (2\pi^2 \sin \theta_p)^2 \times \frac{F_\pi^2}{f_G^2} \times \frac{m_a^4 \Gamma_{\eta'}(m_a)}{(m_a^2 - m_{\eta'}^2)^2 + m_{\eta'}^2 \Gamma_{\eta'}^2(m_a)}, \quad (\text{A.20})$$

where $\Gamma_\eta(m)$ and $\Gamma_{\eta'}(m)$ are the energy-dependent widths $\Gamma(E)$ evaluated at $E = m_a$. Value for mixing angles, $\cos \theta_p \simeq 0.6$ and $\sin \theta_p \simeq 0.8$, are taken from [361]. More details on mixing coefficients are given in the appendix.

Theoretical input is required in deriving $\Gamma_{\eta(\eta')}(E)$, where the main effect is due to the available phase space for 3π and $\eta 2\pi$ final states. PBC suggest using a simple approximate formula that reflects the growth of phases space. For η meson we take

$$\Gamma_\eta(E) = \Gamma_\eta \times \frac{f(E)}{f(m_\eta)}; \quad f(E) = \frac{(E - 3m_\pi)^{1.5}}{(E - 3m_\pi)^{1.5} + (300 \text{ MeV})^{1.5}} \text{ for } E > 3m_\pi; \\ f(E) = 0 \text{ for } E < 3m_\pi, \quad (\text{A.21})$$

where Γ_η is the total width of (physical) η meson. For η' , the same formula applies, with

$\Gamma_\eta \rightarrow \Gamma_{\eta'}$ and $3m_\pi \rightarrow 2m_\pi + m_\eta$ substitutions. Better description can be achieved with the use of hadronic models.

Appendix B. ALPs: production via π^0, η, η' mixing

If m_a is below the hadronic scale of $\sim 4\pi F_\pi$ ($F_\pi = 93$ MeV), one can neglect heavy flavors and try to use chiral perturbation theory by replacing $G\tilde{G}$ operator with using the anomaly equation. We use this equation for three light quarks ($q_i = u, d, s$) in the following form

$$\frac{\alpha_s}{8\pi} G^b \tilde{G}^b = \sum_i \frac{m_*}{2m_i} \partial_\mu \bar{q}_i \gamma_\mu \gamma_5 q_i - m_* \sum_i \bar{q}_i i \gamma_5 q_i - \frac{\alpha}{4\pi} F \tilde{F} \sum_i \frac{N_c Q_i^2 m_*}{m_i}, \quad (\text{B.1})$$

where we suppress the Lorentz indices over the gluon and photon fields strength, G and F . Here Q_i are the quark charges in units of e , $N_c = 3$ and $m_* \equiv (\sum_i m_i^{-1})^{-1}$. Dropping terms suppressed by $m_{u(d)}/m_s$, we have $m_* = m_u m_d / (m_u + m_d)$ and

$$\begin{aligned} \frac{\alpha_s}{8\pi} G^b \tilde{G}^b &= \frac{m_d}{2(m_u + m_d)} \partial_\mu \bar{u} \gamma_\mu \gamma_5 u + \frac{m_u}{2(m_u + m_d)} \partial_\mu \bar{d} \gamma_\mu \gamma_5 d \\ &\quad - m_* \sum_i \bar{q}_i i \gamma_5 q_i - \frac{\alpha}{4\pi} F \tilde{F} \frac{4m_d + m_u}{3(m_u + m_d)}. \end{aligned} \quad (\text{B.2})$$

In the leading chiral order, the flavor-singlet $m_* \sum_i \bar{q}_i i \gamma_5 q_i$ combination can be neglected, and the total Lagrangian at low energy can be rewritten as

$$\begin{aligned} \mathcal{L}_{\text{axion, l.e.}} &= \mathcal{L}_{\text{SM}} + \mathcal{L}_{\text{DS}} + 4\pi^2 \times \frac{a}{f_G} \frac{\alpha}{4\pi} \frac{4m_d + m_u}{3(m_u + m_d)} F_{\mu\nu} \tilde{F}_{\mu\nu} \\ &\quad - 4\pi^2 \times \frac{\partial_\mu a}{2f_G} \left(J_{A,\mu}^S + \frac{m_d - m_u}{m_u + m_d} J_{A,\mu}^T \right), \end{aligned} \quad (\text{B.3})$$

where $J_{A,\mu}^S$ is the singlet, $\frac{1}{2}(\bar{u} \gamma_\mu \gamma_5 u + \bar{d} \gamma_\mu \gamma_5 d)$, and $J_{A,\mu}^T$ is the triplet axial-vector current, $\frac{1}{2}(\bar{u} \gamma_\mu \gamma_5 u - \bar{d} \gamma_\mu \gamma_5 d)$. Interaction with $J_{A,\mu}^S$ leads to $a-\eta$ and $a-\eta'$ mixing, while interaction with $J_{A,\mu}^T$ results in $a-\pi^0$ mixing.

Using the model that relates octet and singlet quark states to physical η and η' [361], and usual rules for $\langle 0 | J_{A,\mu} | \text{pseudoscalar} \rangle$ matrix elements, we transform the last term in (B.3) to an on-shell mixing between a and the pseudoscalars

$$\begin{aligned} \mathcal{L}_{\text{axion, l.e.}} &= \dots 4\pi^2 \times \frac{\partial_\mu a}{2f_G} \left(J_{A,\mu}^S + \frac{m_d - m_u}{m_u + m_d} J_{A,\mu}^T \right) \\ &\rightarrow 4\pi^2 \times \frac{F_\pi}{2f_G} \left(\partial_\mu a \partial_\mu \eta \times \cos \theta_p + \partial_\mu a \partial_\mu \eta' \times \sin \theta_p + \partial_\mu a \partial_\mu \pi_0 \frac{m_d - m_u}{m_u + m_d} \right), \end{aligned} \quad (\text{B.4})$$

where $\cos \theta_p \simeq 0.6$ and $\sin \theta_p \simeq 0.8$ related physical η and η' with octet and singlet combinations [361].

ORCID iDs

J Beacham  <https://orcid.org/0000-0003-3623-3335>

D Curtin  <https://orcid.org/0000-0003-0263-6195>

G Lanfranchi  <https://orcid.org/0000-0002-9467-8001>

References

- [1] Aad G *et al* (ATLAS collaboration) 2012 Observation of a new particle in the search for the Standard Model Higgs boson with the ATLAS detector at the LHC *Phys. Lett. B* **716** 1–29
- [2] Chatrchyan S *et al* (CMS collaboration) 2012 Observation of a new boson at a mass of 125 GeV with the CMS experiment at the LHC *Phys. Lett. B* **716** 30–61
- [3] Degrassi G *et al* 2012 Higgs mass and vacuum stability in the standard model at NNLO *J. High Energy Phys.* **JHEP08(2012)098**
- [4] Buttazzo D *et al* 2013 Investigating the near-criticality of the Higgs boson *J. High Energy Phys.* **JHEP12(2013)089**
- [5] Bezrukov F, Kalmykov M Y, Kniehl B A and Shaposhnikov M 2012 Higgs boson mass and new physics *J. High Energy Phys.* **JHEP10(2012)140**
- [6] Sakharov A D 1967 Violation of CP Invariance, C asymmetry, and baryon asymmetry of the Universe *Pisma Zh. Eksp. Teor. Fiz.* **5** 32–5
- [7] Coleman S R and Glashow S L 1999 High-energy tests of Lorentz invariance *Phys. Rev. D* **59** 116008
- [8] Jackiw R and Kostelecky V A 1999 Radiatively induced Lorentz and CPT violation in electrodynamics *Phys. Rev. Lett.* **82** 3572–5
- [9] Kostelecky V A and Russell N 2011 Data tables for lorentz and CPT violation *Rev. Mod. Phys.* **83** 11–31
- [10] Asaka T, Blanchet S and Shaposhnikov M 2005 The nuMSM, dark matter and neutrino masses *Phys. Lett. B* **631** 151–6
- [11] Asaka T and Shaposhnikov M 2005 The nuMSM, dark matter and baryon asymmetry of the Universe *Phys. Lett. B* **620** 17–26
- [12] Lee B W and Weinberg S 1977 Cosmological lower bound on heavy neutrino masses *Phys. Rev. Lett.* **39** 165–8
- [13] Boehm C, Ensslin T A and Silk J 2004 Can annihilating dark matter be lighter than a few GeVs? *J. Phys. G: Nucl. Part. Phys.* **30** 279–86
- [14] Boehm C and Fayet P 2004 Scalar dark matter candidates *Nucl. Phys. B* **683** 219–63
- [15] Pospelov M, Ritz A and Voloshin M B 2008 Secluded WIMP dark matter *Phys. Lett. B* **662** 53–61
- [16] Feng J L and Kumar J 2008 The WIMPlless miracle: dark-matter particles without weak-scale masses or weak interactions *Phys. Rev. Lett.* **101** 231301
- [17] Feng J L, Tu H and Yu H-B 2008 Thermal relics in hidden sectors *J. Cosmol. Astropart. Phys.* **JCAP10(2008)043**
- [18] Pospelov M 2009 Secluded U(1) below the weak scale *Phys. Rev. D* **80** 095002
- [19] Arkani-Hamed N, Finkbeiner D P, Slatyer T R and Weiner N 2009 A theory of dark matter *Phys. Rev. D* **79** 015014
- [20] Pospelov M and Ritz A 2009 Astrophysical signatures of secluded dark matter *Phys. Lett. B* **671** 391–7
- [21] Patt B and Wilczek F Higgs-field portal into hidden sectors arXiv:[hep-ph/0605188](https://arxiv.org/abs/hep-ph/0605188)
- [22] Batell B, Pospelov M and Ritz A 2009 Exploring portals to a hidden sector through fixed targets *Phys. Rev. D* **80** 095024
- [23] Alekhin S *et al* 2016 A facility to search for hidden particles at the CERN SPS: the SHiP physics case *Rep. Prog. Phys.* **79** 124201
- [24] Holdom B 1986 Two U(1)'s and epsilon charge shifts *Phys. Lett. B* **166** 196–8
- [25] Izaguirre E, Krnjaic G, Schuster P and Toro N 2014 Physics motivation for a pilot dark matter search at Jefferson laboratory *Phys. Rev. D* **90** 014052
- [26] Izaguirre E, Krnjaic G, Schuster P and Toro N 2015 Analyzing the discovery potential for light dark matter *Phys. Rev. Lett.* **115** 251301
- [27] Jaeckel J and Ringwald A 2010 The low-energy frontier of particle physics *Ann. Rev. Nucl. Part. Sci.* **60** 405–37
- [28] Bauer M, Foldenauer P and Jaeckel J 2018 Hunting all the hidden photons *J. High Energy Phys.* **2018** **JHEP07(2018)094**
- [29] O'Connell D, Ramsey-Musolf M J and Wise M B 2007 Minimal extension of the standard model scalar sector *Phys. Rev. D* **75** 037701
- [30] Krnjaic G 2016 Probing light thermal dark-matter with a Higgs portal mediator *Phys. Rev. D* **94** 073009

- [31] Batell B, Pospelov M and Ritz A 2011 Multi-lepton signatures of a hidden sector in rare B decays *Phys. Rev. D* **83** 054005
- [32] Bezrukov F and Gorbunov D 2010 Light inflaton hunter's guide *J. High Energy Phys.* **JHEP05(2010)010**
- [33] Bird C, Jackson P, Kowalewski R V and Pospelov M 2004 Search for dark matter in $b \rightarrow s$ transitions with missing energy *Phys. Rev. Lett.* **93** 201803
- [34] Gorbunov D and Shaposhnikov M 2007 How to find neutral leptons of the ν MSM? *J. High Energy Phys.* **JHEP10(2007)015**
- [35] Peccei R D and Quinn H R 1977 CP conservation in the presence of instantons *Phys. Rev. Lett.* **38** 1440–3
- [36] Weinberg S 1978 A new light Boson? *Phys. Rev. Lett.* **40** 223–6
- [37] Wilczek F 1978 Problem of strong p and t invariance in the presence of instantons *Phys. Rev. Lett.* **40** 279–82
- [38] Abel C *et al* 2017 Search for axionlike dark matter through nuclear spin precession in electric and magnetic fields *Phys. Rev. X* **7** 041034
- [39] Irastorza I G and Redondo J 2018 New experimental approaches in the search for axion-like particles *Prog. Part. Nucl. Phys.* **102** 89–159
- [40] Sikivie P 1983 Experimental tests of the *invisible* axion *Phys. Rev. Lett.* **51** 1415–7
- [41] Maiani L, Petronzio R and Zavattini E 1986 Effects of nearly massless, spin-zero particles on light propagation in a magnetic field *Phys. Lett. B* **175** 359–63
- [42] Van Bibber K, Dagdeviren N R, Koonin S E, Kerman A K and Nelson H N 1987 Proposed experiment to produce and detect light pseudoscalars *Phys. Rev. Lett.* **59** 759–62
- [43] Moody J E and Wilczek F 1984 New macroscopic forces? *Phys. Rev. D* **30** 130–8
- [44] Armengaud E *et al* 2014 Conceptual design of the international axion observatory (IAXO) *JINST* **9** T05002
- [45] Cameron R *et al* 1993 Search for nearly massless, weakly coupled particles by optical techniques *Phys. Rev. D* **47** 3707–25
- [46] Ehret K *et al* 2010 New ALPS results on hidden-sector lightweights *Phys. Lett. B* **689** 149–55
- [47] Ballou R *et al* (OSQAR collaboration) 2015 New exclusion limits on scalar and pseudoscalar axionlike particles from light shining through a wall *Phys. Rev. D* **92** 092002
- [48] Bahre R *et al* 2013 Any light particle search II—technical design report *J. Instrum.* **8** T09001
- [49] Hoogeveen F and Ziegenhagen T 1991 Production and detection of light bosons using optical resonators *Nucl. Phys. B* **358** 3–26
- [50] Sikivie P, Tanner D B and van Bibber K 2007 Resonantly enhanced axion-photon regeneration *Phys. Rev. Lett.* **98** 172002
- [51] Döbrich B, Jaeckel J, Kahlhoefer F, Ringwald A and Schmidt-Hoberg K 2016 ALPtraum: ALP production in proton beam dump experiments *J. High Energy Phys.* **JHEP02(2016)018**
- [52] Oberla E and Frisch H J 2016 The design and performance of a prototype water Cherenkov optical time-projection chamber *Nucl. Instrum. Methods A* **814** 19–32
- [53] Gatto C, Di Benedetto V, Mazzacane A and (T1015 collaboration) 2015 Status of ADRIANO R&D in T1015 Collaboration *J. Phys.: Conf. Ser.* **587** 012060
- [54] Kim T *et al* 2014 Production of scintillating fiber modules for high resolution tracking devices *PoS TIPP2014* 108
- [55] Gninenko S N 2014 Search for MeV dark photons in a light-shining-through-walls experiment at CERN *Phys. Rev. D* **89** 075008
- [56] Andreas S *et al* 2013 Proposal for an experiment to search for light dark matter at the SPS arXiv:1312.3309
- [57] Gninenko S N, Krasnikov N V, Kirsanov M M and Kirpichnikov D V 2016 Missing energy signature from invisible decays of dark photons at the CERN SPS *Phys. Rev. D* **94** 095025
- [58] Gninenko S N, Kirpichnikov D V, Kirsanov M M and Krasnikov N V 2018 The exact tree-level calculation of the dark photon production in high-energy electron scattering at the CERN SPS *Phys. Lett. B* **782** 406–11
- [59] Gninenko S N, Krasnikov N V and Matveev V A 2015 Muon $g-2$ and searches for a new leptophobic sub-GeV dark boson in a missing-energy experiment at CERN *Phys. Rev. D* **91** 095015
- [60] Gninenko S, Kovalenko S, Kuleshov S, Lyubovitskij V E and Zhevlakov A S 2018 Deep inelastic $e - \tau$ and $\mu - \tau$ conversion in the NA64 experiment at the CERN SPS *Phys. Rev. D* **98** 015007

- [61] Gninenko S N and Krasnikov N V 2018 Probing the muon $g_\mu - 2$ anomaly, $L_\mu - L_\tau$ gauge boson and dark matter in dark photon experiments *Phys. Lett. B* **783** 24–8
- [62] Kahn Y, Krnjaic G, Tran N and Whitbeck A 2018 M^3 : a new muon missing momentum experiment to probe $(g-2)_\mu$ and dark matter at Fermilab *J. High Energy Phys.* **JHEP09(2018)153**
- [63] Chen C-Y, Kozaczuk J and Zhong Y-M 2018 Exploring leptophilic dark matter with NA64- μ *J. High Energy Phys.* **JHEP10(2018)154**
- [64] Aaij R *et al* (LHCb collaboration) 2014 Test of lepton universality using $B^+ \rightarrow K^{*\ell^+\ell^-}$ decays *Phys. Rev. Lett.* **113** 151601
- [65] Aaij R *et al* (LHCb collaboration) 2017 Test of lepton universality with $B^0 \rightarrow K^{*0\ell^+\ell^-}$ decays *J. High Energy Phys.* **JHEP08(2017)055**
- [66] Gninenko S N and Krasnikov N V 2015 Invisible K_L decays as a probe of new physics *Phys. Rev. D* **92** 034009
- [67] Gninenko S N 2015 Search for invisible decays of π^0 , η , η' , K_S and K_L : a probe of new physics and tests using the Bell-Steinberger relation *Phys. Rev. D* **91** 015004
- [68] Barducci D, Fabbrichesi M and Gabrielli E 2018 Neutral hadrons disappearing into the darkness *Phys. Rev. D* **98** 035049
- [69] Abada A, Becirevic D, Sumensari O, Weiland C and Zukanovich R 2017 Funchal, Sterile neutrinos facing kaon physics experiments *Phys. Rev. D* **95** 075023
- [70] Banerjee D *et al* (NA64 collaboration) 2017 Search for invisible decays of sub-GeV dark photons in missing-energy events at the CERN SPS *Phys. Rev. Lett.* **118** 011802
- [71] Banerjee D *et al* (NA64 collaboration) 2018 Search for vector mediator of Dark Matter production in invisible decay mode *Phys. Rev. D* **97** 072002
- [72] Banerjee D *et al* (NA64 collaboration) 2018 Search for a hypothetical 16.7 MeV gauge boson and dark photons in the NA64 experiment at CERN *Phys. Rev. Lett.* **120** 231802
- [73] Feng J L *et al* 2016 Protophobic fifth-force interpretation of the observed anomaly in ^8Be nuclear transitions *Phys. Rev. Lett.* **117** 071803
- [74] Feng J L *et al* 2016 Particle physics models for the 17 MeV anomaly in beryllium nuclear decays *Phys. Rev. D* **95** 035017
- [75] Gagnon L 2018 Conventional beams working group to the physics beyond collider study and to the European strategy for particle physics *Technical Report* CERN-PBC-REPORT-2018-002 CERN
- [76] Gonnella F and (NA62 collaboration) 2017 The NA62 experiment at CERN *J. Phys.: Conf. Ser.* **873** 012015
- [77] Lanfranchi G and (NA62 collaboration) 2017 Search for hidden sector particles at NA62 *PoS EPS-HEP2017* 301
- [78] Åkesson T (LDMX collaboration) *et al* 2018 Light dark matter eXperiment (LDMX) arXiv:1808.05219
- [79] Åkesson T, Dutheil Y, Evans L, Grudiev A, Papaphilippou Y and Stapnes S 2018 A primary electron beam facility at CERN arXiv:1805.12379
- [80] Hansson Adrian P and (HPS collaboration) 2016 The silicon vertex tracker for the heavy photon search experiment *Proc., 2015 IEEE Nuclear Science Symp. and Medical Imaging Conf. (NSS/MIC 2015) (: San Diego, California, United States)* p 7581862 arXiv:1511.07844
- [81] Ahdida C C, Calviani M, Goddard B, Jacobsson R and Lamont M 2018 SPS beam dump facility comprehensive design study *Technical Report* CERN-PBC-REPORT -2018-001 CERN
- [82] Feng J L, Galon I, Kling F and Trojanowski S 2018 ForWard search experiment at the LHC *Phys. Rev. D* **97** 035001
- [83] Feng J L, Galon I, Kling F and Trojanowski S 2018 Dark Higgs bosons at the forward search experiment *Phys. Rev. D* **97** 055034
- [84] Batell B, Freitas A, Ismail A and Mckeen D 2018 Flavor-specific scalar mediators *Phys. Rev. D* **98** 055026
- [85] Kling F and Trojanowski S 2018 Heavy neutral leptons at FASER *Phys. Rev. D* **97** 095016
- [86] Helo J C, Hirsch M and Wang Z S 2018 Heavy neutral fermions at the high-luminosity LHC *J. High Energy Phys.* **2018 JHEP07(2018)056**
- [87] Cheng H-C, Li L and Zheng R 2018 Coscattering/Coannihilation dark matter in a fraternal twin Higgs model *J. High Energy Phys.* **JHEP09(2018)098**
- [88] Feng J L, Galon I, Kling F and Trojanowski S 2018 Axionlike particles at FASER: The LHC as a photon beam dump *Phys. Rev. D* **98** 055021

- [89] Hochberg Y, Kuflik E, McGehee R, Murayama H and Schutz K 2018 SIMPs through the axion portal *Phys. Rev. D* **98** 115031
- [90] Berlin A and Kling F 2019 Inelastic dark matter at the LHC lifetime frontier: ATLAS, CMS, LHCb, CODEX-b, FASER, and MATHUSLA *Phys. Rev. D* **99** 015021
- [91] Dercks D, de Vries J, Dreiner H K and Wang Z S 2019 R-parity violation and light neutralinos at CODEX-b, FASER, and MATHUSLA *Phys. Rev. D* **99** 055039
- [92] Ariga A (FASER collaboration) *et al* 2019 FASER's physics reach for long-lived particles *Phys. Rev. D* **99** 095011
- [93] Ferrari A, Sala P R, Fasso A and Ranft J 2005 FLUKA: a multi-particle transport code (Program version 2005)
- [94] Böhlen T T *et al* 2014 The FLUKA code: developments and challenges for high energy and medical applications *Nucl. Data Sheets* **120** 211–4
- [95] Sabate-Gilarte M, Cerutti F and Tsinganis A Characterization of the radiation field for the FASER experiment
- [96] Ariga A (FASER collaboration) *et al* 2018 Letter of intent for FASER: forward search experiment at the LHC arXiv:1811.10243
- [97] Chou J P, Curtin D and Lubatti H J 2017 New detectors to explore the lifetime frontier *Phys. Lett. B* **767** 29–36
- [98] Co R T, D'Eramo F and Hall L J 2017 Gravitino or axino dark matter with reheat temperature as high as 10^{16} GeV *J. High Energy Phys.* **JHEP03(2017)005**
- [99] Bhupal Dev P, Mohapatra R N and Zhang Y 2017 Displaced photon signal from a possible light scalar in minimal left-right seesaw model *Phys. Rev. D* **95** 115001
- [100] Dev P S B, Mohapatra R N and Zhang Y 2017 Long lived light scalars as probe of low scale seesaw models *Nucl. Phys. B* **923** 179–221
- [101] Caputo A, Hernandez P, Lopez-Pavon J and Salvado J 2017 The seesaw portal in testable models of neutrino masses *J. High Energy Phys.* **JHEP06(2017)112**
- [102] Curtin D and Peskin M E 2018 Analysis of long lived particle decays with the MATHUSLA detector *Phys. Rev. D* **97** 015006
- [103] Evans J A, Gori S and Shelton J 2018 Looking for the WIMP next door *J. High Energy Phys.* **JHEP02(2018)100**
- [104] D'Agnolo R T, Mondino C, Ruderman J T and Wang P-J 2018 Exponentially light dark matter from coannihilation *J. High Energy Phys.* **2018 JHEP08(2018)079**
- [105] Berlin A, Gori S, Schuster P and Toro N 2018 Dark sectors at the Fermilab SeaQuest experiment *Phys. Rev. D* **98** 035011
- [106] Deppisch F F, Liu W and Mitra M 2018 Long-lived heavy neutrinos from Higgs decays *J. High Energy Phys.* **2018 JHEP08(2018)181**
- [107] Jana S, Okada N and Raut D 2018 Displaced vertex signature of type-I seesaw *Phys. Rev. D* **98** 035023
- [108] Dev P S B, Ramsey-Musolf M J and Zhang Y 2018 Doubly-charged scalars in the Type-II seesaw mechanism: fundamental symmetry tests and high-energy searches *Phys. Rev. D* **98** 055013
- [109] Curtin D *et al* 2019 Long-lived particles at the energy frontier: the MATHUSLA physics case *Rept. Prog. Phys.* **82** 116201
- [110] Alpigiani C *et al* 2018 A letter of intent for MATHUSLA: a dedicated displaced vertex detector above ATLAS or CMS arXiv:1811.00927
- [111] Aielli G *et al* (Argo-YBJ collaboration) 2006 Layout and performance of RPCs used in the Argo-YBJ experiment *Nucl. Instrum. Methods A* **562** 92–6
- [112] Iuppa R 2015 Potential of RPCs in cosmic ray experiments for the next decade *JINST* **10** C04044
- [113] Aliaga L *et al* (MINERvA collaboration) 2014 Design, calibration, and performance of the MINERvA detector *Nucl. Instrum. Methods A* **743** 130–59
- [114] Aushev T *et al* 2015 A scintillator based endcap K_L and muon detector for the Belle II experiment *Nucl. Instrum. Methods A* **789** 134–42
- [115] Gligorov V V, Knapen S, Papucci M and Robinson D J 2018 Searching for long-lived particles: a compact detector for exotics at LHCb *Phys. Rev. D* **97** 015023
- [116] Lindner R private communication
- [117] Buras A J, Buttazzo D, Girschbach-Noe J and Knegjens R 2014 Can we reach the Zeptouniverse with rare K and $B_{s,d}$ decays? *J. High Energy Phys.* **JHEP11(2014)121**

- [118] Buttazzo D, Greljo A, Isidori G and Marzocca D 2017 B-physics anomalies: a guide to combined explanations *J. High Energy Phys.* **JHEP11(2017)044**
- [119] Bordone M, Buttazzo D, Isidori G and Monnard J 2017 Probing lepton flavour universality with $K \rightarrow \pi \nu \bar{\nu}$ decays *Eur. Phys. J. C* **77** 618
- [120] Fajfer S, Kosnik N and Vale Silva L 2018 Footprints of leptoquarks: from $R_{K^{(*)}}$ to $K \rightarrow \pi \nu \bar{\nu}$ *Eur. Phys. J. C* **78** 275
- [121] Babu K S and Kolda C 2002 Higgs mediated tau \rightarrow 3 mu in the supersymmetric seesaw model *Phys. Rev. Lett.* **89** 241802
- [122] Brignole A and Rossi A 2003 Lepton flavor violating decays of supersymmetric Higgs bosons *Phys. Lett. B* **566** 217–25
- [123] Paradisi P 2005 Constraints on SUSY lepton flavor violation by rare processes *J. High Energy Phys.* **JHEP10(2005)006**
- [124] Hays C, Mitra M, Spannowsky M and Waite P 2017 Prospects for new physics in $\tau \rightarrow l \mu \mu$ at current and future colliders *J. High Energy Phys.* **JHEP05(2017)014**
- [125] Feruglio F, Paradisi P and Pattori A 2017 Revisiting lepton flavor universality in B decays *Phys. Rev. Lett.* **118** 011801
- [126] Crivellin A, Hofer L, Matias J, Nierste U, Pokorski S and Rosiek J 2015 Lepton-flavour violating B decays in generic Z' models *Phys. Rev. D* **92** 054013
- [127] Greljo A, Isidori G and Marzocca D 2015 On the breaking of lepton flavor universality in B decays *J. High Energy Phys.* **JHEP07(2015)142**
- [128] Feruglio F, Paradisi P and Pattori A 2017 On the importance of electroweak corrections for B anomalies *J. High Energy Phys.* **JHEP09(2017)061**
- [129] Atoian G S *et al* 2008 An improved shashlyk calorimeter *Nucl. Instrum. Methods A* **584** 291–303
- [130] Ramberg E, Cooper P and Tschirhart R 2004 A photon veto detector for the CKM experiment *IEEE Trans. Nucl. Sci.* **51** 2201–4
- [131] Atiya M S *et al* 1992 A detector to search for $K^+ \rightarrow \pi^+ \nu \bar{\nu}$ *Nucl. Instrum. Methods A* **321** 129–51
- [132] Ambrosino F *et al* 2007 A Prototype large-angle photon veto detector for the P326 experiment at CERN *Proc., 2007 IEEE Nuclear Science Symp. and Medical Imaging Conf. (NSS/MIC 2007)* vol 1 (Honolulu, Hawaii., 28 October–3 November 2007) pp 57–64
- [133] Hayasaka K *et al* 2010 Search for lepton flavor violating tau decays into three leptons with 719 million produced tau+tau- pairs *Phys. Lett. B* **687** 139–43
- [134] Lees J *et al* (BaBar collaboration) 2010 Limits on τ lepton-flavor violating decays in three charged leptons *Phys. Rev. D* **81** 111101
- [135] Aaij R *et al* (LHCb collaboration) 2015 Search for the lepton flavour violating decay $\tau^- \rightarrow \mu^- \mu^+ \mu^-$ *J. High Energy Phys.* **JHEP02(2015)121**
- [136] Abe T (Belle-II collaboration) *et al* 2010 Belle II technical design report arXiv:1011.0352
- [137] Charles M J, Forty R and (LHCb collaboration) 2011 TORCH: time of flight identification with cherenkov radiation *Nucl. Instrum. Methods A* **639** 173–6
- [138] Harnew N *et al* 2018 Status of the TORCH time-of-flight project arXiv:1812.09773
- [139] Bediaga I (LHCb collaboration) *et al* 2018 Physics case for an LHCb Upgrade II-Opportunities in flavour physics, and beyond, in the HL-LHC era arXiv:1808.08865
- [140] Khriplovich I B and Lamoreaux S K 1997 *CP Violation Without Strangeness: Electric Dipole Moments Of Particles, Atoms, and Molecules* (Berlin: Springer) p 230
- [141] Chupp T and Ramsey-Musolf M 2015 Electric dipole moments: a global analysis *Phys. Rev. C* **91** 035502
- [142] Dekens W, de Vries J, Bsaisou J, Bernreuther W, Hanhart C, Meißner U-G *et al* 2014 Unraveling models of CP violation through electric dipole moments of light nuclei *J. High Energy Phys.* **JHEP07(2014)069**
- [143] Smith J H, Purcell E M and Ramsey N F 1957 Experimental limit to the electric dipole moment of the neutron *Phys. Rev.* **108** 120–2
- [144] Pendlebury J M *et al* 2015 Revised experimental upper limit on the electric dipole moment of the neutron *Phys. Rev. D* **92** 092003
- [145] Golub R and Lamoreaux K 1994 Neutron electric dipole moment, ultracold neutrons and polarized He-3 *Phys. Rep.* **237** 1–62
- [146] Piegsa F M 2013 New concept for a neutron electric dipole moment search using a pulsed beam *Phys. Rev. C* **88** 045502
- [147] Graner B, Chen Y, Lindahl E G and Heckel B R 2016 Reduced limit on the permanent electric dipole moment of Hg199 *Phys. Rev. Lett.* **116** 161601

- [148] Dmitriev V F and Sen'kov R A 2003 Schiff moment of the Mercury nucleus and the proton dipole moment *Phys. Rev. Lett.* **91** 212303
- [149] Sahoo B 2017 Improved limits on the hadronic and semihadronic CP violating parameters and role of a dark force carrier in the electric dipole moment of ^{199}Hg *Phys. Rev. D* **95** 013002
- [150] Andreev V *et al* (ACME collaboration) 2018 Improved limit on the electric dipole moment of the electron *Nature* **562** 355–60
- [151] Cairncross W B *et al* 2017 Precision measurement of the electron's electric dipole moment using trapped molecular ions *Phys. Rev. Lett.* **119** 153001
- [152] Hudson J J, Kara D M, Smallman I J, Sauer B E, Tarbutt M R and Hinds E A 2011 Improved measurement of the shape of the electron *Nature* **473** 493–6
- [153] Aggarwal P(NL-eEDM collaboration) *et al* 2018 Measuring the electric dipole moment of the electron in BaF *Eur. Phys. J. D* **72** 197
- [154] Bennett G W *et al* (Muon (g-2) collaboration) 2009 An improved limit on the muon electric dipole moment *Phys. Rev. D* **80** 052008
- [155] Adelmann A, Kirch K, Onderwater C J G and Schietinger T 2010 Compact storage ring to search for the muon electric dipole moment *J. Phys. G: Nucl. Part. Phys.* **37** 085001
- [156] Botella F J *et al* 2017 On the search for the electric dipole moment of strange and charm baryons at LHC *Eur. Phys. J. C* **77** 181
- [157] Bagli E *et al* 2017 Electromagnetic dipole moments of charged baryons with bent crystals at the LHC *Eur. Phys. J. C* **77** 828
- [158] Sala F 2014 A bound on the charm chromo-EDM and its implications *J. High Energy Phys.* [JHEP03\(2014\)061](#)
- [159] Dainese A(QCD Working Group collaboration) *et al* 2019 Physics beyond colliders: QCD working group report [arXiv:1901.04482](#)
- [160] Fu J *et al* 2019 Novel method for the direct measurement of the τ lepton dipole moments *Phys. Rev. Lett.* **123** 011801
- [161] Fomin A S, Korchin A Y, Stocchi A, Barsuk S and Robbe P 2019 Feasibility of tau lepton electromagnetic dipole moments measurement using bent crystal at the LHC *J. High Energy Phys.* **2019** [JHEP03\(2019\)156](#)
- [162] Alves A A Jr *et al* (LHCb collaboration) 2008 The LHCb detector at the LHC *JINST* **3** S08005
- [163] Aaij R *et al* (LHCb collaboration) 2015 LHCb detector performance *Int. J. Mod. Phys. A* **30** 1530022
- [164] Du N *et al* (ADMX collaboration) 2018 A search for invisible axion dark matter with the axion dark matter experiment *Phys. Rev. Lett.* **120** 151301
- [165] Ballou R *et al* (OSQAR collaboration) 2015 New exclusion limits on scalar and pseudoscalar axionlike particles from light shining through a wall *Phys. Rev. D* **92** 092002
- [166] Della Valle F *et al* 2016 The PVLAS experiment: measuring vacuum magnetic birefringence and dichroism with a birefringent Fabry–Perot cavity *Eur. Phys. J. C* **76** 24
- [167] Della Valle F *et al* 2013 Measurements of vacuum magnetic birefringence using permanent dipole magnets: the PVLAS experiment *New J. Phys.* **15** 053026
- [168] Siemko A 2018 PBC technology subgroup report *Tech. Rep.* CERN-PBC-REPORT-2018-006 CERN
- [169] Anastassopoulos V *et al* (CAST collaboration) 2017 New CAST limit on the axion-photon interaction *Nat. Phys.* **13** 584–90
- [170] Sloan J *et al* 2016 Limits on axion-photon coupling or on local axion density: dependence on models of the milky way dark halo *Phys. Dark Universe* **14** 95–102
- [171] Melcon A A *et al* 2018 Axion searches with microwave filters: the RADES project *J. Cosmol. Astropart. Phys.* [JCAP05\(2018\)040](#)
- [172] Cadamuro D, Hannestad S, Raffelt G and Redondo J 2011 Cosmological bounds on sub-meV mass axions *J. Cosmol. Astropart. Phys.* [JCAP11\(2011\)003](#)
- [173] Cadamuro D and Redondo J 2012 Cosmological bounds on pseudo nambu-goldstone bosons *J. Cosmol. Astropart. Phys.* [JCAP12\(2012\)032](#)
- [174] Ayala A, Domínguez I, Giannotti M, Mirizzi A and Straniero O 2014 Revisiting the bound on axion-photon coupling from globular clusters *Phys. Rev. Lett.* **113** 191302
- [175] Vinyoles N, Serenelli A, Villante F, Basu S, Redondo J and Isern J 2015 New axion and hidden photon constraints from a solar data global fit *J. Cosmol. Astropart. Phys.* [JCAP15\(2015\)015](#)
- [176] Massó E and Toldrà R 1995 Light spinless particle coupled to photons *Phys. Rev. D* **52** 1755–63

- [177] Lazarus D M *et al* 1992 Search for solar axions *Phys. Rev. Lett.* **69** 2333–6
- [178] Moriyama S, Minowa M, Namba T, Inoue Y, Takasu Y and Yamamoto A 1998 Direct search for solar axions by using strong magnetic field and x-ray detectors *Phys. Lett. B* **434** 147
- [179] Anastassopoulos V *et al* 2017 Towards a medium-scale axion helioscope and haloscope *J. Instrum.* **12** P11019
- [180] Brubaker B M *et al* 2017 First results from a microwave cavity axion search at 24 μeV *Phys. Rev. Lett.* **118** 061302
- [181] Alesini D, Babusci D, Di Gioacchino D, Gatti C, Lamanna G and Ligi C 2017 The KLASH proposal arXiv:1707.06010
- [182] Chung W 2018 CULTASK, axion experiment at CAPP in Korea *Proc., 13th Patras Workshop on Axions, WIMPs and WISPs, (PATRAS 2017): Thessaloniki, Greece, 15 May 2017-19, 2017* pp 97–101
- [183] Miceli L 2015 Haloscope axion searches with the cast dipole magnet: the CAST-CAPP/IBS detector *Proc., 11th Patras Workshop on Axions, WIMPs and WISPs (Axion-WIMP 2015): Zaragoza, Spain, June 22-26, 2015* pp 164–8
- [184] Choi J, Themann H, Lee M J, Ko B R and Semertzidis Y K 2017 First axion dark matter search with toroidal geometry *Phys. Rev. D* **96** 061102
- [185] McAllister B T, Flower G, Ivanov E N, Goryachev M, Bourhill J and Tobar M E 2017 The organ experiment: an axion haloscope above 15 GHz *Phys. Dark Universe* **18** 67–72
- [186] Horns D, Jaeckel J, Lindner A, Lobanov A, Redondo J and Ringwald A 2013 Searching for WISPy cold dark matter with a dish antenna *J. Cosmol. Astropart. Phys.* **JCAP04(2013)016**
- [187] Caldwell A *et al* (MADMAX Working Group collaboration) 2017 Dielectric haloscopes: a new way to detect axion dark matter *Phys. Rev. Lett.* **118** 091801
- [188] Silva-Feaver M *et al* 2017 Design overview of DM radio pathfinder experiment *IEEE Trans. Appl. Supercond.* **27** 1400204
- [189] Kahn Y, Safdi B R and Thaler J 2016 Broadband and resonant approaches to axion dark matter detection *Phys. Rev. Lett.* **117** 141801
- [190] Lees J P *et al* (BaBar collaboration) 2014 Search for a dark photon in e^+e^- collisions at BaBar *Phys. Rev. Lett.* **113** 201801
- [191] Batley J R *et al* (NA48/2 collaboration) 2015 Search for the dark photon in π^0 decays *Phys. Lett. B* **746** 178–85
- [192] Merkel H *et al* 2014 Search at the Mainz microtron for light massive gauge bosons relevant for the muon $g-2$ anomaly *Phys. Rev. Lett.* **112** 221802
- [193] Riordan E M *et al* 1987 A search for short lived axions in an electron beam dump experiment *Phys. Rev. Lett.* **59** 755
- [194] Bjorken J D *et al* 1988 Search for neutral metastable penetrating particles produced in the SLAC beam dump *Phys. Rev. D* **38** 3375
- [195] Bross A, Crisler M, Pordes S H, Volk J, Errede S and Wrbanek J 1991 A search for shortlived particles produced in an electron beam dump *Phys. Rev. Lett.* **67** 2942–5
- [196] Archilli F *et al* (KLOE-2 collaboration) 2012 Search for a vector gauge boson in ϕ meson decays with the KLOE detector *Phys. Lett. B* **706** 251–5
- [197] Babusci D *et al* (KLOE-2 collaboration) 2013 Limit on the production of a light vector gauge boson in phi meson decays with the KLOE detector *Phys. Lett. B* **720** 111–5
- [198] Babusci D *et al* (KLOE-2 collaboration) 2014 Search for light vector boson production in $e^+e^- \rightarrow \mu^+\mu^-\gamma$ interactions with the KLOE experiment *Phys. Lett. B* **736** 459–64
- [199] Anastasi A *et al* (KLOE-2 collaboration) 2016 Limit on the production of a new vector boson in $e^+e^- \rightarrow U\gamma$, $U \rightarrow \pi^+\pi^-$ with the KLOE experiment *Phys. Lett. B* **757** 356–61
- [200] Aaij R *et al* (LHCb collaboration) 2018 Search for dark photons produced in 13 TeV pp collisions *Phys. Rev. Lett.* **120** 061801
- [201] Batell B, Essig R and Surujon Z 2014 Strong constraints on Sub-GeV dark sectors from SLAC beam dump E137 *Phys. Rev. Lett.* **113** 171802
- [202] Bergsma F (CHARM collaboration) *et al* 1985 Search for axion like particle production in 400-GeV proton—copper interactions *Phys. Lett. B* **157** 458–62
- [203] Gninenko S N 2012 Constraints on sub-GeV hidden sector gauge bosons from a search for heavy neutrino decays *Phys. Lett. B* **713** 244–8
- [204] Blumlein J *et al* 1991 Limits on neutral light scalar and pseudoscalar particles in a proton beam dump experiment *Z. Phys. C* **51** 341–50

- [205] Ahn J K(KOTO collaboration) *et al* 2019 Search for the $K_L \rightarrow \pi^0 \nu \bar{\nu}$ and $K_L \rightarrow \pi^0 X^0$ decays at the J-PARC KOTO experiment *Phys. Rev. Lett.* **122** 021802
- [206] Kou E and (Belle II collaboration) 2018 *The Belle II Physics Book KEK Preprint 2018-27, BELLE2-PUB-PH-2018-001, FERMILAB-PUB-18-398-T, JLAB-THY-18-2780, INT-PUB-18-047, UWThPh 2018-26* Belle II Collaboration arXiv:1808.10567
- [207] Ilten P, Soreq Y, Thaler J, Williams M and Xue W 2016 Proposed inclusive dark photon search at LHCb *Phys. Rev. Lett.* **116** 251803
- [208] Ilten P, Thaler J, Williams M and Xue W 2015 Dark photons from charm mesons at LHCb *Phys. Rev. D* **92** 115017
- [209] Adrian P H(HPS collaboration) *et al* 2018 Search for a dark photon in electro-produced e^+e^- pairs with the heavy photon search experiment at JLab *Phys. Rev. D* **98** 091101(R)
- [210] Battaglieri M *et al* 2015 The heavy photon search test detector *Nucl. Instrum. Meth. A* **777** 91–101
- [211] Abrahamyan S *et al* (APEX collaboration) 2011 Search for a new gauge boson in electron-nucleus fixed-target scattering by the APEX experiment *Phys. Rev. Lett.* **107** 191804
- [212] Essig R, Schuster P, Toro N and Wojtsekhowski B 2011 An electron fixed target experiment to search for a new vector boson A' decaying to e^+e^- *J. High Energy Phys.* **JHEP02(2011)009**
- [213] Shiltsev V 2017 Fermilab proton accelerator complex status and improvement plans *Mod. Phys. Lett. A* **32** 1730012
- [214] Wojtsekhowski B, Nikolenko D and Rachek I 2012 Searching for a new force at VEPP-3 arXiv:1207.5089
- [215] Doria L, Achenbach P, Christmann M, Denig A, Gülker P and Merkel H 2018 Search for light dark matter with the MESA accelerator *13th Conf. on the Intersections of Particle and Nuclear Physics (CIPANP 2018) (Palm Springs, California, USA, 29 May–3 June 2018)* arXiv:1809.07168
- [216] Lees J P *et al* (BaBar collaboration) 2017 Search for invisible decays of a dark photon produced in e^+e^- collisions at BaBar *Phys. Rev. Lett.* **119** 131804
- [217] deNiverville P, Pospelov M and Ritz A 2011 Observing a light dark matter beam with neutrino experiments *Phys. Rev. D* **84** 075020
- [218] Essig R, Manalaysay A, Mardon J, Sorensen P and Volansky T 2012 First direct detection limits on sub-GeV dark matter from XENON10 *Phys. Rev. Lett.* **109** 021301
- [219] Essig R, Volansky T and Yu T-T 2017 New constraints and prospects for sub-GeV dark matter scattering off electrons in xenon *Phys. Rev. D* **96** 043017
- [220] Adler S *et al* (E787 collaboration) 2002 Further evidence for the decay $K^+ \rightarrow \pi^+ \nu \bar{\nu}$ anti-neutrino *Phys. Rev. Lett.* **88** 041803
- [221] Artamonov A V *et al* (BNL-E949 collaboration) 2009 Study of the decay $K^+ \rightarrow \pi^+ \nu \bar{\nu}$ in the momentum region $140 < P_\pi < 199$ MeV/c *Phys. Rev. D* **79** 092004
- [222] Bennett G W *et al* (Muon g-2 collaboration) 2006 Final report of the muon E821 anomalous magnetic moment measurement at BNL *Phys. Rev. D* **73** 072003
- [223] Angloher G *et al* (CRESST collaboration) 2016 Results on light dark matter particles with a low-threshold CRESST-II detector *Eur. Phys. J. C* **76** 25
- [224] Angle J *et al* (XENON10 collaboration) 2011 A search for light dark matter in XENON10 data *Phys. Rev. Lett.* **107** 051301
- [225] Aprile E *et al* (XENON collaboration) 2016 Low-mass dark matter search using ionization signals in XENON100 *Phys. Rev. D* **94** 092001
- [226] Agnese R *et al* (SuperCDMS collaboration) 2017 Projected sensitivity of the super CDMS SNOLAB experiment *Phys. Rev. D* **95** 082002
- [227] Battaglieri M(BDX collaboration) *et al* 2016 Dark matter search in a beam-dump experiment (BDX) at Jefferson lab arXiv:1607.01390
- [228] Aguilar-Arevalo A A(MiniBooNE DM collaboration) *et al* 2018 Dark matter search in nucleon, pion, and electron channels from a proton beam dump with MiniBooNE *Phys. Rev. D* **98** 112004
- [229] deNiverville P, Pospelov M and Ritz A 2015 Light new physics in coherent neutrino-nucleus scattering experiments *Phys. Rev. D* **92** 095005
- [230] Tiffenberg J *et al* (SENSEI collaboration) 2017 Single-electron and single-photon sensitivity with a silicon Skipper CCD *Phys. Rev. Lett.* **119** 131802
- [231] Magill G, Plestid R, Pospelov M and Tsai Y-D 2018 Millicharged particles in neutrino experiments *Phys. Rev. Lett.* **122** 071801

- [232] Aguilar-Arevalo A A (MiniBooNE collaboration) *et al* 2018 Significant excess of electronlike events in the MiniBooNE short-baseline neutrino experiment *Phys. Rev. Lett.* **121** 221801
- [233] Athanassopoulos C *et al* (LSND collaboration) 1997 The Liquid scintillator neutrino detector and LAMPF neutrino source *Nucl. Instrum. Methods A* **388** 149–72
- [234] Antonello M (LAr1-ND, ICARUS-WA104, MicroBooNE collaboration) *et al* A proposal for a three detector short-baseline neutrino oscillation program in the fermilab booster neutrino beam arXiv:1503.01520
- [235] Acciarri R (DUNE collaboration) *et al* 2015 Long-baseline neutrino facility (LBNF) and deep underground neutrino experiment (DUNE) arXiv:1512.06148
- [236] Prinz A A *et al* 1998 Search for millicharged particles at SLAC *Phys. Rev. Lett.* **81** 1175–8
- [237] Davidson S, Hannestad S and Raffelt G 2000 Updated bounds on millicharged particles *J. High Energy Phys.* **JHEP05(2000)003**
- [238] Monsalve R A *et al* 2018 Results from EDGES High-Band: II. Constraints on parameters of early galaxies *Astrophys. J.* **863** 11
- [239] Muñoz J B and Loeb A 2018 A small amount of mini-charged dark matter could cool the baryons in the early Universe *Nature* **557** 684
- [240] Barkana R 2018 Possible interaction between baryons and dark-matter particles revealed by the first stars *Nature* **555** 71–4
- [241] Kovetz E D, Poulin V, Gluscevic V, Boddy K K, Barkana R and Kamionkowski M 2018 Tighter limits on dark matter explanations of the anomalous EDGES 21 cm Signal arXiv:1807.11482
- [242] Barkana R, Outmezguine N J, Redigolo D and Volansky T 2018 Strong constraints on light dark matter interpretation of the EDGES signal *Phys. Rev. D* **98** 103005
- [243] Crisler M *et al* (SENSEI collaboration) 2018 SENSEI: first direct-detection constraints on sub-GeV dark matter from a surface run *Phys. Rev. Lett.* **121** 061803
- [244] Chuzhoy L and Kolb E W 2009 Reopening the window on charged dark matter *J. Cosmol. Astropart. Phys.* **JCAP07(2009)014**
- [245] Ball A *et al* 2016 A letter of intent to install a milli-charged particle detector at LHC P5 arXiv:1607.04669
- [246] Kelly K J and Tsai Y-D 2019 Proton fixed-target scintillation experiment to search for minicharged particles *Phys. Rev. D* **100** 015043
- [247] Clarke J D, Foot R and Volkas R R 2014 Phenomenology of a very light scalar ($100 \text{ MeV} < m_h < 10 \text{ GeV}$) mixing with the SM Higgs *J. High Energy Phys.* **JHEP02(2014)123**
- [248] Winkler M W 2019 Decay and detection of a light scalar boson mixing with the Higgs *Phys. Rev. D* **99** 015018
- [249] Aaij R *et al* (LHCb collaboration) 2017 Search for long-lived scalar particles in $B^+ \rightarrow K^+ \chi (\mu^+ \mu^-)$ decays *Phys. Rev. D* **95** 071101
- [250] Aaij R *et al* (LHCb collaboration) 2015 Search for hidden-sector bosons in $B^0 \rightarrow K^{*0} \mu^+ \mu^-$ decays *Phys. Rev. Lett.* **115** 161802
- [251] Wei J T *et al* 2009 Measurement of the differential branching fraction and forward-backward asymmetry for $B \rightarrow K^{(*)} \ell^+ \ell^-$ *Phys. Rev. Lett.* **103** 171801
- [252] Artamonov A V *et al* (E949 collaboration) 2008 New measurement of the $K^+ \rightarrow \pi^+ \nu \bar{\nu}$ branching ratio *Phys. Rev. Lett.* **101** 191802
- [253] Turner M S 1988 Axions from SN 1987a *Phys. Rev. Lett.* **60** 1797
- [254] Frieman J A, Dimopoulos S and Turner M S 1987 Axions and stars *Phys. Rev. D* **36** 2201
- [255] Burrows A, Turner M S and Brinkmann R P 1989 Axions and SN 1987a *Phys. Rev. D* **39** 1020
- [256] Essig R, Harnik R, Kaplan J and Toro N 2010 Discovering new light states at neutrino experiments *Phys. Rev. D* **82** 113008
- [257] Minkowski P 1977 $\mu \rightarrow e \gamma$ at a rate of one out of 10^9 muon decays? *Phys. Lett. B* **67** 421–8
- [258] Gell-Mann M, Ramond P and Slansky R 1979 Complex spinors and unified theories *Conf. Proc.* vol 790927, pp 315–21
- [259] Mohapatra R N and Senjanovic G 1980 Neutrino mass and spontaneous parity violation *Phys. Rev. Lett.* **44** 912
- [260] Yanagida T 1980 Horizontal symmetry and masses of neutrinos *Prog. Theor. Phys.* **64** 1103
- [261] Schechter J and Valle J W F 1980 Neutrino masses in $SU(2) \times U(1)$ theories *Phys. Rev. D* **22** 2227
- [262] Schechter J and Valle J W F 1982 Neutrino decay and spontaneous violation of lepton number *Phys. Rev. D* **25** 774

- [263] D’Onofrio M, Rummukainen K and Tranberg A 2014 Sphaleron rate in the minimal standard model *Phys. Rev. Lett.* **113** 141602
- [264] Kuzmin V A, Rubakov V A and Shaposhnikov M E 1985 On the anomalous electroweak baryon number nonconservation in the early universe *Phys. Lett. B* **155** 36
- [265] Fukugita M and Yanagida T 1986 Baryogenesis without grand unification *Phys. Lett. B* **174** 45–7
- [266] Akhmedov E K, Rubakov V A and Smirnov A Y 1998 Baryogenesis via neutrino oscillations *Phys. Rev. Lett.* **81** 1359–62
- [267] Hambye T and Teresi D 2016 Higgs doublet decay as the origin of the baryon asymmetry *Phys. Rev. Lett.* **117** 091801
- [268] Canetti L, Drewes M and Shaposhnikov M 2012 Matter and antimatter in the Universe *New J. Phys.* **14** 095012
- [269] Viel M, Lesgourgues J, Haehnelt M G, Matarrese S and Riotto A 2005 Constraining warm dark matter candidates including sterile neutrinos and light gravitinos with WMAP and the Lyman-alpha forest *Phys. Rev. D* **71** 063534
- [270] Ruchayskiy O and Ivashko A 2012 Restrictions on the lifetime of sterile neutrinos from primordial nucleosynthesis *J. Cosmol. Astropart. Phys.* **JCAP10(2012)014**
- [271] Fuller G M, Kusenko A and Petraki K 2009 Heavy sterile neutrinos and supernova explosions *Phys. Lett. B* **670** 281–4
- [272] Drewes M 2013 The phenomenology of right-handed neutrinos *Int. J. Mod. Phys. E* **22** 1330019
- [273] Canetti L, Drewes M, Frossard T and Shaposhnikov M 2013 Dark matter, baryogenesis and neutrino oscillations from right-handed neutrinos *Phys. Rev. D* **87** 093006
- [274] Abreu P *et al* (DELPHI collaboration) 1997 Search for neutral heavy leptons produced in Z decays *Z. Phys. C* **74** 57–71
- [275] Bernardi G *et al* 1988 Further limits on heavy neutrino couplings *Phys. Lett. B* **203** 332–4
- [276] Bergsma F (CHARM collaboration) *et al* 1986 A search for decays of heavy neutrinos in the mass range 0.5 GeV to 2.8 GeV *Phys. Lett. B* **166** 473–8
- [277] Vaitaitis A *et al* (NuTeV, E815 collaboration) 1999 Search for neutral heavy leptons in a high-energy neutrino beam *Phys. Rev. Lett.* **83** 4943–6
- [278] Artamonov A V *et al* (E949 collaboration) 2015 Search for heavy neutrinos in $K^+ \rightarrow \mu^+ \nu_H$ decays *Phys. Rev. D* **91** 052001
- [279] Aoki M *et al* (PIENU collaboration) 2011 Search for massive neutrinos in the decay $\pi \rightarrow e \nu$ *Phys. Rev. D* **84** 052002
- [280] Britton D I *et al* 1992 Improved search for massive neutrinos in $\pi^+ \rightarrow e^+ \nu$ neutrino decay *Phys. Rev. D* **46** R885–7
- [281] Badier J *et al* (NA3 collaboration) 1986 Direct photon production from pions and protons at 200 GeV/c *Z. Phys. C* **31** 341
- [282] Cortina Gil E *et al* (NA62 collaboration) 2018 Search for heavy neutral lepton production in K^+ decays *Phys. Lett. B* **778** 137–45
- [283] Izaguirre E and Shuve B 2015 Multilepton and lepton jet probes of sub-weak-scale right-handed neutrinos *Phys. Rev. D* **91** 093010
- [284] Antusch S, Cazzato E and Fischer O 2016 Displaced vertex searches for sterile neutrinos at future lepton colliders *J. High Energy Phys.* **JHEP12(2016)007**
- [285] Gago A M, Hernández P, Jones-Pérez J, Losada M and Moreno Briceño A 2015 Probing the type I seesaw mechanism with displaced vertices at the LHC *Eur. Phys. J. C* **75** 470
- [286] Antusch S, Cazzato E and Fischer O 2017 Sterile neutrino searches via displaced vertices at LHCb *Phys. Lett. B* **774** 114–8
- [287] Antusch S, Cazzato E and Fischer O 2017 Sterile neutrino searches at future e^-e^+ , pp , and e^-p colliders *Int. J. Mod. Phys. A* **32** 1750078
- [288] Antusch S *et al* 2018 Probing leptogenesis at future colliders *J. High Energy Phys.* **JHEP09(2018)124**
- [289] Deppisch F F, Bhupal Dev P S and Pilaftsis A 2015 Neutrinos and collider physics *New J. Phys.* **17** 075019
- [290] Cai Y, Han T, Li T and Ruiz R 2018 Lepton number violation: seesaw models and their collider tests *Front. Phys.* **6** 40
- [291] Liventsev D *et al* (Belle collaboration) 2013 Search for heavy neutrinos at Belle *Phys. Rev. D* **87** 071102
- [292] Sirunyan A M *et al* (CMS collaboration) 2018 Search for heavy neutral leptons in events with three charged leptons in proton-proton collisions at $\sqrt{s} = 13$ TeV *Phys. Rev. Lett.* **120** 221801

- [293] Canetti L and Shaposhnikov M 2010 Baryon asymmetry of the Universe in the NuMSM *J. Cosmol. Astropart. Phys.* **JCAP09(2010)001**
- [294] Drewes M, Hajer J, Klaric J and Lanfranchi G 2018 NA62 sensitivity to heavy neutral leptons in the low scale seesaw model *J. High. Energ. Phys.* **2018 JHEP07(2018)105**
- [295] Adams C (LBNE collaboration) *et al* 2013 The long-baseline neutrino experiment: exploring fundamental symmetries of the Universe arXiv:1307.7335
- [296] Blondel A, Graverini E, Serra N, Shaposhnikov M and (FCC-ee study Team collaboration) 2016 Search for heavy right-handed neutrinos at the FCC-ee *Nucl. Part. Phys. Proc.* **273–275 1883–90**
- [297] Aaij R *et al* (LHCb collaboration) 2014 Search for Majorana neutrinos in $B^- \rightarrow \pi^+ \mu^- \mu^-$ decays *Phys. Rev. Lett.* **112 131802**
- [298] Orloff J, Rozanov A N and Santoni C 2002 Limits on the mixing of tau neutrino to heavy neutrinos *Phys. Lett. B* **550 8–15**
- [299] Astier P *et al* (NOMAD collaboration) 2001 Search for heavy neutrinos mixing with tau neutrinos *Phys. Lett. B* **506 27–38**
- [300] Peccei R D and Quinn H R 1977 Constraints imposed by CP conservation in the presence of instantons *Phys. Rev. D* **16 1791–7**
- [301] Freytsis M and Ligeti Z 2011 On dark matter models with uniquely spin-dependent detection possibilities *Phys. Rev. D* **83 115009**
- [302] Dienes K R, Kumar J, Thomas B and Yaylali D 2014 Overcoming velocity suppression in dark-matter direct-detection experiments *Phys. Rev. D* **90 015012**
- [303] Akerib D S *et al* (LUX collaboration) 2014 First results from the LUX dark matter experiment at the sanford underground research facility *Phys. Rev. Lett.* **112 091303**
- [304] Agnese R *et al* (SuperCDMS collaboration) 2014 Search for low-mass weakly interacting massive particles using voltage-assisted calorimetric ionization detection in the super CDMS experiment *Phys. Rev. Lett.* **112 041302**
- [305] Agnese R *et al* (SuperCDMS collaboration) 2014 Search for low-mass weakly interacting massive particles with super CDMS *Phys. Rev. Lett.* **112 241302**
- [306] Angloher G *et al* (CRESST-II collaboration) 2014 Results on low mass WIMPs using an upgraded CRESST-II detector *Eur. Phys. J. C* **74 3184**
- [307] Aad G *et al* (ATLAS collaboration) 2014 Search for invisible decays of a Higgs boson produced in association with a Z boson in ATLAS *Phys. Rev. Lett.* **112 201802**
- [308] Chatrchyan S *et al* (CMS collaboration) 2014 Search for invisible decays of Higgs bosons in the vector boson fusion and associated ZH production modes *Eur. Phys. J. C* **74 2980**
- [309] Chatrchyan S *et al* (CMS collaboration) 2011 Search for new physics with a mono-jet and missing transverse energy in pp collisions at $\sqrt{s} = 7$ TeV *Phys. Rev. Lett.* **107 201804**
- [310] Halprin A, Andersen C M and Primakoff H 1966 Photonic decay rates and nuclear-coulomb-field coherent production processes *Phys. Rev.* **152 1295–303**
- [311] Dolan M J, Ferber T, Hearty C, Kahlhoefer F and Schmidt-Hoberg K 2017 Revised constraints and Belle II sensitivity for visible and invisible axion-like particles *J. High Energy Phys.* **JHEP12(2017)094**
- [312] Krasny M W *et al* 1987 Recent searches for shortlived pseudoscalar bosons in electron beam dump experiments *High-energy physics. Proc., Int. Europhysics Conf. Vols. 1, 2 (Uppsala, Sweden, 25 June 25–1 July 1987)*
- [313] Döbrich B Axion-like Particles from Primakov production in beam-dumps *Photon 2017: Int. Conf. on the Structure and the Interactions of the Photon and 22th Int. Workshop on Photon-Photon Collisions and the Int. Workshop on High Energy Photon Colliders CERN (Geneva, Switzerland, 22–26 May 2017)* arXiv:1708.05776
- [314] 2012 Fundamental physics at the intensity frontier (<https://doi.org/10.2172/1042577>)
- [315] Jaeckel J and Spannowsky M 2016 Probing MeV to 90 GeV axion-like particles with LEP and LHC *Phys. Lett. B* **753 482–7**
- [316] Acciarri M *et al* (L3 collaboration) 1995 Search for anomalous $Z \rightarrow \gamma \gamma \gamma$ events at LEP *Phys. Lett. B* **345 609–16**
- [317] Abreu P *et al* (DELPHI collaboration) 1991 The reaction $e^+ e^- \rightarrow \gamma \gamma (\gamma)$ at Z0 energies *Phys. Lett. B* **268 296–304**
- [318] Abreu P *et al* (DELPHI collaboration) 1994 Measurement of the $e^+ e^- \rightarrow \gamma \gamma (\gamma)$ cross-section at LEP energies *Phys. Lett. B* **327 386–96**

- [319] Acciarri M *et al* (L3 collaboration) 1995 Tests of QED at LEP energies using $e+e- \rightarrow$ gamma gamma (gamma) and $e+e- \rightarrow$ lepton+ lepton- gamma gamma *Phys. Lett. B* **353** 136–44
- [320] Abdallah J *et al* (DELPHI collaboration) 2009 Search for one large extra dimension with the DELPHI detector at LEP *Eur. Phys. J. C* **60** 17–23
- [321] Aaboud M *et al* (ATLAS collaboration) 2017 Search for dark matter at $\sqrt{s} = 13$ TeV in final states containing an energetic photon and large missing transverse momentum with the ATLAS detector *Eur. Phys. J. C* **77** 393
- [322] Duffy M E *et al* 1988 Neutrino production by 400-GeV/c protons in a beam-dump experiment *Phys. Rev. D* **38** 2032
- [323] Anisimovsky V V *et al* (E949 collaboration) 2004 Improved measurement of the $K^+ \rightarrow \pi^+\nu\bar{\nu}$ branching ratio *Phys. Rev. Lett.* **93** 031801
- [324] Alavi-Harati A *et al* (KTeV collaboration) 2000 Search for the Decay $K_L \rightarrow \pi^0\mu^+\mu^-$ *Phys. Rev. Lett.* **84** 5279–82
- [325] Dolan M J, Kahlhoefer F, McCabe C and Schmidt-Hoberg K 2015 A taste of dark matter: flavour constraints on pseudoscalar mediators *J. High Energy Phys.* **JHEP03(2015)171**
- [326] Dobrich B, Ertas F, Kahlhoefer F and Spadaro T 2019 Model-independent bounds on light pseudoscalars from rare B-meson decays *Phys. Lett. B* **790** 537–44
- [327] Lees J P *et al* (BaBar collaboration) 2013 Search for di-muon decays of a low-mass Higgs boson in radiative decays of the $\Upsilon(1S)$ *Phys. Rev. D* **87** 031102
- [328] Yamazaki T *et al* 1984 Search for a neutral boson in a two-body decay of $K^+ \rightarrow \pi^+ X^0$ *Phys. Rev. Lett.* **52** 1089–91
- [329] Ammar R *et al* (CLEO collaboration) 2001 Search for the familon via $B^{+-} \rightarrow \pi^+\pi^- X^0$, $B^{+-} \rightarrow K^+ X^0$, and $B^0 \rightarrow K^0(S)X^0$ decays *Phys. Rev. Lett.* **87** 271801
- [330] Lees J P *et al* (BaBar collaboration) 2013 Search for a low-mass scalar Higgs boson decaying to a tau pair in single-photon decays of $\Upsilon(1S)$ *Phys. Rev. D* **88** 071102
- [331] Aaij R *et al* (LHCb collaboration) 2013 Differential branching fraction and angular analysis of the $B^+ \rightarrow K^+\mu^+\mu^-$ decay *J. High Energy Phys.* **JHEP02(2013)105**
- [332] Aloni D, Soreq Y and Williams M 2019 Coupling QCD-scale axion-like particles to gluons *Phys. Rev. Lett.* **123** 031803
- [333] Knapen S, Lin T, Lou H K and Melia T 2017 Searching for axionlike particles with ultraperipheral heavy-ion collisions *Phys. Rev. Lett.* **118** 171801
- [334] Abbiendi G *et al* (OPAL collaboration) 2003 Multiphoton production in $e+e^-$ collisions at $s^{**}(1/2) = 181$ GeV to 209 GeV *Eur. Phys. J. C* **26** 331–44
- [335] Tanabashi M *et al* (Particle Data Group collaboration) 2018 Review of particle physics *Phys. Rev. D* **98** 030001
- [336] Aubert B *et al* (BaBar collaboration) 2008 Study of B meson decays with excited eta and eta-prime mesons *Phys. Rev. Lett.* **101** 091801
- [337] Lees J P *et al* (BaBar collaboration) 2011 Measurements of branching fractions and CP asymmetries and studies of angular distributions for $B \rightarrow \phi\phi K$ decays *Phys. Rev. D* **84** 012001
- [338] Chobanova V *et al* (Belle collaboration) 2014 Measurement of branching fractions and CP violation parameters in $B \rightarrow \omega K$ decays with first evidence of CP violation in $B^0 \rightarrow \omega K_S^0$ *Phys. Rev. D* **90** 012002
- [339] Lazzeroni C *et al* (NA62 collaboration) 2014 Study of the $K^\pm \rightarrow \pi^\pm\gamma\gamma$ decay by the NA62 experiment *Phys. Lett. B* **732** 65–74
- [340] Abouzaid E *et al* (KTeV collaboration) 2008 Final Results from the KTeV Experiment on the Decay $K_L \rightarrow \pi^0\gamma\gamma$ *Phys. Rev. D* **77** 112004
- [341] Bauer M, Neubert M and Thamm A 2017 Collider probes of axion-like particles *J. High Energy Phys.* **JHEP12(2017)044**
- [342] Hiller G 2004 B physics signals of the lightest CP odd Higgs in the NMSSM at large tan beta *Phys. Rev. D* **70** 034018
- [343] Bobeth C, Ewerth T, Kruger F and Urban J 2001 Analysis of neutral Higgs boson contributions to the decays $\bar{B}(s) \rightarrow \ell^+\ell^-$ and $\bar{B} \rightarrow K\ell^+\ell^-$ *Phys. Rev. D* **64** 074014
- [344] Choi K, Im S H, Park C B and Yun S 2017 Minimal flavor violation with axion-like particles *J. High Energy Phys.* **JHEP11(2017)070**
- [345] Buras A J, Buttazzo D, Girschbach-Noe J and Knegjens R 2015 $K^+ \rightarrow \pi^+\nu\bar{\nu}$ and $K_L \rightarrow \pi^0\nu\bar{\nu}$ in the standard model: status and perspectives *J. High Energy Phys.* **JHEP11(2015)033**

- [346] Grossman Y and Nir Y 1997 $K(L) \rightarrow \pi^0$ neutrino anti-neutrino beyond the standard model *Phys. Lett. B* **398** 163–8
- [347] Buras A J, Buttazzo D and Kneijens R 2015 $K \rightarrow \pi\nu\bar{\nu}$ and ϵ'/ϵ in simplified new physics models *J. High Energy Phys.* [JHEP11\(2015\)166](#)
- [348] Bai Z *et al* (RBC, UKQCD collaboration) 2015 Standard model prediction for direct CP violation in $K \rightarrow \pi\pi$ decay *Phys. Rev. Lett.* **115** 212001
- [349] Buras A J and Gerard J-M 2015 Upper bounds on ϵ'/ϵ parameters $B_6^{(1/2)}$ and $B_8^{(3/2)}$ from large N QCD and other news *J. High Energy Phys.* [JHEP12\(2015\)008](#)
- [350] Bobeth C and Buras A J 2018 Leptoquarks meet ϵ'/ϵ and rare Kaon processes *J. High Energy Phys.* [JHEP02\(2018\)101](#)
- [351] Bobeth C, Buras A J, Celis A and Jung M 2017 Patterns of flavour violation in models with vector-like quarks *J. High Energy Phys.* [JHEP04\(2017\)079](#)
- [352] Endo M, Kitahara T, Mishima S and Yamamoto K 2017 Revisiting Kaon physics in general Z scenario *Phys. Lett. B* **771** 37–44
- [353] Endo M, Mishima S, Ueda D and Yamamoto K 2016 Chargino contributions in light of recent ϵ'/ϵ *Phys. Lett. B* **762** 493–7
- [354] Endo M, Goto T, Kitahara T, Mishima S, Ueda D and Yamamoto K 2018 Gluino-mediated electroweak penguin with flavor-violating trilinear couplings *J. High Energy Phys.* [JHEP04\(2018\)019](#)
- [355] Tanimoto M and Yamamoto K 2016 Probing SUSY with 10 TeV stop mass in rare decays and CP violation of kaon *PTEP* **2016** 123B02
- [356] Crivellin A, D'Ambrosio G, Kitahara T and Nierste U 2017 $K \rightarrow \pi\nu\bar{\nu}$ in the MSSM in light of the ϵ'_K/ϵ_K anomaly *Phys. Rev. D* **96** 015023
- [357] Blanke M, Buras A J and Recksiegel S 2016 Quark flavour observables in the Littlest Higgs model with T-parity after LHC Run 1 *Eur. Phys. J. C* **76** 182
- [358] Kamenik J F, Soreq Y and Zupan J 2018 Lepton flavor universality violation without new sources of quark flavor violation *Phys. Rev. D* **97** 035002
- [359] Barbieri R, Isidori G, Pattori A and Senia F 2016 Anomalies in B -decays and $U(2)$ flavour symmetry *Eur. Phys. J. C* **76** 67
- [360] Gasser J and Leutwyler H 1985 $\eta \rightarrow 3\pi$ to one loop *Nucl. Phys. B* **250** 539–60
- [361] Fariborz A H and Schechter J 1999 η' decay as a probe of a possible lowest lying scalar nonet *Phys. Rev. D* **60** 034002